

Cold Trap CFD Modeling for TEF KTI
[project 20.06002.01.091 (use to be 20.01402.661)]

1/29/03

STG

This notebook is intended to document the technical support provided for the effort on modeling the heat transfer and fluid flow phenomenon in the underground storage tunnels (drifts) for nuclear waste packages. This includes review and analysis of laboratory scale cold trap experiments and predictions of the actual field conditions at the actual storage facility.

The other team members for the overall effort are Randy Fedors (team leader), David Walter, and Frank Dodge.

My part of the task will involve standard engineering analysis and acting as a technical advisor to David Walter in his use of the FLOW-3D[®] CFD software package.

3/25/03

STG

Problem:

The CFD model of the cold trap phenomenon simulates dry air only. The CFD results are used to conduct a water vapor transport analysis to estimate the flow of water vapor from the hot end of the drift to the cold end. The analysis assumes that the air is saturated. The water vapor concentration is dictated by the vapor pressure of water at the local value of air temperature and some way of approximating the tabulated values of water saturation pressure is required. The temperature range of the air is approximately 20°C to 100°C

Required:

Determine a reasonably accurate correlation for the saturation vapor pressure of water in the specified temperature range.

Solution:

Investigate and compare the three correlations presented in Chapter 5 of ASHRAE Handbook of Fundamentals (1977):

Goff Formula (vapor pressure over liquid water for the temperature range of -50°C to 100°C):

$$\begin{aligned}\log_{10}(P_{v,sat}) = & 10.79586(1 - \theta) + 5.82808 \log_{10}(\theta) \\ & + 1.50474 \times 10^{-4} \left(1 - 10^{-8.29692(1/\theta - 1)}\right) \\ & + 4.2873 \times 10^{-3} \left(10^{4.76955(1 - \theta)} - 1\right) \\ & - 2.2195983\end{aligned}$$

where

$$\theta = \frac{273.16}{T}$$

T = absolute temperature, Kelvin

$P_{v,sat}$ = water liquid - vapor saturation pressure, atmospheres

IMPORTANT NOTE:

The ASHRAE Fundamentals text had the coefficient of the Goff formula fourth term, 4.2873, listed as 0.42873. In conducting this review, it was discovered that the value, 4.2873, provided results that were more accurate than those given by the as-printed equation. I did not locate the original reference to verify the formula; rather, I assumed that the 'modified' equation listed here is the intended form

The citation for this equation is:

Goff, J. A., "Saturation Pressure of Water on the new Kelvin Scale," ***Humidity and Moisture Measurement and Control in Science and Industry***, Jwexler, A., and Wildhack, W. H., eds., Reinhold Publishing Corp., New York, 1965, p. 289. As cited in Chapter 5 of ***ASHRAE Handbook and Product Directory, 1977 Fundamentals***, Third Printing, American Society of Heating Refrigeration and Air Conditioning Engineers, Inc., New York, p. 5.12

Keenan, Keyes, Hill, and Moore Formula (vapor pressure over liquid water for the temperature range of 0°C to 374°C):

$$\ln\left(\frac{P_{v,sat}}{217.99}\right) = \frac{0.01}{T} (374.136 - t) \left[-741.9242 + \sum_{i=1}^7 F_i (0.65 - 0.01t)^i \right]$$

where

$$F_1 = -29.72100 \quad F_5 = +0.439993$$

$$F_2 = -11.55286 \quad F_6 = +0.2520658$$

$$F_3 = -0.8685635 \quad F_7 = +0.05218684$$

$$F_4 = +0.1094098$$

$$t = T - 273.15K = \text{degreed Celsius}$$

$$T = \text{absolute temperature, Kelvin}$$

$$P_{v,sat} = \text{water liquid - vapor saturation pressure, atmospheres}$$

The citation for this equation is:

Keenan, J. H., Keyes, F. G., Hill, P. G., Moore, J. G., **Steam Tables: Thermodynamic Properties of Water, Including Vapor, Liquid, and Solid Phases**, John Wiley and Sons, Inc, 1969. As cited in Chapter 5 of **ASHRAE Handbook and Product Directory, 1977 Fundamentals**, Third Printing, American Society of Heating Refrigeration and Air Conditioning Engineers, Inc., New York, p. 5.12.

Keenan-Keyes Formula (vapor pressure over liquid water for the temperature range of 10°C to 150°C):

$$\log_{10} \left(\frac{P_{v,sat}}{218.167} \right) = \frac{\beta}{T} \left(\frac{a + b\beta + c\beta^3}{1 + d\beta} \right)$$

where

$$a = 3.2437814$$

$$b = 5.868276 \times 10^{-3}$$

$$c = 1.1702379 \times 10^{-8}$$

$$d = 2.1878462 \times 10^{-3}$$

$$\beta = 647.27 - T$$

T = absolute temperature, Kelvin

$P_{v,sat}$ = water liquid - vapor saturation pressure, atmospheres

The citation for this equation is:

Keenan, J. H., and Keyes, F. G., Hill, P. G., Moore, J. G., ***Thermodynamic Properties of Steam***, John Wiley and Sons, Inc, 1936, p. 14. As cited in Chapter 5 of ***ASHRAE Handbook and Product Directory, 1977 Fundamentals***, Third Printing, American Society of Heating Refrigeration and Air Conditioning Engineers, Inc., New York, p. 5.12.

These three equations were programmed into Excel (located in S. Green's desktop computer as C:\Projects\div20\Notebook\Water_Pvsat.xls) and compared to the tabulated values for the saturation pressure of water vapor in equilibrium with liquid water in the temperature range of 0.01°C to 200°C. The tabulated values are taken from

Keenan, J. H., Keyes, F. G., Hill, P. G., Moore, J. G., ***Steam Tables***, John Wiley and Sons, Inc, New York, 1978. As cited in Appendix A of Van Wylen, G. J., and Sonntag, R. E., ***Fundamentals of Classical Thermodynamics***, Third Edition, John Wiley and Sons, Inc, New York, 1985, p 613.

The tabulated values of the calculation results are shown on the following page and are compared graphically in the subsequent two figures.

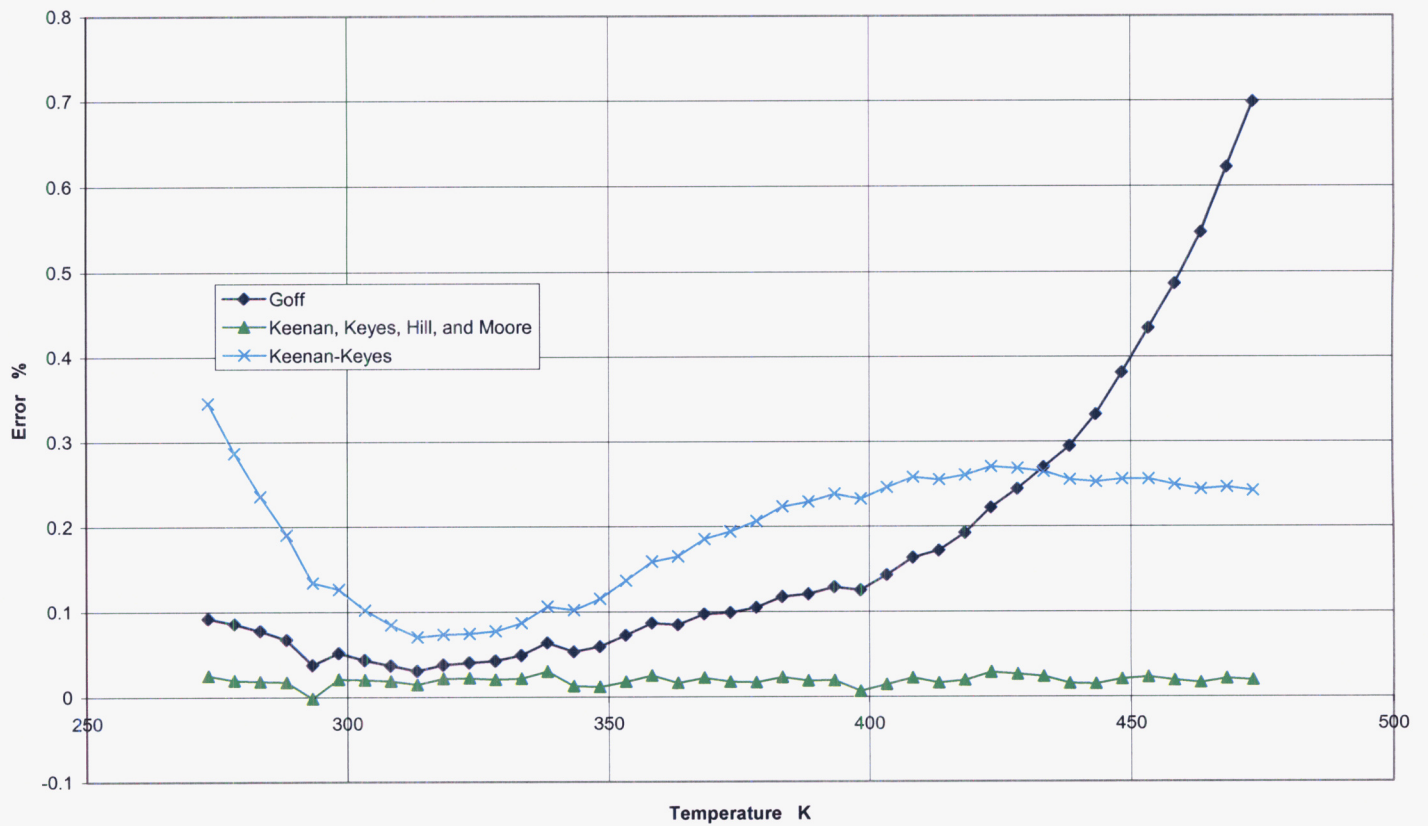
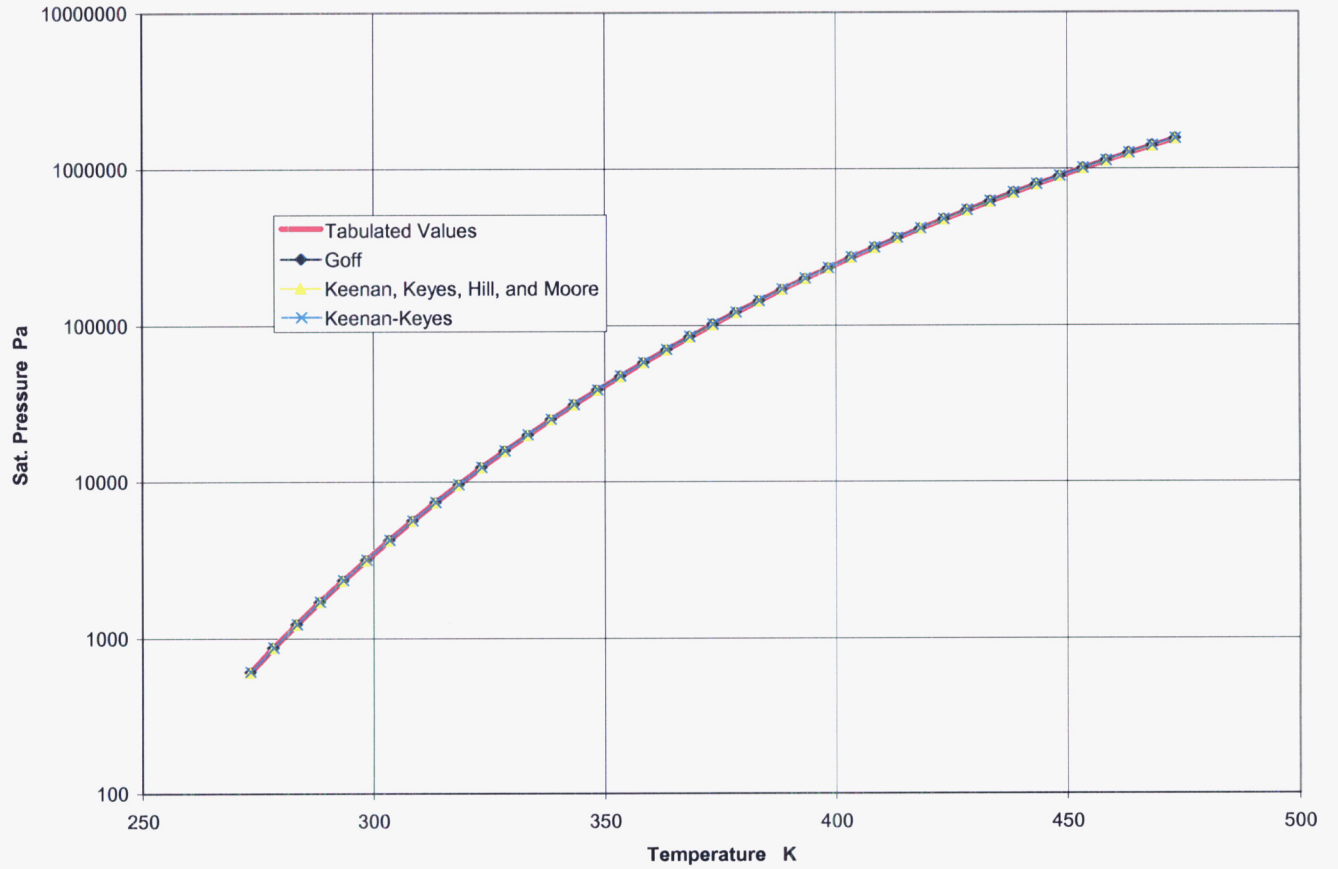
Conclusion/Recommendation

The saturation pressure graph shows that there are no serious deviations from the tabulated values in the recommended temperature range for each correlation. The correlation error graph, however, shows clearly that the Keenan, Keyes, Hill, and Moore correlation is superior to the other two. With current software packages, it is not much more difficult to code that correlation than the other two correlations.

It is recommended that the Keenan, Keyes, Hill, and Moore correlation be used for estimating the saturation pressure of water when the use of the tabulated experimental measurements is inconvenient.

Tabulated Values				Goff (-50°C to 100°C)				Keenan, Keyes, Hill, and Moore (0° to 374°C)				Keenan, Keyes (10° to 150°C)			
T	P _{v,sat}	T	P _{v,sat}	q	P _{v,sat}	P _{v,sat}	Error	t	P _{v,sat}	P _{v,sat}	Error	b	P _{v,sat}	P _{v,sat}	Error
C	kPa	K	Pa	1/K	atm	Pa	%	°C	atm	Pa	%	K	atm	Pa	%
0.01	0.6113	273.16	611.3	1	0.006037	611.863	0.092097	0.01	0.006033082	611.4529	0.025005	374.11	0.006052	613.411	0.345322
5	0.8721	278.15	872.1	0.98206	0.008612	872.848	0.085768	5	0.008606513	872.2701	0.01951	369.12	0.008629	874.5984	0.286483
10	1.2276	283.15	1227.6	0.964718	0.012122	1228.551	0.077465	10	0.012114683	1227.823	0.018171	364.12	0.012141	1230.491	0.235486
15	1.7051	288.15	1705.1	0.947978	0.016835	1706.24	0.066878	15	0.016826788	1705.395	0.017302	359.12	0.016856	1708.349	0.190519
20	2.339	293.15	2339	0.93181	0.023087	2339.88	0.037609	20	0.023078024	2338.958	-0.00181	354.12	0.023109	2342.132	0.133895
25	3.169	298.15	3169	0.916183	0.031284	3170.627	0.051348	25	0.031274455	3169.666	0.021017	349.12	0.031307	3173.004	0.12634
30	4.246	303.15	4246	0.901072	0.041913	4247.833	0.043167	30	0.041902799	4246.849	0.019987	344.12	0.041937	4250.332	0.102032
35	5.628	308.15	5628	0.886451	0.055551	5630.078	0.036928	35	0.055540631	5629.043	0.018532	339.12	0.055577	5632.736	0.084159
40	7.384	313.15	7384	0.872298	0.072879	7386.249	0.030456	40	0.072866911	7385.061	0.014374	334.12	0.072907	7389.165	0.06995
45	9.593	318.15	9593	0.858589	0.094688	9596.625	0.037785	45	0.094672707	9595.079	0.021671	329.12	0.094721	9599.996	0.072925
50	12.349	323.15	12349	0.845304	0.121894	12353.98	0.040319	50	0.121872015	12351.73	0.022096	324.12	0.121935	12358.14	0.074017
55	15.758	328.15	15758	0.832424	0.155547	15764.67	0.042329	55	0.155512524	15761.19	0.020271	319.12	0.155601	15770.15	0.077074
60	19.94	333.15	19940	0.819931	0.19684	19949.72	0.048729	60	0.196786237	19944.29	0.02149	314.12	0.196914	19957.27	0.086615
65	25.03	338.15	25030	0.807807	0.247122	25045.84	0.063286	65	0.247039798	25037.48	0.029898	309.12	0.247228	25056.54	0.106033
70	31.19	343.15	31190	0.796037	0.307908	31206.47	0.052813	70	0.307784428	31193.95	0.01267	304.12	0.308059	31221.74	0.101764
75	38.58	348.15	38580	0.784604	0.380885	38602.71	0.058853	75	0.380705361	38584.49	0.011634	299.12	0.381099	38624.37	0.115017
80	47.39	353.15	47390	0.773496	0.467925	47424.19	0.072153	80	0.467670679	47398.42	0.017774	294.12	0.468224	47454.54	0.136187
85	57.83	358.15	57830	0.762697	0.571109	57879.98	0.086431	85	0.570739467	57844.44	0.024978	289.12	0.571502	57921.74	0.158644
90	70.14	363.15	70140	0.752196	0.692642	70199.28	0.084518	90	0.692169212	70151.35	0.016181	284.12	0.693198	70255.64	0.164863
95	84.55	368.15	84550	0.74198	0.835048	84632.15	0.097164	95	0.834422398	84568.71	0.022129	279.12	0.835783	84706.65	0.185271
100	101.35	373.15	101350	0.732038	1.000988	101450.1	0.09881	100	1.00017224	101367.5	0.017224	274.12	1.001939	101546.6	0.19394
105	120.82	378.15	120820	0.722359	1.193358	120946.8	0.104987	105	1.192307562	120840.4	0.016861	269.12	1.194563	121069	0.20607
110	143.27	383.15	143270	0.712932	1.415278	143438.4	0.117526	110	1.413936779	143302.5	0.022679	264.12	1.416771	143589.7	0.223144
115	169.06	388.15	169060	0.703749	1.670092	169263.8	0.120573	115	1.66839102	169091.4	0.018591	259.12	1.6719	169447	0.228938

120	198.53	393.15	198530	0.694798	1.961378	198785.7	0.12878	120	1.959226397	198567.6	0.018937	254.12	1.963513	199002	0.237768
125	232.1	398.15	232100	0.686073	2.292945	232390	0.124937	125	2.290225478	232114.4	0.006184	249.12	2.295398	232638.6	0.232051
130	270.1	403.15	270100	0.677564	2.668839	270486.9	0.143233	130	2.665398004	270138.1	0.014101	244.12	2.671569	270763.5	0.245659
135	313	408.15	313000	0.669264	3.093347	313510.7	0.163163	135	3.088980926	313068.2	0.021795	239.12	3.096267	313806.6	0.257707
140	361.3	413.15	361300	0.661164	3.570995	361920.3	0.171686	140	3.565437834	361357.1	0.015811	234.12	3.573957	362220.6	0.254789
145	415.4	418.15	415400	0.653258	4.106554	416199.3	0.192411	145	4.099457859	415480.1	0.019272	229.12	4.109332	416480.8	0.260182
150	475.8	423.15	475800	0.645539	4.705044	476856.2	0.221989	150	4.695954148	475935	0.028363	224.12	4.707306	477085.5	0.270176
155	543.1	428.15	543100	0.638001	5.371732	544425	0.243973	155	5.360061992	543242.3	0.026198	219.12	5.373018	544555.3	0.267968
160	617.8	433.15	617800	0.630636	6.112137	619465.1	0.269522	160	6.097136702	617944.8	0.023439	214.12	6.111824	619433.3	0.264376
165	700.5	438.15	700500	0.623439	6.932036	702561.9	0.294343	165	6.912751325	700607.3	0.015324	209.12	6.929301	702284.6	0.254763
170	791.7	443.15	791700	0.616405	7.837464	794327	0.331815	170	7.812694287	791816.6	0.014724	204.12	7.831242	793696.4	0.252166
175	892	448.15	892000	0.609528	8.83472	895398.9	0.381042	175	8.802967022	892180.7	0.020259	199.12	8.823657	894277.7	0.255342
180	1002.1	453.15	1002100	0.602803	9.930374	1006443	0.433426	180	9.889781683	1002329	0.022889	194.12	9.912768	1004659	0.255367
185	1122.7	458.15	1122700	0.596224	11.13127	1128154	0.485798	185	11.07955896	1122913	0.018999	189.12	11.10501	1125493	0.248752
190	1254.4	463.15	1254400	0.589787	12.44453	1261253	0.546336	190	12.37892608	1254604	0.016275	184.12	12.40703	1257452	0.243343
195	1397.8	468.15	1397800	0.583488	13.87758	1406493	0.621878	195	13.794715	1398094	0.021059	179.12	13.82569	1401233	0.245632
200	1553.8	473.15	1553800	0.577322	15.43813	1564654	0.698561	200	15.33396087	1554097	0.01911	174.12	15.36805	1557552	0.241487



3/26/03

STG

Problem:

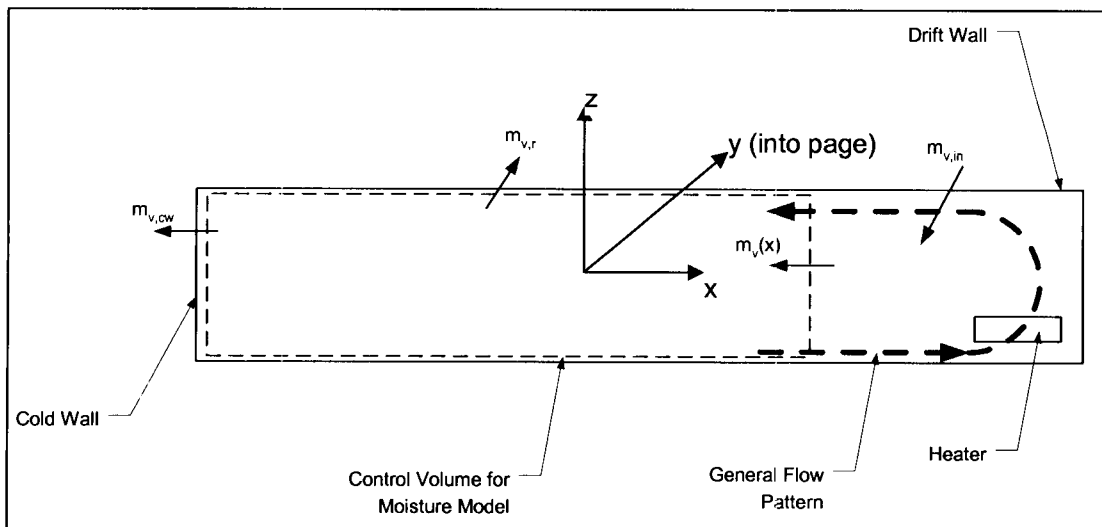
The FLOW-3D® CFD package used to analyze the coldtrap natural convection process does not directly compute the transport of water vapor in the drift. Rather, the CFD analysis predicts the heat and mass transport of air alone due to buoyancy effects.

Required:

Develop a method of using the CFD results of air velocity, temperature, and density to estimate the transport of water vapor in the drift

Solution:

Consider the control volume inside the drift as shown in the figure below



The assumptions underlying this approach are

1. The CFD velocity and thermal predictions for dry air are indicative of those for moist air.
2. The air in the drift is saturated at the local air temperature.
3. The vapor diffusion velocity is much greater than the advection velocity.
4. The thermal effect of evaporation is negligible compared to the dry air heat transfer rates.
5. Water vapor and air both act as ideal gases.

Assumption 1 is simply stating that the air and water vapor are well mixed and there is no slip velocity between these two components.

Assumption 2 is actually a result of assumption 3 and are closely related. This assumption is probably not valid in the area directly over the heater since the vapor will not have enough time to diffuse completely into the hot air from the walls. This analysis is primarily concerned with transport of vapor away from the heater and assumption 2 should be OK 1-2 drift diameters away from the heater.

Assumption 4 does not come into play for the analysis presented below, but is a key assumption in the thermal analysis performed by the CFD code.

Assumption 5 is a typical assumption for thermodynamic calculations of mixture at moderate temperatures. It is shown to be valid for air and water vapor in most engineering thermo texts.

The net mass flow of water vapor into the control volume, m_v , is represented mathematically by

$$m_v(x) = \int_{A_x} c_v \rho u dA \quad (\text{S-1})$$

where c_v = mass concentration of water vapor, ρ = local density, u = local axial velocity component. The integration is carried out over the face of the control volume at the axial location, 'x'.

Following the ideal gas assumption, the mass concentration of water vapor can be expressed as

$$c_v = \left[\left(\frac{P_{v,sat}}{P} - 1 \right) \frac{M_a}{M_v} + 1 \right]^{-1}$$

where $M_a=28.96$ gm/mol and $M_v=18.02$ gm/mol are the molecular weights of air and water vapor, respectively; P = total pressure, $P_{v,sat}$ = saturation pressure of water vapor at the local temperature.

The saturation pressure of water vapor is approximated by the Keenan, Keyes, Hill, and Moore formula (see notebook entry for 3-25-03),

$$\ln(P_{v,sat} / 217.99) = \frac{0.01}{T} (374.136 - t) \left[-741.9242 + \sum_{i=1}^7 F_i (0.65 - 0.01t)^i \right]$$

$$F_1 = -29.72100 \quad F_5 = +0.439993$$

$$F_2 = -11.55286 \quad F_6 = +0.2520658$$

$$F_3 = -0.8685635 \quad F_7 = +0.05218684$$

$$F_4 = +0.1094098$$

In this correlation T is expressed in Kelvin, t is expressed in °C and $P_{v,sat}$ is expressed in atmospheres. All the elements are now defined for carrying out the integration in Eq. (S-1). Because the CFD analysis uses finite volumes and areas for the discrete analysis, the integral in Eq. S-1 is approximated as

$$m_v(x_i) \approx \sum_{k=1}^{N_k} \sum_{j=1}^{N_j} C_v(T_{i,j,k}) \rho(T_{i,j,k}) \mu_{i,j,k} f_{x,i,j,k} \Delta A_{x,i,j,k} \quad (S-2)$$

where f_x = fraction of the computational cell face in the axial direction that is open to flow, ΔA_x = the computational cell face area. (Some of the elemental volumes include both the drift wall and open flow area and the parameter, f_x , describes this flow blockage effect.) As indicated, the summations are carried out over the all the cells in a particular axial plane at $x=x_i$. The number of cells in the transverse direction is N_j , and the number of cells in the vertical direction is N_k .

The indices, i,j,k , refer to the structured grid indices used by FLOW-3D.

Equation (S-2) is an expression of the net mass flow of vapor into the control volume. Part of this mass flow is condensed and returned to the drift wall, m_r , and the remainder is condensed at the cold wall and drained from the drift. The amount of water vapor condensed at the cold wall is estimated by computing m_v at each axial station along the drift and extrapolating the resulting curve to $x=x_{cw}$.

Conclusion/Recommendation:

Equation (S-2) can be coded into a spreadsheet and combined with the FLOW-3D results to estimate the flow of net mass flow water vapor and the condensation rate along the drift wall.

3/27/03

STG

In mid-February, Randy Fedors requested that I review the heat transfer aspects of the Total Performance Assessment (TPA) to support their planned release of a new version of the code. The heat transfer analysis performed by the TPA is described in a document provided by R. Fedors titled "5 NFENV MODULE DESCRIPTION". I assume that this is Section 5 of the TPA Users' Manual. My assignment was to focus on how the TPA computes the waste package temperature from the input data describing the thermal properties of the rock, invert, drift air, and waste package materials.

3/27/03

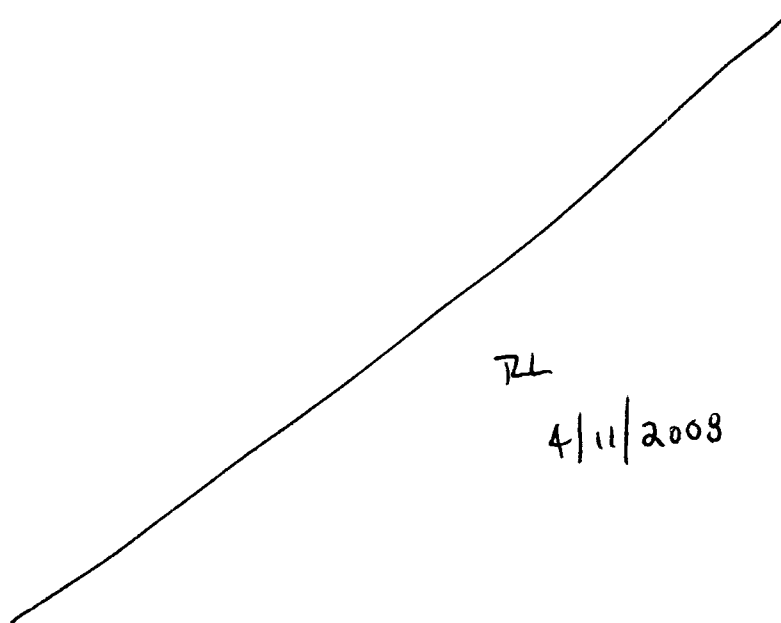
STG

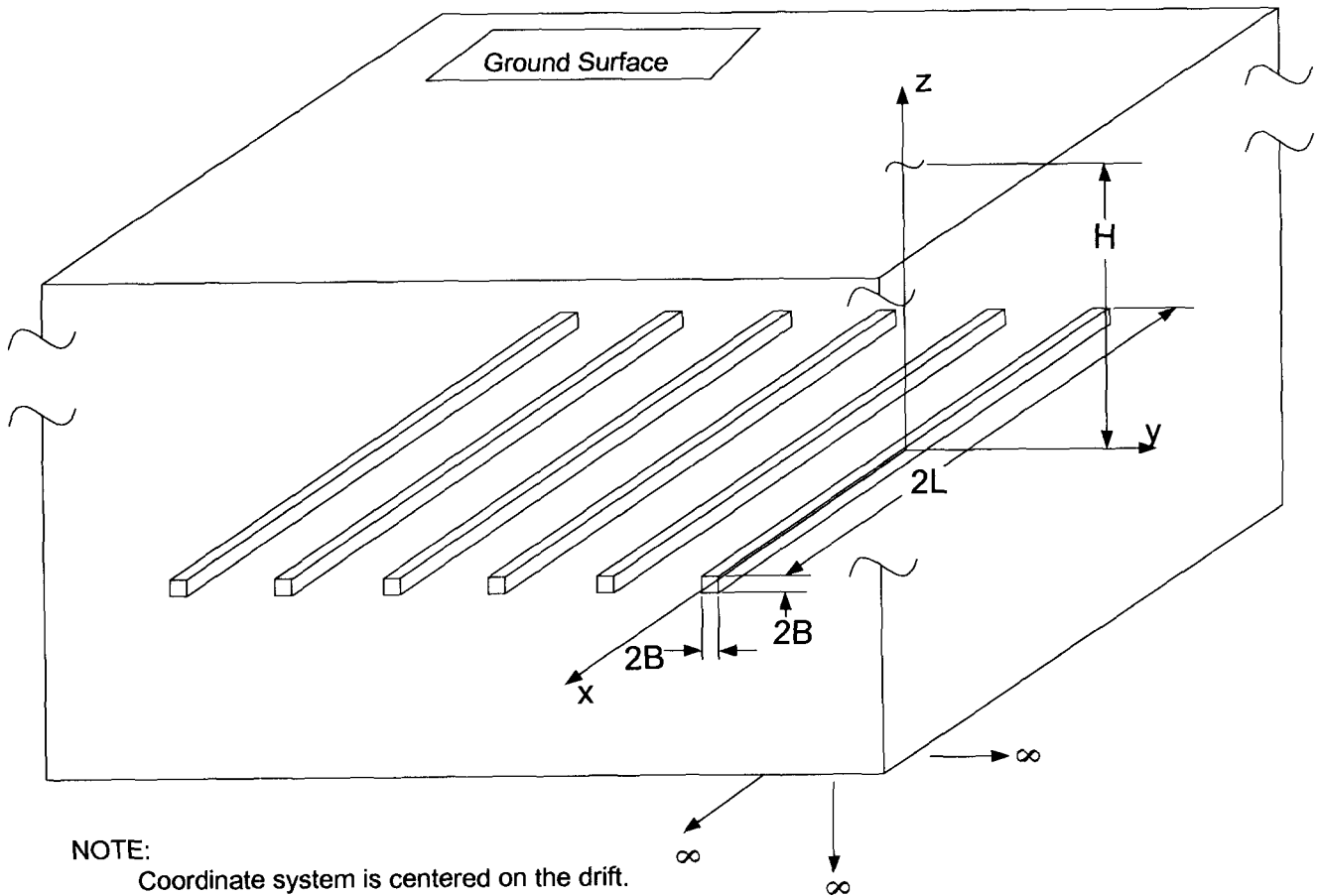
Problem:

The waste packages will be stored end-to-end in long drifts excavated underground. The long drifts are parallel. The underground situation is idealized as shown in the figure below.

Required:

Derive an equation that expresses the three-dimensional temperature field in the ground at any time after the waste packages are installed.



**NOTE:**

Coordinate system is centered on the drift.
 Drift center is at H below the ground.
 Domain extends to infinity in the $\pm x$, $\pm y$, and $-z$ directions

Solution:

Several simplifying assumptions will be made to make the problem tractable:

1. The waste packages are closely spaced in the drifts and that the heat is liberated uniformly along the drift length.
2. The ground properties are uniform throughout the domain and are not temperature dependent.
3. The ground surface temperature is uniform and constant for all times.
4. The drift has a square section.

According to Carslaw and Jaeger and Özişik,

Carslaw, H. S., and Jaeger, J. C., **Conduction of Heat in Solids**, 2nd ed., Clarendon Press, Oxford.

Özişik, M. N., **Heat Conduction**, John Wiley and Sons, Inc., New York, 1993.

the assumptions result in the problem being linear and the principle of superposition can be applied to this problem. That is, the thermal response at a specific location in the ground to the heat liberated from a single drift alone can be derived. The results of this calculation for multiple drifts (accounting for the coordinate system transformations in each case) can then be summed to yield the net thermal response to the heat liberated from multiple drifts.

A Green's Function (no relation, ha!) can be applied to this problem. The general expression for the solution is given by Özişik (pp. 214-251),

$$\begin{aligned}
 T(x, y, z, t) = & \iiint G(x, y, z, t | x', y', z', t') \Big|_{t'=0} T_{init}(x', y', z') dx' dy' dz' \\
 & + \frac{\alpha}{k} \int_{t'=0}^t \left\{ \iiint G(x, y, z, t | x', y', z', t') g(x', y', z', t') dx' dy' dz' \right\} dt' \\
 & + \alpha \int_{t'=0}^t \left\{ \sum_{i=1}^N \iint \left(\frac{\partial G(x, y, z, t | x', y', z', t')}{\partial n_i} \right)_{s_i} f_i(x', y', z', t') dA' \right\} dt'
 \end{aligned} \tag{1}$$

where

$G(x, y, z, t | x', y', z', t')$ = Green's function representing the response at position (x, y, z) to an instantaneous source pulse at time t' , located at position (x', y', z') . The units of G are L^{-3} (e.g. m^{-3})

$T_{init}(x, y, z)$ = initial temperature distribution at $t=0$.

$g(x, y, z, t)$ = volumetric heat source distribution (energy per unit volume)

α = ground thermal diffusivity

k = ground thermal conductivity

$f(x,y,z,t)$ = surface temperature

n = normal direction for the domain boundaries

The three terms in Eq. (1) have the following physical significance:

Term 1 represents the effect that the diffusion of the initial energy distribution has on the transient solution. For this analysis, we will assume that there is a initial uniform temperature within the domain. If we set $T_i=0$ everywhere in Eq.(1), then the left side of Eq. (1) is the temperature difference between the initial temperature and the local temperature at position (x,y,z) at time, t .

Term 2 represents the diffusion of energy from a heat source located within the domain. This form of the solution allows for the heat source to be both spatially and temporally dependent.

Term 3 is the diffusion of energy from each of the boundary faces of the domain. The form for the third term shown in Eq. (1) is for the specification of a boundary temperature through the function, f_i . Alternate forms for the third term can be developed for heat flux or convective boundary conditions. We will assume here that the ground surface temperature is constant and uniform at $f(x,y,z=H,t) = T_i(x,y,z) = 0$.

Under these special boundary conditions, the method of images described by Carslaw and Jaeger (p. 273) can be used here to include the boundary condition at $z=H$ into the second term. Consider an energy source of equal magnitude but opposite sign (i.e. an energy sink) sink located at $z=2H$ in a domain that went to $z=\infty$ instead of $z=H$. . The integral in the second term would thus include both sources. The antisymmetry of the two sources would ensure that the temperature at $z=H$ would remain at its initial value.

So, the solution to the domain temperature is reduced to the single term,

$$T(x,y,z,t) = \frac{\alpha}{k} \int_{t'=0}^t \left\{ \int_{z'=-\infty}^{+\infty} \int_{y'=-\infty}^{+\infty} \int_{x'=-\infty}^{+\infty} G(x,y,z,t|x',y',z',t') g(x',y',z',t') dx' dy' dz' \right\} dt' \tag{2}$$

For the infinite solid, the appropriate Green's function is

$$\begin{aligned}
 G(x, y, z, t | x', y', z', t') = & \left[\frac{1}{2\sqrt{\pi\alpha(t-t')}} \exp\left(-\frac{(x-x')^2}{4\alpha(t-t')}\right) \right] \\
 & \times \left[\frac{1}{2\sqrt{\pi\alpha(t-t')}} \exp\left(-\frac{(y-y')^2}{4\alpha(t-t')}\right) \right] \\
 & \times \left[\frac{1}{2\sqrt{\pi\alpha(t-t')}} \exp\left(-\frac{(z-z')^2}{4\alpha(t-t')}\right) \right]
 \end{aligned} \tag{3}$$

Similarly, the principle of separation of variables can be applied to the source term,

$$g(x, y, z, t) = q(t)g_x(x)g_y(y)g_z(z) \tag{4}$$

where

$q(t)$ = uniform volumetric heat generation over the drift volume, $2L \times 2B \times 2B$

$$g_x(x) = \begin{cases} 0 & -\infty < x < -L \\ 1 & -L \leq x \leq +L \\ 0 & L < x < +\infty \end{cases}$$

$$g_y(y) = \begin{cases} 0 & -\infty < y < -B \\ 1 & -B \leq y \leq +B \\ 0 & B < y < +\infty \end{cases}$$

$$g_z(z) = \begin{cases} 0 & -\infty < z < -B \\ 1 & -B \leq z \leq +B \\ 0 & +B < z < 2H - B \\ -1 & 2H - B \leq z \leq 2H + B \\ 0 & 2H + B < z < +\infty \end{cases}$$

Continuing to follow the scheme of separation of variables, Eq. (2) can now be rewritten as

$$\begin{aligned}
T(x, y, z, t) = \frac{\alpha}{k} \int_0^t q(t') & \left\{ \int_{-\infty}^{+\infty} g_x(x') \frac{1}{2\sqrt{\pi\alpha(t-t')}} \exp\left(-\frac{(x-x')^2}{4\alpha(t-t')}\right) dx' \right. \\
& \times \int_{-\infty}^{+\infty} g_y(y') \frac{1}{2\sqrt{\pi\alpha(t-t')}} \exp\left(-\frac{(y-y')^2}{4\alpha(t-t')}\right) dy' \\
& \left. \times \int_{-\infty}^{+\infty} g_z(z') \frac{1}{2\sqrt{\pi\alpha(t-t')}} \exp\left(-\frac{(z-z')^2}{4\alpha(t-t')}\right) dz' \right\} dt'
\end{aligned} \tag{5}$$

or, simplify the notation to

$$T(x, y, z, t) = \frac{\alpha}{k} \int_0^t q(t') I_x I_y I_z dt' \tag{6}$$

Consider the first of the three spatial integrals,

$$I_x = \int_{-\infty}^{+\infty} g_x(x') \frac{1}{2\sqrt{\pi\alpha(t-t')}} \exp\left(-\frac{(x-x')^2}{4\alpha(t-t')}\right) dx' = \frac{1}{2\sqrt{\pi\alpha(t-t')}} \int_{-L}^{+L} \exp\left(-\frac{(x-x')^2}{4\alpha(t-t')}\right) dx' \tag{7}$$

Substitute

$$\beta = \frac{x-x'}{\sqrt{4\alpha(t-t')}} \qquad d\beta = -\frac{1}{\sqrt{4\alpha(t-t')}} dx'$$

into Eq. 7,

$$\begin{aligned}
I_x &= -\frac{1}{\sqrt{\pi}} \int_{\frac{x+L}{\sqrt{4\alpha(t-t')}}}^{\frac{x-L}{\sqrt{4\alpha(t-t')}}} \exp(-\beta^2) d\beta \\
&= \frac{1}{\sqrt{\pi}} \int_0^{\frac{x-L}{\sqrt{4\alpha(t-t')}}} \exp(-\beta^2) d\beta - \frac{1}{\sqrt{\pi}} \int_0^{\frac{x-L}{\sqrt{4\alpha(t-t')}}} \exp(-\beta^2) d\beta \\
&= \frac{1}{2} \left[\operatorname{erf}\left(\frac{L+x}{\sqrt{4\alpha(t-t')}}\right) + \operatorname{erf}\left(\frac{L-x}{\sqrt{4\alpha(t-t')}}\right) \right]
\end{aligned} \tag{8}$$

Similarly,

$$I_y = \frac{1}{2} \left[\operatorname{erf}\left(\frac{B+y}{\sqrt{4\alpha(t-t')}}\right) + \operatorname{erf}\left(\frac{B-y}{\sqrt{4\alpha(t-t')}}\right) \right] \tag{9}$$

Finally, the third integral, I_z , must be broken up into two intervals to cover both the source and the sink. The logic is identical to that used in the first two integrals to yield,

$$I_z = \frac{1}{2} \left[\operatorname{erf}\left(\frac{B+z}{\sqrt{4\alpha(t-t')}}\right) + \operatorname{erf}\left(\frac{B-z}{\sqrt{4\alpha(t-t')}}\right) + \operatorname{erf}\left(\frac{z-(2H+B)}{\sqrt{4\alpha(t-t')}}\right) + \operatorname{erf}\left(\frac{(2H-B)-z}{\sqrt{4\alpha(t-t')}}\right) \right] \tag{10}$$

Finally, the complete solution is given by

$$\begin{aligned}
T(x, y, z, t) &= \frac{\alpha}{8k} \int_0^t q(t') \left\{ \left[\operatorname{erf}\left(\frac{L+x}{\sqrt{4\alpha(t-t')}}\right) + \operatorname{erf}\left(\frac{L-x}{\sqrt{4\alpha(t-t')}}\right) \right] \right. \\
&\quad \times \left[\operatorname{erf}\left(\frac{B+y}{\sqrt{4\alpha(t-t')}}\right) + \operatorname{erf}\left(\frac{B-y}{\sqrt{4\alpha(t-t')}}\right) \right] \\
&\quad \left. \times \left[\operatorname{erf}\left(\frac{B+z}{\sqrt{4\alpha(t-t')}}\right) + \operatorname{erf}\left(\frac{B-z}{\sqrt{4\alpha(t-t')}}\right) + \operatorname{erf}\left(\frac{z-(2H+B)}{\sqrt{4\alpha(t-t')}}\right) + \operatorname{erf}\left(\frac{(2H-B)-z}{\sqrt{4\alpha(t-t')}}\right) \right] \right\} dt'
\end{aligned}$$

(11)

Now, consider the idealized condition that the heat source is a thin strip of width $2B$ at $z=0$. The functions $g_x(x)$, and $g_y(y)$ remain as described above, but the function $g_z(z)$ becomes

$$g_z(z) = \delta(0) - \delta(2H) \quad (12)$$

where δ is the Dirac delta function, defined as $\delta(z) = 1$ at $z=z'$ and $\delta(z) = 0$ elsewhere. In this application, the units of δ are L^{-1} . The integral of a function multiplied by the Dirac delta is defined as

$$\int_{-\infty}^{+\infty} f(z')\delta(z_1)dz' = f(z_1)$$

Now the z-integral, I_z becomes

$$\begin{aligned} I_z &= \frac{1}{\sqrt{4\pi\alpha(t-t')}} \left\{ \int_{-\infty}^{+\infty} \exp\left[-\frac{(z-z')^2}{4\alpha(t-t')}\right] \delta(0) dz' - \int_{-\infty}^{+\infty} \exp\left[-\frac{(z-z')^2}{4\alpha(t-t')}\right] \delta(2H) dz' \right\} \\ &= \frac{1}{\sqrt{4\pi\alpha(t-t')}} \left\{ \exp\left[\frac{-z^2}{4\alpha(t-t')}\right] - \exp\left[\frac{-(z-2H)^2}{4\alpha(t-t')}\right] \right\} \end{aligned} \quad (13)$$

Going another step further, if we now consider a pure line source in which all the heat is generated in a line along the x-axis, the function $g_y(y)$ becomes,

$$g_y(y) = \delta(0) \quad (14)$$

The y-spatial integral is now expressed as

$$I_y = \frac{1}{\sqrt{4\pi\alpha(t-t')}} \int_{-\infty}^{+\infty} \exp\left[-\frac{(y-y')^2}{4\alpha(t-t')}\right] \delta(0) dy' = \frac{1}{\sqrt{4\pi\alpha(t-t')}} \exp\left[\frac{-y^2}{4\alpha(t-t')}\right] \quad (15)$$

We can now use the various forms of the spatial integrals to arrive at temperature responses to heat sources distributed throughout a volume, a planar strip (in either the $z=0$ plane or the $y=0$ plane), and a line along the x-axis.

Case 1: Volumetric heat source distributed over the range, $-L \leq x \leq L$, $-B \leq y \leq B$, $-B \leq z \leq B$

$$\begin{aligned}
T(x, y, z, t) = \frac{\alpha}{8k} \int_0^t q_{3D}(t') & \left\{ \left[\operatorname{erf} \left(\frac{L+x}{\sqrt{4\alpha(t-t')}} \right) + \operatorname{erf} \left(\frac{L-x}{\sqrt{4\alpha(t-t')}} \right) \right] \right. \\
& \times \left[\operatorname{erf} \left(\frac{B+y}{\sqrt{4\alpha(t-t')}} \right) + \operatorname{erf} \left(\frac{B-y}{\sqrt{4\alpha(t-t')}} \right) \right] \\
& \times \left[\operatorname{erf} \left(\frac{B+z}{\sqrt{4\alpha(t-t')}} \right) + \operatorname{erf} \left(\frac{B-z}{\sqrt{4\alpha(t-t')}} \right) + \operatorname{erf} \left(\frac{z-(2H+B)}{\sqrt{4\alpha(t-t')}} \right) + \operatorname{erf} \left(\frac{(2H-B)-z}{\sqrt{4\alpha(t-t')}} \right) \right] \left. \right\} dt'
\end{aligned} \tag{16}$$

where $q_{3D}(t) = q_{\text{wastepackage}}(t)/(8LB^2)$ (units of energy per unit volume)

Case 2: Planar heat source at $z=0$, distributed over the range, $-L \leq x \leq L$, $-B \leq y \leq B$

$$\begin{aligned}
T(x, y, z, t) = \frac{\alpha}{8k\sqrt{\pi\alpha}} \int_0^t q_{2D}(t') & \left\{ \left[\operatorname{erf} \left(\frac{L+x}{\sqrt{4\alpha(t-t')}} \right) + \operatorname{erf} \left(\frac{L-x}{\sqrt{4\alpha(t-t')}} \right) \right] \right. \\
& \times \left[\operatorname{erf} \left(\frac{B+y}{\sqrt{4\alpha(t-t')}} \right) + \operatorname{erf} \left(\frac{B-y}{\sqrt{4\alpha(t-t')}} \right) \right] \\
& \times \left[\frac{1}{\sqrt{(t-t')}} \left\{ \exp \left[\frac{-z^2}{4\alpha(t-t')} \right] - \exp \left[\frac{-(z-2H)^2}{4\alpha(t-t')} \right] \right\} \right] \left. \right\} dt'
\end{aligned} \tag{17}$$

where $q_{2D}(t) = q_{\text{wastepackage}}(t)/(4LB)$ (units of energy per unit area)

Case 3: Linear heat source at $z=0$, $y=0$ distributed over the range, $-L \leq x \leq L$

$$\begin{aligned}
 T(x, y, z, t) = & \frac{1}{8k\pi} \int_0^t q_{1D}(t') \left\{ \left[\operatorname{erf} \left(\frac{L+x}{\sqrt{4\alpha(t-t')}} \right) + \operatorname{erf} \left(\frac{L-x}{\sqrt{4\alpha(t-t')}} \right) \right] \right. \\
 & \times \left[\exp \left[\frac{-y^2}{4\alpha(t-t')} \right] \right] \\
 & \times \left[\frac{1}{\sqrt{(t-t')}} \left\{ \exp \left[\frac{-z^2}{4\alpha(t-t')} \right] - \exp \left[\frac{-(z-2H)^2}{4\alpha(t-t')} \right] \right\} \right] \left. \right\} dt'
 \end{aligned}
 \tag{18}$$

where $q_{1D}(t) = q_{\text{wastepackage}}(t)/(2L)$ (units of energy per unit length)

Conclusion/Recommendation:

The underground temperature response to a single drift as represented by Eq. 17 agrees with the equation described in Section 5 (NFENV MODULE DESCRIPTION) of the TPA Users' Manual.

=====

====

Entries made into Scientific Notebook #536E for the period September 2002, to April 3, 2002, have been made by Steven Green (April 3, 2003).

No original text or figures entered into this Scientific Notebook has been removed

STG 04/03/2003

=====

====

5/07/03 *STG*

This entry is to document some CFD analyses that were accomplished to support the theoretical and experimental investigations of the coldtrap phenomenon. This work was included in a report of the overall coldtrap activities but not recorded in his notebook.

Problem:

Some drifts in the repository may not be completely filled with waste packages. This could result in there being a long section of a drift between the last waste package in a line and the endwall of the drift. If a long thermal convection cell is set up between the waste packages and the endwall, moisture will be carried with the hot air toward the cold end of the drift, where it will then condense.

As a precursor to the analysis and experiments of the complete thermal and moisture transport phenomenon, a simplified 2-D theoretical solution to the Navier-Stokes and fluid energy equations was developed by Frank Dodge. In that analysis, the scenario was idealized as flow between tunnel endwalls of different temperatures with the tunnel walls being perfectly insulated. That analysis is described in F. Dodge's MathCAD sheet submitted in Scientific Notebook #432, Volume VII, page 59 (maintained by Randy Fedors) ; Frank's MathCAD sheet was renamed and saved on S. Green's desktop computer as

C:\Projects\div20\Notebook\notebook_5-7-03\FTD_model_exp.mcd)

Required:

Prepare a 3-D computational fluid dynamics (CFD) solution equivalent of the 2-D analysis to establish mutual confidence in the theory-based 2-D approach and the 3-D CFD approach to modeling the coldtrap phenomenon.

Solution:

The computer program FLOW-3D was used for this study. Version 8.0.1 of this code installed on a LINUX server in Div. 18 (server name: 18bdb.div18.swri.edu). The installation validation of this code version is described in memo from S. Green to B. Mabrito, dated 25 September 2003.

The FLOW-3D input file for this simulation is listed here (the file is also contained in S. Green's desktop computer as

C:\Projects\div20\Notebook\notebook_5-7-03\prepin.3d-hotwallf)

++++
+

3D, Actual Test Setup, Coldtrap Experiment

Cylinder Version of Test run of analytical solution derived by Frank Dodge

```

$xput
  ipdis=1,    remark=' initial hydrostatic pressure distribution',
  ifenrg=3,   remark=' solve for internal energy and temperature',
  ifrho=1,    remark=' evaluate density from temperature ',
  itb=0,      remark=' no free surface ',
  nmat=1,     remark=' one fluid',
  iwsh=1,     remark=' include wall shear ',
  gz=-9.807,  remark=' gravity in -z-direction',
  delt=0.001, remark=' initial time step size ',
  twfin=100.0, remark=' final time',
  prtdt=100.0, remark=' only print at end of calculaiton ',
  pltdt=10.,  remark=' modified to plot at ten intermediate times ',
  ihtc=1,     remark=' evaluate wall heat transfer ',
  impvis=1,   imphtc=1,
$end
$limits
  ilpr=2, irpr=2,
  jfpr=2, jbkpr=2,
  kbpr=2, ktpr=2,
$end
$props
  remark=' equation of state parameters for air',
  cv1=770.,   remark=' specific heat ',
  rhof=1.18,  remark=' density ',
  thc1=0.026, remark=' conductivity',
  mui=1.85e-05, remark=' viscosity set to give the ',
               remark=' correct prandtl number ',
  thexf1=3.33e-03, remark=' thermal expansion coefficient ',
  tstar=300., remark=' reference temperature for thermal',
               remark=' expansion',
$end
$bcdata
  remark=' walls on physical edges of the box ',
  wl=2,
    tbc(1)=295., remark=' constant left boundary temperature',
  wr=2,
    tbc(2)=305., remark=' constant right boundary temperature',
  wf=2,
    rwall(3)=0.0, remark=' insulated front boundary ',
  wbk=2,
    rwall(4)=0.0, remark=' insulated back boundary',

  wb=2,
    rwall(5)=0.0, remark=' insulated bottom boundary ',
  wt=2,
    rwall(6)=0.0, remark=' insulated top boundary',

$end
$mesh

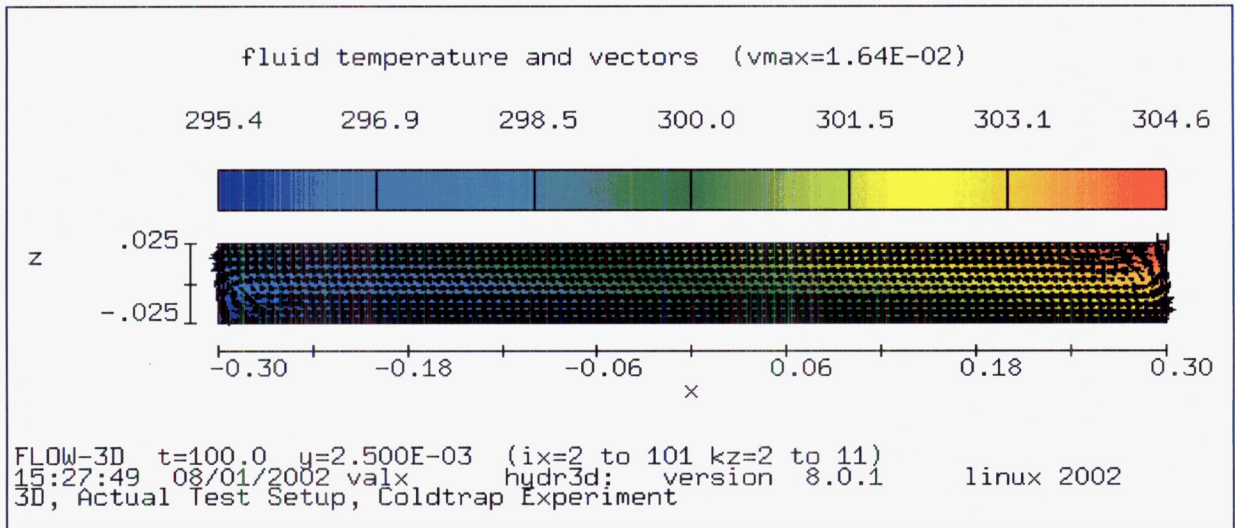
```

```

    remark=' define a simple, uniform mesh ',
    px(1)=-0.30, py(1)=-0.025, pz(1)=-0.025,
    px(2)= 0.30, py(2)= 0.025, pz(2)= 0.025,
    nxcelt=50, nycelt=20,  nzcelt=20,
$end
$obs
    nob=1,
    cc(1)= 6.25e-04, cy2=-1., cz2=-1.,
$end
$fl
    flht=1.0,
$end
$bf
$end
$temp
    remark=' start from uniform temperature ',
    tempi=300.,
$end
$grafic
    remark=' place a history probe close to upper right corner of rectangle ',
    xloc(1)=0.25, zloc(1)=0.02, yloc(1)=0.02,
    nvplts=5,    remark='5 velocity vector plots ',
    contpv(1)='tn',    remark=' fluid temperature vertical mid-plane',
    yv1(1)=0.0, yv2(1)=0.0,
    contpv(2)='tn',    remark=' fluid temperature horizontal mid-plane',
    zv1(2)=0.0, zv2(2)=0.0,
    contpv(3)='tn',    remark=' fluid temperature horizontal tunnel cross-section',
    xv1(3)=-0.02, xv2(3)=-0.02,
    contpv(4)='tn',    remark=' fluid temperature horizontal tunnel cross-section',
    xv1(4)=0., xv2(4)=0.,
    contpv(5)='tn',    remark=' fluid temperature horizontal tunnel cross-section',
    xv1(5)=0.2, xv2(5)=0.2,
$end
$parts
$end
+++++
+++++

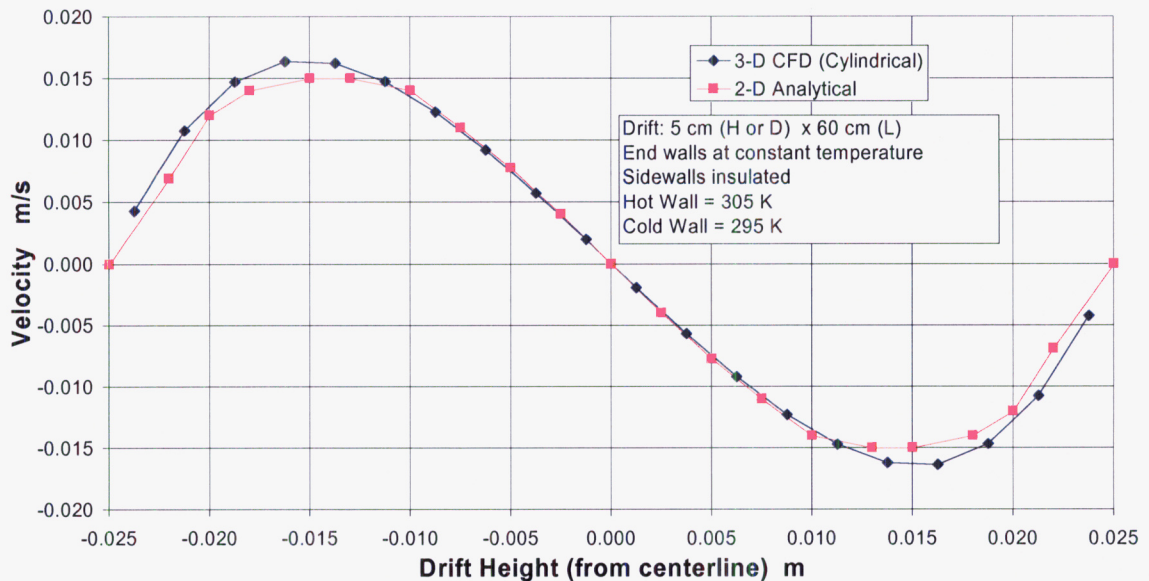
```

The results obtained with FLOW-3D for the fluid temperature and velocity are shown in the following graphic (created with the graphic processor as part of the FLOW-3D package)



In this figure the length dimensions are meters and the temperature is Kelvin. This shows that a single long convection cell is established between the two end walls as predicted by the 2-D theory described above. The warmer air travels along the top of the drift from the hot wall to the cold wall and returns from the cold wall to the hot wall along the bottom of the drift.

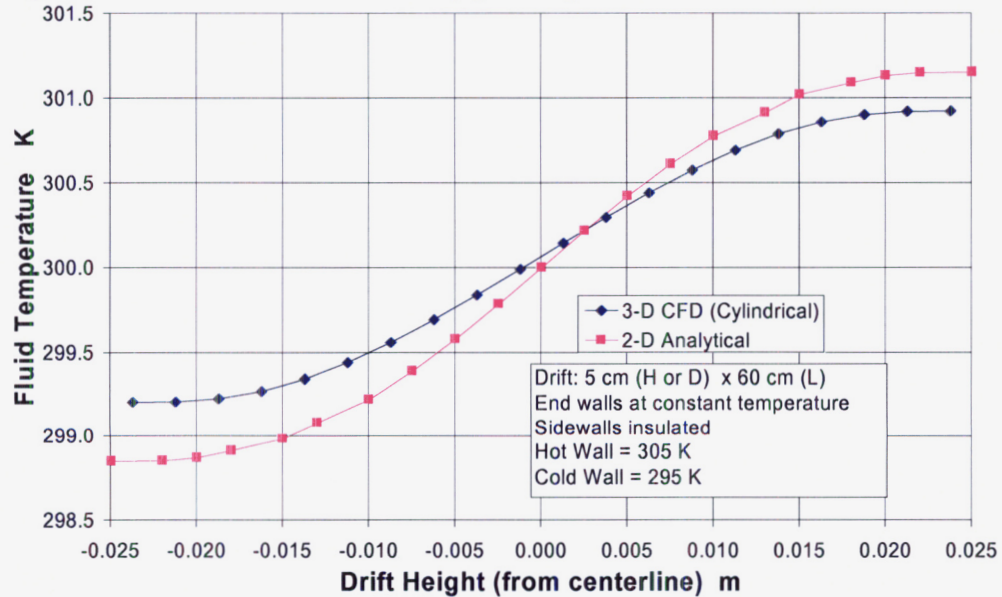
The predicted air velocity from the 2-D theory and the 3-D CFD analyses are directly compared here.



This graph shows the horizontal velocity profile along a vertical line at the center of the drift near the midway point between the two end walls. The peak velocity magnitude predicted by the 2-D theory is slightly greater than that predicted by the 3-D CFD

simulation. The position of the velocity peak is also slightly different. Nonetheless, this is considered to be excellent agreement between the two predictions.

The temperature profile at this same position is shown in the following graph. The temperature difference from top to bottom of the drift is predicted by the 2-D theory to be slightly greater than is predicted by the 3-D CFD simulation. This is expected given the difference in the ratio of endwall surface area to enclosed volume between the two models. Again, this is considered to be very good agreement between the two sets of



predictions.

9/30/03

STG

The computer files in which this scientific notebook are kept was reorganized by S. Green such that Notebook updates are separated into different directories. References to file names made in entries prior to 5/7/03 should be modified to reflect this. The file path for entries prior to 5/7/03 is shown as

C:\Projects\div20\Notebook\

The file path has been updated to

C:\Projects\div20\Notebook\notebook_5-7-03

9/30/03 *STG*

This entry is to document some analyses that were accomplished to support the review of the models used in the TPA Code as of May 2003.

**Analysis of Heat Transfer Processes from Waste Package to Rock Wall
including Comments on
Section 5, "NFENV MODULE DESCRIPTION" of the TPA Users' Manual**

INTRODUCTION

Nuclear waste packages are placed end-to-end in long underground vaults or tunnels as shown schematically in Figure 1.

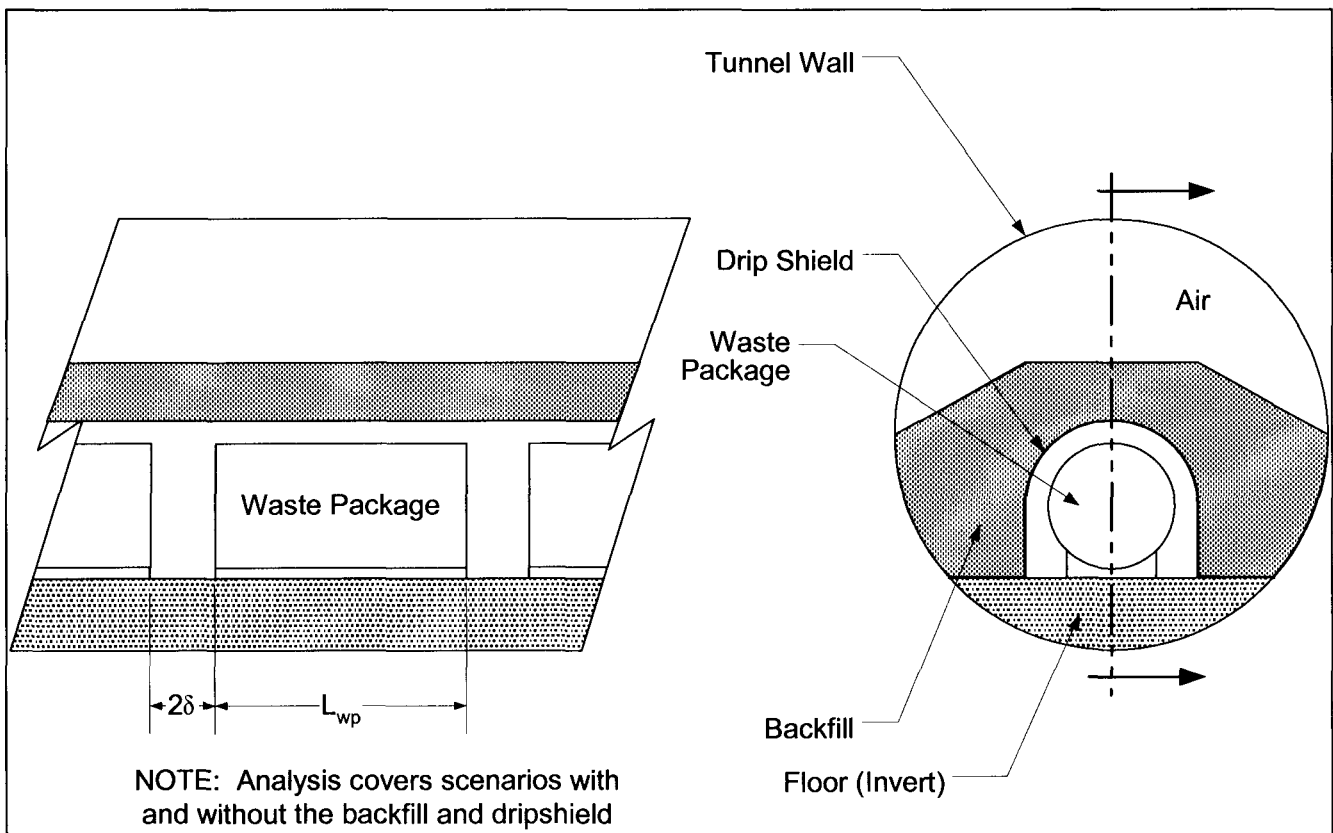


Figure 1. Sketch of Waste Packages in Tunnel.

The rock wall temperature is computed from a separate large-scale mathematical model of the entire tunnel system in the mountain. In that analysis, the tunnels are idealized as nominally linear heat sources that cause the underground rock strata to thermally respond over many hundreds of years.

The objective of this analysis is to define a method of estimating the waste package temperature. The tunnel wall temperature is given as a function of time by the mountain-scale model. The waste package temperature, however, is computed at each instant

using a steady state approach. This follows from the assumption that the thermal response of the tunnel internal structures (waste package, floor, drip shield, backfill, etc.) is much faster than the surrounding rock. This basic approach is in agreement with that taken in the TPA Users' manual although it is not so explicitly stated.

It could be argued that it is desirable to take a conservative approach and bias the analysis to produce predicted waste package temperatures that are greater than those likely to be experienced. The waste package temperature, however, will be a significant factor in the drift moisture analysis and the waste package corrosion assessment. As such, it is not prudent to overestimate the temperatures since too high a temperature might place the waste package in a condition wherein the waste package is too dry and the corrosion is underestimated. So, a careful analysis is needed to prevent overly conservative predictions.

The following references are cited in this report:

Incropera, F. P. and DeWitt, D. P., ***Fundamentals of Heat and Mass Transfer***, 2nd Edition, John Wiley and Sons, New York, 1985.

Raithby, G. D. and Hollands, K. G. T., "A General Method of Obtaining Approximate Solutions to Laminar and Turbulent Heat Transfer Problems," in Irvine, T. F. and Hartnett, J. P., eds., ***Advances in Heat Transfer***, Vol. 11, Academic Press, New York, 1975, pp 265-315.

Kuehn, T. H. and Goldstein, R. J., "An Experimental Study of Natural Convection Heat Transfer in Concentric and Eccentric Horizontal Cylindrical Annuli," ***ASME Journal of Heat Transfer***, Vol. 100, November 1978m pp. 635-640.

Lowry, W., "Atlas Natural Convection Test Plan," Report No. SITP0-02-EBS-002 Rev 00, Bechtel SAIC Company, January 2002.

Siegel, R. and Howell, J. R., ***Thermal Radiation Heat Transfer***, Hemisphere Publishing Corporation, Washington, D. C., 1992.

ASSUMPTIONS

A list of the modeling assumptions will be maintained here for easy access and summarization:

1. The rock wall temperature and waste package heat generation change slowly with respect to the thermal response of the waste package structures.
2. Material properties are constant and uniform.
3. Axial variations in temperature and heat flux are negligible.
4. Temperature is uniform over the entire waste package surface.
5. All surfaces are gray-diffuse emitters of thermal radiation.
6. Drip shield thermal resistance is negligible compared to other components in the tunnel.

Following the 2-D assumption, the analysis is further simplified by assuming that all components are radially oriented and centered on the tunnel centerline. This is shown schematically in Figure 2.

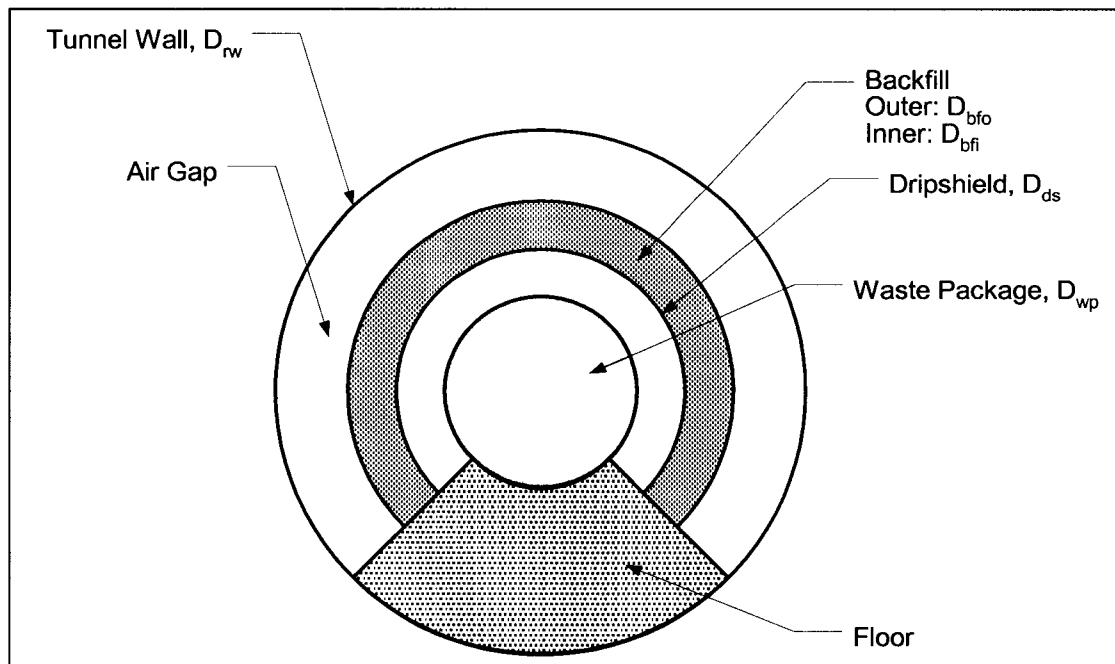


Figure 2. Radial 2-D Model for Tunnel Heat Transfer Analysis

NOTE: The effects of the drip shield and backfill are considered in separate scenarios

Several scenarios are considered for different configurations of the internal components:

- Case 1 – Only the waste package is in the tunnel; there is no drip shield or backfill. The waste package rests on the floor and can ‘see’ the tunnel walls.
- Case 2 – The waste package is in the tunnel and is covered by a drip shield. The waste package rests on the floor and can ‘see’ the drip shield but not the tunnel walls. The drip shield can ‘see’ the tunnel walls.
- Case 3 – The waste package is covered by a drip shield that is itself covered by backfill. There is an air gap between the backfill and the in the tunnel. The waste package rests on the floor and can ‘see’ the drip shield but not the tunnel walls. The backfill can ‘see’ the tunnel walls.

Each case is considered separately.

CASE 1

An electrical circuit analog to this heat transfer situation is shown on Figure 3.

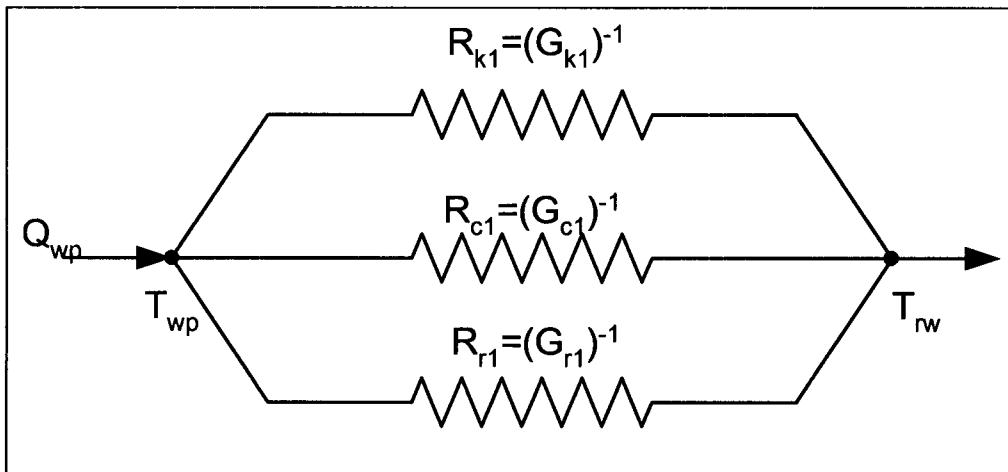


Figure 3. Electrical Analogy for Tunnel Heat Transfer without Drip Shield or Backfill

Figure 3 highlights the assumed scenario in which the waste package heat is transferred to the rock wall through three parallel paths. The 'resistors' in this circuit represent the resistance to heat transfer in the respective paths

R_{k1} – conduction through the floor

R_{c1} – convection across the air gap

R_{r1} – radiation directly from the waste package to the rock wall

The heat generated by a single waste package Q_{wp} is assumed to be spread along its unit length consisting of the length of the waste package and the gap between one waste package and the next. This is the same as taking the total heat generated by all waste packages and spreading it over the entire length of the line of packages.

Following this electrical analog, the heat transfer rate can be defined as

$$Q_{wp} = \left[\frac{1}{R_{k1}} + \frac{1}{R_{c1}} + \frac{1}{R_{r1}} \right] (T_{wp} - T_{rw}) = [G_{k1} + G_{c1} + G_{r1}] (T_{wp} - T_{rw}) \quad (1)$$

where the 'G' terms are thermal conductance values, the inverse of thermal resistance. The '1' in the subscripts refers to values for Case 1.

Conduction

The heat transfer by conduction through the tunnel floor can be estimated in this radial 2-D model as described in many basic engineering heat transfer texts (e.g., Incropera and Dewitt).

$$q_k'' = k_{floor} \frac{\partial T}{\partial r} \quad (2)$$

where q_k'' = radial heat flux, k_{floor} = thermal conductivity of floor material, T = local temperature. Eq. (2) can be integrated over the surface area through which the conduction heat transfer occurs along a radial direction to yield,

$$Q_{wp,k} = \frac{2\pi(L_{wp} + 2\delta)(1 - f_c)k_{floor}}{\ln\left(\frac{D_{rw}}{D_{wp}}\right)}(T_{wp} - T_{rw}) = G_{k1}(T_{wp} - T_{rw}) \quad (3)$$

where

$Q_{wp,k}$ = heat transfer rate by conduction (units of Energy/time)

L_{wp} = waste package length

2δ = distance between waste packages

f_c = fraction of waste package cylindrical surface available for convection and radiation

k_{floor} = thermal conductivity of floor material

D_{rw} = inner diameter of tunnel wall

D_{wp} = outer diameter of waste package

T_{wp} = waste package temperature

T_{rw} = tunnel wall temperature

G_{k1} = effective conductance for conduction heat transfer path (Case 1)

A typical value for G_{k1} can be found by assuming the following hypothetical scenario,

$$D_{wp} = 1.5 \text{ m}, \quad D_{rw} = 5 \text{ m}, \quad L_{wp} + 2\delta = 3 \text{ m}, \quad f_c = 0.75,$$

$$k_{floor} = 0.2 \text{ watt/m}\cdot\text{K}$$

The resulting value is $G_{k1} = 0.78$

NOTE

Eq. (3) agrees with the corresponding equation in the current version of the TPA Users' Manual.

Convection

The convective heat transfer across the air gap between the waste package and the rock wall (or the drip shield when it is in place) is driven by buoyancy forces causing the air to circulate. Engineering texts and the technical literature describe many ways of computing the convective heat transfer. Raithby and Hollands describe a technique for evaluating the natural convection heat transfer between concentric cylinders in which the heat transfer rate per unit length is given by the following correlation,

$$q' = \frac{2\pi k_{eff}}{\ln\left(\frac{D_o}{D_i}\right)} (T_i - T_o) \quad (4)$$

where k_{eff} = effective thermal conductivity of the circulating medium, D_o = outer cylinder inside diameter, D_i = inner cylinder outer diameter, T_o = outer cylinder inner surface temperature, and T_i = inner cylinder outer surface temperature. Recall that for conduction heat transfer in the radial direction,

$$Q = q'' A_i = \frac{2k_{eff} A_i}{D_i \ln\left(\frac{D_o}{D_i}\right)} (T_i - T_o) \quad (5)$$

For the tunnel, $A_i = f_c \pi D_{wp} (L_{wp} + 2\delta)$. So, Eq. (4) can be adapted to this scenario as

$$Q_{wp,c} = \frac{2\pi f_c (L_{wp} + 2\delta) k_{eff}}{\ln\left(\frac{D_{rw}}{D_{wp}}\right)} (T_{wp} - T_{rw}) \quad (6)$$

In the nomenclature of Eq. (1), the convection conductance for this case is

$$G_{c1} = \frac{2\pi f_c (L_{wp} + 2\delta) k_{eff}}{\ln\left(\frac{D_{rw}}{D_{wp}}\right)} \quad (7)$$

Raithby and Hollands define the effective thermal conductivity as

$$k_{eff} = k_{fluid} \left[0.386 \left(\frac{Pr}{0.861 + Pr} \right)^{0.25} \right] Ra_c^{0.25} \quad (8)$$

where k_{fluid} = fluid thermal conductivity, Pr = fluid Prandtl Number, and Ra_c is a modified Rayleigh Number,

$$Ra_c = \frac{\left[\ln \left(\frac{D_{rw}}{D_{wp}} \right) \right]^4}{(D_{rw} - D_{wp})^3 (D_{rw}^{-0.6} + D_{wp}^{-0.6})^5} Ra_{gap} \quad (9)$$

The air gap Rayleigh Number, Ra_{gap} is defined as

$$Ra_{gap} = \frac{\rho^2 g \beta Pr}{\mu^2} (D_{rw} - D_{wp})^3 (T_{wp} - T_{rw}) \quad (10)$$

It should be noted that the Raithby and Hollands correlation described here is valid for the Rayleigh Number range, $10^2 < Ra_{gap} < 10^7$

Kuehn and Goldstein report an alternate calculation procedure for estimating the natural convection heat transfer that is more complicated than the one described here. That method, however, includes a calculation for the bulk average air temperature in the gap, but still requires an iterative solution involving the unknown waste package temperature. The goal here is to remove the need for iterations (without sacrificing much in the way of accuracy); so, we will keep using the slightly simpler Raithby and Hollands method.

It is instructive to combine Eqs. (8), (9), and (10) to demonstrate the parameters affecting the value of k_{eff} ,

$$k_{eff} = 0.386 \left[\frac{\ln \left(\frac{D_{rw}}{D_{wp}} \right)}{(D_{rw}^{-0.6} + D_{wp}^{-0.6})^{1.25}} \right] k_{fluid} \left[\frac{\rho^2 g \beta Pr^2}{(0.861 + Pr) \mu^2} \right]^{0.25} (T_{wp} - T_{rw})^{0.25} \quad (11)$$

The term in the first set of brackets is related to the geometric properties of the model, the next two factors are related to the fluid properties, which should be evaluated at some bulk average temperature between the temperature of the rock wall and the waste package. Finally, the effective thermal conductivity is affected by the last factor in Eq.(11), the one-quarter power of the temperature across the gap. Clearly, the effective thermal conductivity is a highly non-linear function of the waste package temperature which means that the convective part of the overall heat transfer rate will require an iterative approach.

Reasonable approximations to the properties of air are given by the following relations,

$$\rho = \frac{P}{RT} \quad \text{ideal gas assumption} \quad (12)$$

$$\beta = \frac{1}{T} \quad \text{ideal gas assumption} \quad (13)$$

$$\mu = 3.8 \times 10^{-8} T + 7.8 \times 10^{-6} \quad T \text{ in Kelvin, } \mu \text{ in Pa}\cdot\text{sec} \quad (14)$$

$$k = 6.3 \times 10^{-5} T + 8.5 \times 10^{-3} \quad T \text{ in Kelvin, } k \text{ in watt/m}\cdot\text{K} \quad (15)$$

$$Pr = 0.702 \quad (\text{constant within 0.2\% over temperature range}) \quad (16)$$

The correlations for μ , k , and Pr are valid over the temperature range $350\text{K} < T < 700\text{K}$.

To understand the magnitude of the possible variations in the effective thermal conductivity and convection conductance with respect to the waste package temperature, consider the following hypothetical case for the tunnel geometry and the rock wall temperature,

$$T_{rw} = 100^{\circ}\text{C}, D_{rw}=5 \text{ m}, D_{wp}=1.5 \text{ m}, f_c=0.75$$

Define the temperature at which fluid properties are to be defined as the average of the waste package and rock wall temperatures. The results of these sample calculations are summarized in Table 1

Table 1. Effective Thermal Conductivity of a Drift Air Gap

$T_{wp}, ^{\circ}\text{C}$	$k_{eff}, \text{ watt}/(\text{m}\cdot\text{K})$	$G_{c1}, \text{ watt}/\text{K}$
150	2.00	23.5
350	2.81	33.1
550	3.07	36.1
750	3.17	37.2

These results show that the effective thermal conductivity is a relatively weak function of the fluid temperature. In light of this it might be advantageous to eliminate the need for an iterative solution by simply approximating the basis temperature for thermal properties as some constant value above the rock wall temperature. The choice of this approximate temperature difference can be made after some trial calculations are made.

Typical waste package peak heat generation rates described by Lowry are listed in Table 2. Each of these values has been used in conjunction with a range of plausible rock wall temperatures in the complete procedure described in Eqs. (6)-(11) above to estimate the waste package temperature. Conduction and radiation have been neglected in these example calculations. The results listed in Table 2 show that the

**Table 2. Reference Temperature Estimates for use in Eq. (11)
(assumes Q_{wp} is by convection heat transfer only)**

Waste Package	Q_{wp} (peak) watt	T_{rw} (assumed) $^{\circ}\text{C}$	$T_{wp}-T_{rw}$ (computed) $^{\circ}\text{C}$	Mean ΔT $^{\circ}\text{C}$	Mean G_{c1} watt/K
5-DHLW-Long	2	25	0.30	0.31	6.4
		100	0.31		
		200	0.33		
5-DHLW-Short	31	25	2.6	2.8	11.0
		100	2.8		
		200	3.0		
44-BWR	600	25	28.6	30.4	19.8
		100	30.4		
		200	32.3		
21-PWR	1380	25	56.4	59.9	23.1
		100	59.8		
		200	63.5		

The calculations required for obtaining the results shown in Table 1 and 2 were performed in Excel. The Excel file is maintained in S. Green's desktop computer as C:\Projects\div20\Notebook\notebook_10-2-03\WP_Drift_HT.xls.

These results show that the waste package temperature, and hence the air temperature is a nearly constant value greater than the wall temperature for a given waste package heat generation rate. The air temperature is a strong function of the waste package heat generation rate. This suggests that the following shortcuts to the computation procedure can be adopted,

$$T_{fluid} - T_{rw} = 0.5(0.043Q_{wp} + 1.67) \quad (17)$$

$$T_{wp} - T_{rw} = 0.043Q_{wp} + 1.67 \quad (18)$$

In both these expressions, Q_{wp} is expressed in watts and the temperatures are in Kelvin. Eq. (18) is used to provide a reasonable estimate for the last factor in Eq. (11) and Eq. (17) is used as the estimated reference temperature for the fluid property correlations in Eqs. (12)-(15). Eqs. (17) and (18) essentially pre-estimate the waste package and air temperatures based on the waste package heat generation rate before these values are computed by the overall method. Using Eqs (17) and (18) in conjunction with Eqs. (11) and (7) provide a way of computing the convection thermal conductance without the need to iterate on the waste package and air temperatures. It has been shown that this procedure introduces some slight error in the predictions, but this is hopefully outweighed by the elimination of the iterative solution required by the more accurate procedure.

It is important to note that the correlations of Eq. (17) and (18) do not include the effects of conduction and radiation. The combined effects of all three modes, described below, will alter the coefficients in these two equations.

The computed values of G_{c1} are included in Table 1 and Table 2 as a comparison to the conduction and radiation conductance values. These results show that the heat transfer from the waste package via convection is predicted to be over an order of magnitude greater than by conduction through the floor.

NOTE

Eq. (6) agrees with the corresponding equation in the TPA Users' Manual.

Eqs. (11)-(18) provide a means of computing the value of k_{eff} from the boundary and initial conditions rather the specifying a fixed value for the entire analysis time period.

Radiation

If we keep to the assumption of a purely 2-D geometry, then the only surface that we can consider for radiative exchange with the tunnel wall is the cylindrical barrel of the waste package. As in the case of the convection heat transfer, we will assume that all of the radiation heat transfer occurs over the cylindrical length, $L_{wp} + 2\delta$, assigned as the unit length for a single waste package.

As the first step in the radiation heat transfer analysis, the radiation configuration factors for this scenario are defined. By inspection, the configuration factor for radiation from the waste package to the wall is

$$F_{wp-rw} = 1 \quad (19)$$

From the reciprocity relation of configuration factor algebra,

$$A_{wp}F_{wp-rw} = A_{rw}F_{rw}$$

$$F_{rw-wp} = F_{wp-rw} \frac{f_c \pi D_{wp} L_{wp}}{f_c \pi D_{rw} L_{wp}}$$

$$F_{rw-wp} = \frac{D_{wp}}{D_{rw}} \quad (20)$$

Finally, the rules of configuration factor algebra state that

$$F_{rw-wp} + F_{rw-rw} = 1 \quad (\text{the wall can 'see' part of itself})$$

$$F_{rw-rw} = 1 - \frac{D_{wp}}{D_{rw}} \quad (21)$$

The general relation for radiation exchange in an enclosure with gray-diffuse surfaces is given by Siegel and Howell,

$$\sum_{j=1}^N \left(\frac{\delta_{jk}}{\varepsilon_j} - F_{k-j} \frac{1-\varepsilon_j}{\varepsilon_j} \right) \frac{Q_j}{A_j} = \sum_{j=1}^N F_{k-j} \sigma (T_k^4 - T_j^4) \quad (22)$$

where Q_j = net heat transfer into surface j

A_j = surface area for surface j

ε_j = emissivity of surface j

σ = Stefan-Boltzmann constant = 5.67×10^{-8} watt/m²/K⁴

F_{k-j} = configuration factor for surface k to surface j

T_k = temperature of surface k

T_j = temperature of surface j

δ_{kj} = Kronecker delta = 1 for $k=j$, otherwise $\delta_{kj}=0$

N = number of surfaces

Eq. (22) is applied to all the surfaces, k , in the enclosure resulting in a set of N equation in N unknowns. Some of the unknowns are surface temperature and some are heat transfer rates.

For the waste package in the tunnel, there are two equations that can be formed. These are written here in their full form:

Waste Package:

$$\left[\frac{1}{\varepsilon_{wp}} - F_{wp-wp} \frac{1 - \varepsilon_{wp}}{\varepsilon_{wp}} \right] \frac{Q_{wp,r}}{A_{wp}} + \left[-F_{wp-rw} \frac{1 - \varepsilon_{rw}}{\varepsilon_{rw}} \right] \frac{Q_{rw,r}}{A_{rw}} = F_{wp-wp} \sigma (T_{wp}^4 - T_{wp}^4) + F_{wp-rw} \sigma (T_{wp}^4 - T_{rw}^4) \quad (23)$$

Rock Wall:

$$\left[-F_{rw-wp} \frac{1 - \varepsilon_{wp}}{\varepsilon_{wp}} \right] \frac{Q_{wp,r}}{A_{wp}} + \left[\frac{1}{\varepsilon_{rw}} - F_{rw-rw} \frac{1 - \varepsilon_{rw}}{\varepsilon_{rw}} \right] \frac{Q_{rw,r}}{A_{rw}} = F_{rw-wp} \sigma (T_{rw}^4 - T_{wp}^4) + F_{rw-rw} \sigma (T_{rw}^4 - T_{rw}^4) \quad (24)$$

The subscript 'r' in $Q_{wp,r}$ and $Q_{rw,r}$ is used in these equations to highlight the fact that we are considering on the portion of the total waste package heat transfer rate that is attributable to radiation.

Eliminate the terms that are zero from each equation,

$$\frac{1}{\varepsilon_{wp}} \frac{Q_{wp,r}}{A_{wp}} - F_{wp-rw} \frac{1 - \varepsilon_{rw}}{\varepsilon_{rw}} \frac{Q_{rw,r}}{A_{rw}} = F_{wp-rw} \sigma (T_{wp}^4 - T_{rw}^4) \quad (25)$$

$$-F_{rw-wp} \frac{1 - \varepsilon_{wp}}{\varepsilon_{wp}} \frac{Q_{wp,r}}{A_{wp}} + \left[\frac{1}{\varepsilon_{rw}} - F_{rw-rw} \frac{1 - \varepsilon_{rw}}{\varepsilon_{rw}} \right] \frac{Q_{rw,r}}{A_{rw}} = F_{rw-wp} \sigma (T_{rw}^4 - T_{wp}^4) \quad (26)$$

The term, $Q_{rw,r}$, can be eliminated between these two equations resulting in a single expression that can be solved for T_{wp} :

$$\frac{Q_{wp,r}}{A_{wp}} = \frac{\sigma (T_{wp}^4 - T_{rw}^4)}{\frac{1}{\varepsilon_{wp}} + \frac{D_{wp}}{D_{rw}} \frac{1 - \varepsilon_{rw}}{\varepsilon_{rw}}} \quad (27)$$

Recall that the heat transfer rate, $Q_{wp,r}$, is spread over the area, $A_{wp} = f_c \pi D_{wp} (L_{wp} + 2\delta)$. Now solve for the radiation heat transfer,

$$Q_{wp,r} = \frac{\sigma(T_{wp}^4 - T_{rw}^4) f_c \pi (L_{wp} + 2\delta)}{\frac{1}{D_{wp}\epsilon_{wp}} + \frac{1}{D_{rw}\epsilon_{rw}}} = G_{r1}(T_{wp} - T_{rw}) \quad (28)$$

where the conductance for radiation heat transfer is given by,

$$G_{r1} = \frac{\sigma f_c \pi (L_{wp} + 2\delta)}{\frac{1}{D_{wp}\epsilon_{wp}} + \frac{1}{D_{rw}\epsilon_{rw}}} (T_{wp}^2 + T_{rw}^2)(T_{wp} + T_{rw}) \quad (29)$$

As in the case of the convection heat transfer conductance, this value is a function of the waste package temperature.

The temperature terms in Eq. (29) can be linearized as follows to eliminate the dependence on the waste package temperature. Make the substitution, $T_{wp} = T_{rw} + \Delta T$,

$$(T_{wp}^2 + T_{rw}^2)(T_{wp} + T_{rw}) = 4T_{rw}^3 + 6T_{rw}^2\Delta T + 4T_{rw}\Delta T^2 + \Delta T^3 \quad (30)$$

One could argue that for small ΔT , only the first term in eq. (30) is significant, resulting in

$$(T_{wp}^2 + T_{rw}^2)(T_{wp} + T_{rw}) \approx 4T_{rw}^3 \quad (31)$$

Alternately, consider the results presented above for the convection heat transfer analysis of the example waste packages. Those results showed that

$$\left. \frac{\Delta T}{T_{rw}} \right)_{max} \approx \frac{60K}{300K} = 0.2 \quad (32)$$

Using this as an upper bound on ΔT , in Eq. (30) yields

$$(T_{wp}^2 + T_{rw}^2)(T_{wp} + T_{rw}) \approx 5.368T_{rw}^3 \quad (33)$$

So, appreciable error can be introduced by not including some estimate of the waste package temperature in the linearization if there is a large temperature difference between the rock wall and the waste package.

As an example of this procedure, consider the sample problem described above for the convection heat transfer case. Include in this list of sample values

$$\epsilon_{rw} = 0.8, \quad \epsilon_{wp} = 0.8$$

Considering only the radiation heat transfer effects, the radiation thermal conductance values are estimated as shown in Table 3.

**Table 3. Example Radiation Thermal Conductance Values
(assumes Q_{wp} is by radiation heat transfer only)**

Waste Package	Q_{wp} (peak) watt	T_{rw} (assumed) °C	T_{wp} (computed) °C	G_{r1} (actual) watt/K	G_{r1} (linearized) watt/K
5-DHLW-Long	2	27	27.0	49.0	49.0
		100	100.0	94.2	94.2
		200	200.0	192.1	192.1
5-DHLW-Short	31	27	27.6	49.2	49.0
		100	100.3	94.3	94.2
		200	200.2	192.2	192.1
44-BWR	600	27	38.6	51.9	49.0
		100	106.2	96.6	94.2
		200	203.1	194.0	192.1
21-PWR	1380	27	51.9	55.4	49.0
		100	113.9	99.6	94.2
		200	207.0	196.4	192.1

The calculations required for obtaining the results shown in Table 3 were performed in Excel. The Excel file is maintained in S. Green's desktop computer as C:\Projects\div20\Notebook\notebook_10-2-03\WP_Drift_HT.xls.

These results show that if the entire waste package heat loss is by radiation only, the waste package temperatures will be close to those of the rock wall. The thermal conductance values for radiation are greater than those for convection, indicating that most of the heat transfer from the package will be by thermal radiation. This is not surprising given the fact that natural convection is a poor heat transfer mode. Finally, the linearization used in Eq. (31) is reasonable since the temperature differences are small.

NOTE

Eq. (29) does not agree with the corresponding equation in the TPA Users' Manual. There is a discrepancy in the $L_{wp}+2\delta$ terms in the denominator of Eq. (29)

Combined Heat Transfer Modes

In the example calculations described above for the single mode convection and radiation heat transfer, it was shown that considerable errors could be introduced in the linearized solutions for situations with large waste package to rock wall temperature differences. To fully examine this condition, this case should be analyzed with all three modes acting simultaneously.

The complete combined mode solution is obtained by the following procedure

1. Specify values for Q_{wp} and T_{rw}

2. Compute G_{k1} using Eq. (3)
3. Assume a value for T_{wp} ($T_{rw} + 20^\circ\text{C}$ is a reasonable first choice)
4. Compute k_{eff} from Eq. (11) using air properties evaluated at a temperature of $T_{fluid} = 0.5(T_{wp} + T_{rw})$
5. Compute G_{c1} using Eq. (7)
6. Compute G_{r1} using Eq. (29)
7. Compute a new value of T_{wp} using Eq.(1)
8. Repeat steps 4-7 until T_{wp} converges sufficiently

Conversely, the linearized solution is obtained by the following shorter procedure:

1. Specify values for Q_{wp} and T_{rw}
2. Compute G_{k1} using Eq. (3)
3. Assume a value for T_{wp} for use in Eq. (11) ($T_{rw} + 20^\circ\text{C}$ is reasonable)
4. Compute k_{eff} using air properties evaluated at a temperature of T_{rw}
5. Compute G_{c1} using Eq. (7)
6. Compute G_{r1} using Eq. (31)
7. Compute the value of T_{wp} using Eq.(1)

To compare these two procedures the following geometric and property values are used

$$D_{wp} = 1.5 \text{ m}$$

$$D_{rw} = 5 \text{ m}$$

$$L_{wp} + 2\delta = 3 \text{ m}$$

$$f_c = 0.75$$

$$k_{floor} = 0.2 \text{ watt/m}\cdot\text{K}$$

$$\varepsilon_{rw} = 0.8$$

$$\varepsilon_{wp} = 0.8$$

Eqs. (12)-(16) are used for air properties

The values shown above for D_{wp} and $L_{wp} + 2\delta$ are used for all the waste packages even though the actual values are different. These are example calculations only for purposes of demonstrating the computation procedure results.

The results of these calculations for four typical waste packages are listed in Table 4. First, it is clear that thermal radiation is the dominant heat transfer mode in Case 2. The values of G_{r1} are much greater than G_{c1} , even for low T_{rw} values. Second, the computed values of T_{wp} are less than 20°C different than the assumed rock wall temperature. As a

result of these low temperature differences, the linearized solution is a good representation of the complete, but iterative, solution.

Table 4. Heat Transfer Analysis for Case 1 - Complete and Linearized Solutions

Waste Package	Q_{wp} watt	T_{rw} K	Complete (Iterative) Solution				Linearized Solution			
			G_{c1} watt/K	G_{r1} watt/K	G_{k1} watt/K	T_{wp} K	G_{c1} watt/K	G_{r1} watt/K	G_{k1} watt/K	T_{wp} K
5-DHLW-Long	2	300	4.1	49.0	0.8	300.0	19.5	49.0	0.8	300.0
		373	3.2	94.2	0.8	373.0	18.0	94.2	0.8	373.0
		473	2.5	192.1	0.8	473.0	16.5	204.6	0.8	473.0
5-DHLW-Short	31	300	7.9	49.1	0.8	300.5	19.5	49.0	0.8	300.5
		373	6.3	94.3	0.8	373.3	18.0	94.2	0.8	373.3
		473	5.0	192.2	0.8	473.2	16.5	204.6	0.8	473.1
44-BWR	600	300	15.9	51.2	0.8	308.9	19.5	49.0	0.8	308.7
		373	13.0	96.3	0.8	378.5	18.0	94.2	0.8	378.3
		473	10.3	193.9	0.8	475.9	16.5	204.6	0.8	475.7
21-PWR	1380	300	19.0	53.8	0.8	318.9	19.5	49.0	0.8	320.1
		373	15.8	98.8	0.8	385.0	18.0	94.2	0.8	385.3
		473	12.6	196.1	0.8	479.6	16.5	204.6	0.8	479.2

For Linearized Solution:

Air properties use the rock wall temp as reference.

G_{c1} assumes a $\Delta T = 20^\circ C$.

G_{r1} uses $4T_{rw}^3$ instead of complete temperature term.

The calculations required for obtaining the results shown in Table 4 were performed in Excel. The Excel file is maintained in S. Green's desktop computer as C:\Projects\div20\Notebook\notebook_10-2-03\WP_Drift_HT.xls.

Recommendation

For the scenario described here for Case 1 the linearized approach is adequate for calculating the waste package temperature in a single calculation step.

CASE 2

In this case, there is a drip shield over the waste package which blocks direct communication across the air gap between the waste package and the rock wall. There is still a direct conductive heat transfer path between the package and the wall through the floor.

An electrical circuit analog to this heat transfer situation is shown on Figure 4.

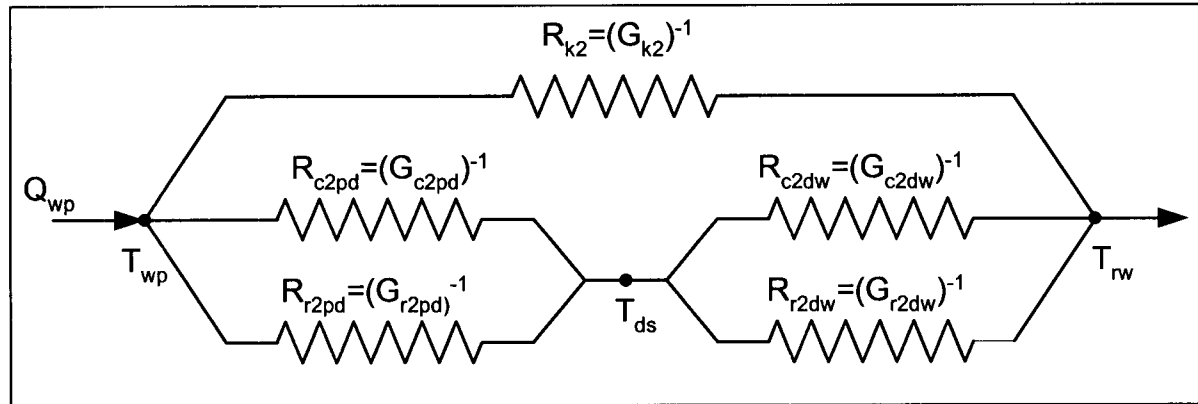


Figure 4. Electrical Analogy for Tunnel Heat Transfer with Drip Shield

Figure 4 highlights the assumed scenario in which the waste package heat is transferred to the rock wall through parallel paths; one of which is complicated by the presence of the drip shield. The 'resistors' in this circuit represent the resistance to heat transfer in the respective paths

- R_{k2} – conduction through the floor
- R_{c2pd} – convection between package and drip shield
- R_{r2pd} – radiation between package and drip shield
- R_{c2dw} – convection between drip shield and wall
- R_{r2dw} – radiation between drip shield and wall
- R_{rc2} – combined radiation and convection between the waste package and wall through the drip shield

The heat generated by a single waste package Q_{wp} is assumed to be spread along its unit length consisting of the length of the waste package and the gap between one waste package and the next. This is the same as taking the total heat generated by all waste packages and spreading it over the entire length of the line of packages.

Following this electrical analog, the heat transfer rate can be defined as

$$Q_{wp} = [R_{k2}^{-1} + R_{rc2}^{-1}] (T_{wp} - T_{rw}) = [G_{k2} + G_{rc2}] (T_{wp} - T_{rw})$$

$$Q_{wp} = \left\{ G_{k2} + \left[\frac{1}{G_{c2pd} + G_{r2pd}} + \frac{1}{G_{c2dw} + G_{r2dw}} \right]^{-1} \right\} (T_{wp} - T_{rw}) \tag{34}$$

where the 'G' terms are thermal conductance values, the inverse of thermal resistance. The '2' in the subscript refers to values for Case 2. G_{rc2} is the effective thermal conductance for the complete heat transfer path from the waste package to the wall through the drip shield.

The drip shield temperature can be computed as well from the relation

$$Q_{wp} - G_{k2}(T_{wp} - T_{rw}) = (G_{c2dw} + G_{r2dw})(T_{ds} - T_{rw}) = (G_{c2pd} + G_{r2pd})(T_{wp} - T_{ds}) \tag{35}$$

The thermal resistance of the drip shield itself is negligible compared to the other resistances. A sample calculation is shown below

IMPORTANT NOTE:

The thermal circuit described in Figure 4 does not agree with the apparent approach adopted by the TPA Users' Manual. In the TPA User's Manual the convection and radiation paths across the air gaps are each put in series independently of the combinatorial effect of the drip shield. This is depicted in Figure 5. In addition, the radiation mode of heat transfer is in considered only between the waste package and the drip shield. It will be shown that radiation is the dominant mode of heat transfer and neglecting the effects of radiation between the drip shield and the wall is significant.

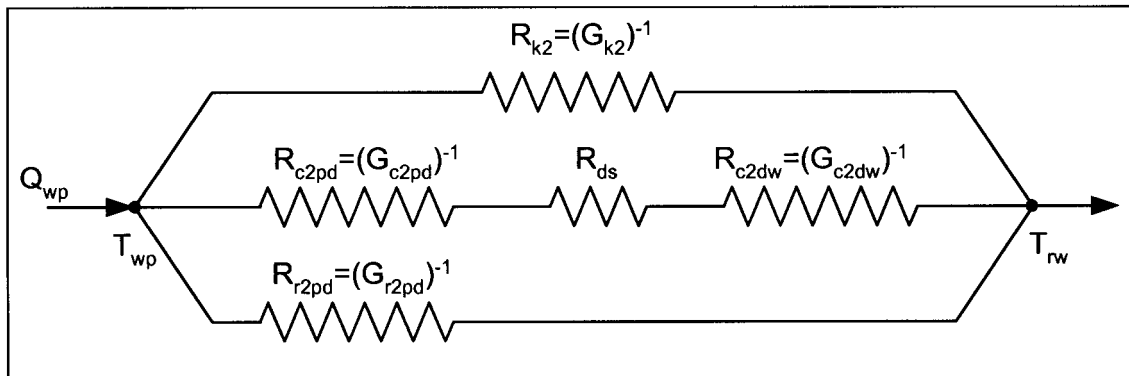


Figure 5. Electrical Analogy for Tunnel Heat Transfer with Dripshield used in the TPA Users' Manual (INCORRECT)

Conduction through Floor

The conduction heat transfer through the floor in Case 2 is identical to that of Case 1,

$$G_{k2} = G_{k1} = \frac{2\pi(L_{wp} + 2\delta)(1 - f_c)k_{floor}}{\ln\left(\frac{D_{rw}}{D_{wp}}\right)} \quad (36)$$

Convection

There is convection heat transfer between the waste package and the drip shield and between the drip shield and the rock wall. Each of these processes can be analyzed similarly to that described above for Case 1. By inspection, the pertinent equations can be written as

$$G_{c2pd} = \frac{2\pi f_c(L_{wp} + 2\delta)k_{eff2,pd}}{\ln\left(\frac{D_{ds}}{D_{wp}}\right)} \quad (37)$$

$$G_{c2dw} = \frac{2\pi f_c(L_{wp} + 2\delta)k_{eff2,dw}}{\ln\left(\frac{D_{rw}}{D_{ds}}\right)} \quad (38)$$

The respective effective thermal conductivities are defined similar to Eq. (11),

$$k_{eff2,pd} = 0.386 \left[\frac{\ln\left(\frac{D_{ds}}{D_{wp}}\right)}{(D_{ds}^{-0.6} + D_{wp}^{-0.6})^{1.25}} \right] k_{fluid} \left[\frac{\rho^2 g \beta Pr^2}{(0.861 + Pr)\mu^2} \right]^{0.25} (T_{wp} - T_{ds})^{0.25} \quad (39)$$

$$k_{eff2,dw} = 0.386 \left[\frac{\ln\left(\frac{D_{rw}}{D_{ds}}\right)}{(D_{rw}^{-0.6} + D_{ds}^{-0.6})^{1.25}} \right] k_{fluid} \left[\frac{\rho^2 g \beta Pr^2}{(0.861 + Pr)\mu^2} \right]^{0.25} (T_{ds} - T_{rw})^{0.25} \quad (40)$$

Eqs. (39) and (40) are the complete forms for the thermal conductance values. The presence of the unknown temperatures, T_{ds} and T_{wp} in these expression (and their affect on the fluid property values) required that Eq. (34) be solved iteratively.

As in Case 1 above, we can provide a noniterative computation by assuming the following in order to compute G_{c2pd} and G_{c2dw} :

$$T_{ds} = T_{rw} + 10^\circ\text{C}$$

$$T_{wp} = T_{rw} + 20^{\circ}\text{C}$$

Radiation

There is radiation heat transfer between the waste package and the drip shield and between the drip shield and the rock wall. Each of these processes can be analyzed similarly to that described above for Case 1. By inspection, the pertinent equations can be written as

$$G_{r2pd} = \frac{\sigma f_c \pi (L_{wp} + 2\delta)}{\frac{1}{D_{wp} \epsilon_{wp}} + \frac{1 - \epsilon_{ds}}{D_{ds} \epsilon_{ds}}} (T_{wp}^2 + T_{ds}^2) (T_{wp} + T_{ds}) \quad (41)$$

$$G_{r2dw} = \frac{\sigma f_c \pi (L_{wp} + 2\delta)}{\frac{1}{D_{ds} \epsilon_{ds}} + \frac{1 - \epsilon_{rw}}{D_{rw} \epsilon_{rw}}} (T_{ds}^2 + T_{rw}^2) (T_{ds} + T_{rw}) \quad (42)$$

The temperatures T_{ds} and T_{wp} are not known *a priori*; so, the linearization proposed above is adopted here as well for both expressions:

$$G_{r2pd} = \frac{\sigma f_c \pi (L_{wp} + 2\delta)}{\frac{1}{D_{wp} \epsilon_{wp}} + \frac{1}{D_{ds} \epsilon_{ds}}} 4T_{rw}^3 \quad (43)$$

$$G_{r2dw} = \frac{\sigma f_c \pi (L_{wp} + 2\delta)}{\frac{1}{D_{ds} \epsilon_{ds}} + \frac{1}{D_{rw} \epsilon_{rw}}} 4T_{rw}^3 \quad (44)$$

This eliminates the need for an iterative solution procedure. The use of T_{rw} in both Eqs (43) and (44) may seem too extreme an approximation. As will be seen below, however, the waste package and drip shield temperatures are low enough so that this approximation leads to reasonable predictions for T_{wp} .

Drip Shield Thermal Resistance

The drip shield thermal resistance was neglected in forming the overall thermal resistance from the waste package to the wall. This is substantiated by the following sample calculation.

The thermal conductance of the drip shield is given by

$$G_{kds} = \frac{2\pi(L_{wp} + 2\delta) f_c k_{steel}}{\ln\left(\frac{D_{dso}}{D_{dsi}}\right)} \quad (45)$$

where

$$L_{wp} + 2\delta = 3 \text{ m}$$

$$f_c = 0.75$$

$$k_{ds} = 15.1 \text{ watt/m}\cdot\text{K} \text{ (302 stainless steel)}$$

$$D_{dso} = 2 \text{ m (assumed)}$$

$$D_{dsi} = 1.975 \text{ m (assumed 1" thick)}$$

Using these sample values, $G_{kds} = 16,971 \text{ watt/K}$. This conductance will be seen to be much greater than any of the other values in the system; that is, the thermal resistance is much less than any other component's and can be neglected.

Combined Heat Transfer Modes

The complete and linearized solutions for Case 2 are very similar to those for Case 1:

1. Specify values for Q_{wp} and T_{rw}
2. Compute G_{k2} using Eq. (36)
3. Assume a value for T_{wp} ($T_{rw} + 20^\circ\text{C}$ is a reasonable first choice)
4. Assume a value for T_{ds} ($T_{rw} + 10^\circ\text{C}$ is a reasonable first choice)
5. Compute k_{eff2pd} from Eq. (39) using air properties evaluated at a temperature of $T_{fluid} = 0.5(T_{wp} + T_{ds})$
6. Compute k_{eff2dw} from Eq. (40) using air properties evaluated at a temperature of $T_{fluid} = 0.5(T_{ds} + T_{rw})$
7. Compute G_{c2pd} using Eq. (37)
8. Compute G_{c2dw} using Eq. (38)
9. Compute G_{r2pd} using Eq. (41)
10. Compute G_{r2dw} using Eq. (42)
11. Compute a new value of T_{wp} using Eq.(34)
12. Compute a new value of T_{ds} using Eq.(35)
13. Repeat steps 5-12 until T_{wp} converges sufficiently

Conversely, the linearized solution is obtained by the following shorter procedure:

1. Specify values for Q_{wp} and T_{rw}
2. Compute G_{k2} using Eq. (36)

3. Assume a value for T_{wp} for use in Eq. (39) ($T_{rw} + 20^\circ\text{C}$ is reasonable)
4. Assume a value for T_{ds} for use in Eq. (40) ($T_{rw} + 10^\circ\text{C}$ is reasonable)
5. Compute k_{eff2pd} using air properties evaluated at a temperature of T_{rw}
6. Compute k_{eff2dw} using air properties evaluated at a temperature of T_{rw}
7. Compute G_{c2pd} using Eq. (37)
8. Compute G_{c2dw} using Eq. (38)
9. Compute G_{r2pd} using Eq. (41)
10. Compute G_{r2dw} using Eq. (42)
11. Compute a value of T_{wp} using Eq.(34)
12. Compute a value of T_{ds} using Eq.(35), if necessary

To compare these two procedures the following geometric and property values are used

$$D_{wp} = 1.5 \text{ m}$$

$$D_{rw} = 5 \text{ m}$$

$$D_{ds} = 3 \text{ m}$$

$$L_{wp} + 2\delta = 3 \text{ m}$$

$$f_c = 0.75$$

$$k_{floor} = 0.2 \text{ watt/m}\cdot\text{K}$$

$$\varepsilon_{rw} = 0.8$$

$$\varepsilon_{wp} = 0.8$$

$$\varepsilon_{ds} = 0.8$$

Eqs. (12)-(16) are used for air properties

The values shown above for D_{wp} and $L_{wp} + 2\delta$ are used for all the waste packages even though the actual values are different. These are example calculations only for purposes of demonstrating the computation procedure results.

The results of these calculations for four typical waste packages are listed in Table 5. First, it is clear that thermal radiation is the dominant heat transfer mode in this scenario. The values of G_{r2pd} and G_{r2dw} are much greater than G_{c2ps} , and G_{c2dw} even for low T_{rw} values. Second, the computed values of T_{wp} are less than 35°C different than the assumed rock wall temperature. As a result of these low temperature differences, the linearized solution is a good representation of the complete, but iterative, solution.

Table 5. Heat Transfer Analysis for Case 2 - Complete and Linearized Solutions

Waste Package	Q_{wp} watt	T_{rw} K	Complete (Iterative) Solution						Linearized Solution					
			G_{k2} watt/K	G_{c2pd} watt/K	G_{r2pd} watt/K	G_{c2dw} watt/K	G_{r2dw} watt/K	T_{wp} K	G_{k2} watt/K	G_{c2pd} watt/K	G_{r2pd} watt/K	G_{c2dw} watt/K	G_{r2dw} watt/K	T_{wp} K
5-DHLW-Long	2	300	0.8	3.2	45.2	4.4	64.1	300.1	0.8	12.3	45.2	18.8	64.1	300.1
		373	0.8	2.5	86.8	3.5	123.3	373.0	0.8	11.4	86.8	17.4	123.3	373.0
		473	0.8	2.0	177.0	2.7	251.3	473.0	0.8	10.6	177.0	16.0	251.3	473.0
5-DHLW-Short	31	300	0.8	6.2	45.5	8.5	64.3	301.0	0.8	12.3	45.2	18.8	64.1	300.9
		373	0.8	4.9	87.1	6.8	123.4	373.6	0.8	11.4	86.8	17.4	123.3	373.5
		473	0.8	3.9	177.3	5.3	251.4	473.3	0.8	10.6	177.0	16.0	251.3	473.3
44-BWR	600	300	0.8	12.2	50.7	17.2	66.4	316.4	0.8	12.3	45.2	18.8	64.1	317.3
		373	0.8	10.1	91.9	14.1	125.4	383.1	0.8	11.4	86.8	17.4	123.3	383.2
		473	0.8	8.0	181.4	11.1	253.1	478.4	0.8	10.6	177.0	16.0	251.3	478.4
21-PWR	1380	300	0.8	14.3	57.2	20.7	69.1	334.0	0.8	12.3	45.2	18.8	64.1	339.7
		373	0.8	12.1	98.2	17.1	128.0	394.8	0.8	11.4	86.8	17.4	123.3	396.5
		473	0.8	9.7	186.8	13.6	255.4	485.1	0.8	10.6	177.0	16.0	251.3	485.4

For Linearized Solution:

Air properties use the rock wall temp as reference.

G_{c2pd} and G_{c2dw} assume $T_{wp}=T_{rw}+20^{\circ}\text{C}$, and $T_{ds}=T_{rw}+10^{\circ}\text{C}$.

G_{r2pd} and G_{r2dw} use $4T_{rw}^3$ instead of complete temperature term.

The calculations required for obtaining the results shown in Table 5 were performed in Excel. The Excel file is maintained in S. Green's desktop computer as C:\Projects\div20\Notebook\notebook_10-2-03\WP_Drift_HT.xls.

47/320

CASE 3

In this case, there is a drip shield and backfill over the waste package which blocks direct communication across the air gap between the waste package and the rock wall. There is still a direct conductive heat transfer path between the package and the wall through the floor.

An electrical circuit analog to this heat transfer situation is shown on Figure 4.

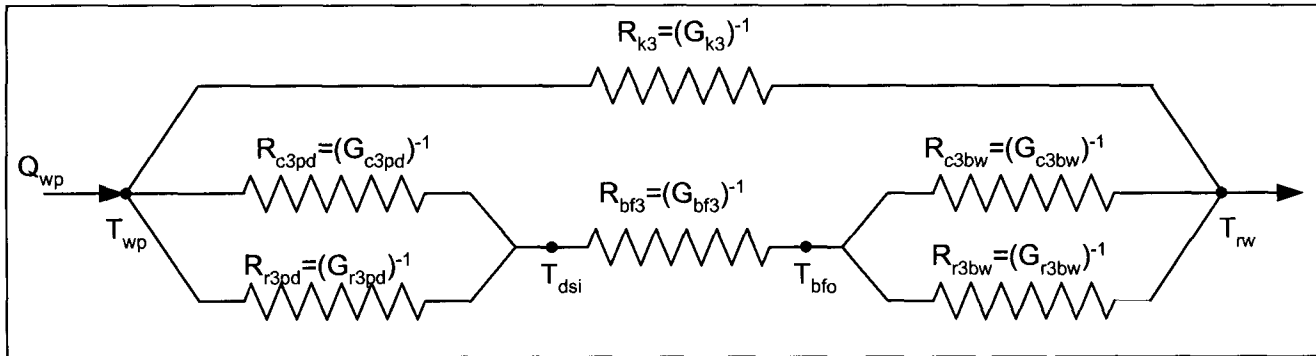


Figure 6. Electrical Analogy for Tunnel Heat Transfer with Dripshield and Backfill

Figure 6 highlights the assumed scenario in which the waste package heat is transferred to the rock wall through parallel paths; one of which is complicated by the presence of the drip shield and the backfill. The 'resistors' in this circuit represent the resistance to heat transfer in the respective paths

- R_{k3} – conduction through the floor
- R_{c3pd} – convection between package and drip shield
- R_{r3pd} – radiation between package and drip shield
- R_{bf3} – conduction through the backfill
- R_{c3bw} – convection between backfill and wall
- R_{r3bw} – radiation between backfill and wall
- R_{rcbf3} – combined radiation/convection/conduction waste package and wall through the backfill

The heat generated by a single waste package Q_{wp} is assumed to be spread along its unit length consisting of the length of the waste package and the gap between one waste package and the next. This is the same as taking the total heat generated by all waste packages and spreading it over the entire length of the line of packages.

Following this electrical analog, the heat transfer rate can be defined as

$$Q_{wp} = [R_{k3}^{-1} + R_{rcbf3}^{-1}] (T_{wp} - T_{rw}) = [G_{k3} + G_{rcbf3}] (T_{wp} - T_{rw})$$

$$Q_{wp} = \left\{ G_{k3} + \left[\frac{1}{G_{c3pd} + G_{r3pd}} + \frac{1}{G_{bf3}} + \frac{1}{G_{c3bw} + G_{r3bw}} \right]^{-1} \right\} (T_{wp} - T_{rw}) \quad (46)$$

where the 'G' terms are thermal conductance values, the inverse of thermal resistance. The '3' in the subscript refers to values for Case 3. The thermal resistance of the drip shield has been neglected here because it was shown previously to be significantly less than the other resistances.

If necessary, the drip shield inner surface and backfill outer surface temperatures can be computed as well from the relations

$$Q_{wp} - G_{k3} (T_{wp} - T_{rw}) = (G_{c3pd} + G_{r3pd}) (T_{wp} - T_{dsi}) \quad (47)$$

$$Q_{wp} - G_{k3} (T_{wp} - T_{rw}) = (G_{c3bw} + G_{r3bw}) (T_{bfo} - T_{rw}) \quad (48)$$

IMPORTANT NOTE:

The thermal circuit described in Figure 6 does not agree with the apparent approach adopted by the TPA Users' Manual for the case of backfill over the drip shield. In the TPA User's Manual the convection and radiation paths across the air gaps are each put in series independently of the combinatorial effect of the drip shield and backfill. This situation is similar to that described for Case 2.

Conduction through Floor

The conduction heat transfer through the floor in Case 3 is identical to that of Case 1,

$$G_{k3} = G_{k1} = \frac{2\pi(L_{wp} + 2\delta)(1 - f_c)k_{floor}}{\ln\left(\frac{D_{rw}}{D_{wp}}\right)} \quad (49)$$

Convection

There is convection heat transfer between the waste package and the drip shield and between the backfill and the rock wall. Each of these processes can be analyzed similarly to that described above for Case 2. By inspection, the pertinent equations can be written as

$$G_{c3pd} = \frac{2\pi f_c (L_{wp} + 2\delta) k_{eff3,pd}}{\ln\left(\frac{D_{dsi}}{D_{wp}}\right)} \quad (50)$$

$$G_{c3bw} = \frac{2\pi f_c (L_{wp} + 2\delta) k_{eff2,bw}}{\ln\left(\frac{D_{rw}}{D_{bfo}}\right)} \quad (51)$$

The respective effective thermal conductivities are defined similar to Eq. (11),

$$k_{eff3,pd} = 0.386 \left[\frac{\ln\left(\frac{D_{ds}}{D_{wp}}\right)}{(D_{ds}^{-0.6} + D_{wp}^{-0.6})^{1.25}} \right] k_{fluid} \left[\frac{\rho^2 g \beta Pr^2}{(0.861 + Pr) \mu^2} \right]^{\frac{1}{4}} (T_{wp} - T_{dsi})^{\frac{1}{4}} \quad (52)$$

$$k_{eff3,bw} = 0.386 \left[\frac{\ln\left(\frac{D_{rw}}{D_{bf}}\right)}{(D_{rw}^{-0.6} + D_{bf}^{-0.6})^{1.25}} \right] k_{fluid} \left[\frac{\rho^2 g \beta Pr^2}{(0.861 + Pr) \mu^2} \right]^{\frac{1}{4}} (T_{bfo} - T_{rw})^{\frac{1}{4}} \quad (53)$$

Eqs. (50) and (51) are the complete forms for the thermal conductance values. The presence of the unknown temperatures, T_{dsi} , T_{bfo} , and T_{wp} in the expression (and their affect on the fluid property values) require that Eq. (46) be solved iteratively.

As in Case 2 above, we can provide a noniterative computation by assuming the following in order to compute G_{c3pd} and G_{c3bw} :

$$T_{bfo} = T_{rw} + 5^\circ\text{C}$$

$$T_{dsi} = T_{rw} + 10^\circ\text{C}$$

$$T_{wp} = T_{rw} + 20^\circ\text{C}$$

Radiation

There is radiation heat transfer between the waste package and the drip shield and between the backfill and the rock wall. Each of these processes can be analyzed similarly to that described above for Case 2. By inspection, the pertinent equations can be written as

$$G_{r3pd} = \frac{\sigma f_c \pi (L_{wp} + 2\delta)}{1 + \frac{1 - \epsilon_{ds}}{D_{wp} \epsilon_{wp}} + \frac{1 - \epsilon_{ds}}{D_{ds} \epsilon_{ds}}} (T_{wp}^2 + T_{dsi}^2) (T_{wp} + T_{dsi}) \quad (54)$$

$$G_{r2bw} = \frac{\sigma f_c \pi (L_{wp} + 2\delta)}{\frac{1}{D_{bf} \epsilon_{bf}} + \frac{1 - \epsilon_{rw}}{D_{rw} \epsilon_{rw}}} (T_{bfo}^2 + T_{rw}^2) (T_{bfo} + T_{rw}) \quad (55)$$

The temperatures T_{bfo} , T_{bfo} and T_{wp} are not known *a priori*; so, the linearization proposed above is adopted here as well for both expressions:

$$G_{r3pd} = \frac{\sigma f_c \pi (L_{wp} + 2\delta)}{\frac{1}{D_{wp} \epsilon_{wp}} + \frac{1 - \epsilon_{ds}}{D_{ds} \epsilon_{ds}}} 4T_{rw}^3 \quad (56)$$

$$G_{r3bw} = \frac{\sigma f_c \pi (L_{wp} + 2\delta)}{\frac{1}{D_{bf} \epsilon_{bf}} + \frac{1 - \epsilon_{rw}}{D_{rw} \epsilon_{rw}}} 4T_{rw}^3 \quad (57)$$

This eliminates the need for an iterative solution procedure. The use of T_{rw} in both Eqs (56) and (57) may seem too extreme an approximation. As will be seen below, however, the backfill dominates the thermal resistance between of this part of the heat transfer path. This means that errors in the convection and radiation conductance values for Case 3 are not as problematic as in Case 2.

Backfill Conduction

The thermal conductance of the backfill is computed with the following relation

$$G_{bf3} = \frac{2\pi(L_{wp} + 2\delta) f_c k_{bf}}{\ln\left(\frac{D_{bf}}{D_{ds}}\right)} \quad (58)$$

Combined Heat Transfer Modes

The complete and linearized solution procedures for Case 3 are very similar to those for Case 2:

1. Specify values for Q_{wp} and T_{rw}
2. Compute G_{k3} using Eq. (49)
3. Assume a value for T_{wp} ($T_{rw} + 20^\circ\text{C}$ is a reasonable first choice)
4. Assume a value for T_{dsi} ($T_{rw} + 10^\circ\text{C}$ is a reasonable first choice)
5. Assume a value for T_{bfo} ($T_{rw} + 5^\circ\text{C}$ is a reasonable first choice)
6. Compute k_{eff3pd} from Eq. (52) using air properties evaluated at a temperature of $T_{fluid} = 0.5(T_{wp} + T_{dsi})$

7. Compute k_{eff3bw} from Eq. (53) using air properties evaluated at a temperature of $T_{fluid}=0.5(T_{bfo} + T_{rw})$
8. Compute G_{c3pd} using Eq. (50)
9. Compute G_{c3bw} using Eq. (51)
10. Compute G_{bf3} using Eq. (58)
11. Compute G_{r3bw} using Eq. (54)
12. Compute G_{r3bw} using Eq. (55)
13. Compute a new value of T_{wp} using Eq.(46)
14. Compute a new value of T_{dsi} using Eq.(47)
15. Compute a new value of T_{bfo} using Eq.(48)
16. Repeat steps 6-15 until T_{wp} converges sufficiently

Conversely, the linearized solution is obtained by the following shorter procedure:

1. Specify values for Q_{wp} and T_{rw}
2. Compute G_{k3} using Eq. (49)
3. Assume a value for T_{wp} for use in Eq. (39) ($T_{rw} + 20^{\circ}\text{C}$ is reasonable)
4. Assume a value for T_{dsi} for use in Eq. (40) ($T_{rw} + 10^{\circ}\text{C}$ is reasonable)
5. Assume a value for T_{bfo} for use in Eq. (40) ($T_{rw} + 5^{\circ}\text{C}$ is reasonable)
6. Compute k_{eff3pd} using air properties evaluated at a temperature of T_{rw}
7. Compute k_{eff3bw} using air properties evaluated at a temperature of T_{rw}
8. Compute G_{c3pd} using Eq. (50)
9. Compute G_{c3bw} using Eq. (51)
10. Compute G_{bf3} using Eq. (58)
11. Compute G_{r3pd} using Eq. (54)
12. Compute G_{r3bw} using Eq. (55)
13. Compute a value of T_{wp} using Eq.(46)
14. Compute a value of T_{dsi} using Eq.(47), if necessary
15. Compute a value of T_{bfo} using Eq.(48), if necessary

To compare these two procedures the following geometric and property values are used

$$D_{wp} = 1.5\text{m}$$

$$D_{ds} = 2\text{ m}$$

$$D_{bf} = 3\text{ m}$$

$$D_{rw} = 5\text{ m}$$

$$L_{wp} + 2\delta = 3 \text{ m}$$

$$f_c = 0.75$$

$$k_{floor} = 0.2 \text{ watt/m}\cdot\text{K}$$

$$k_{bf} = 0.2 \text{ watt/m}\cdot\text{K}$$

$$\varepsilon_{rw} = 0.8$$

$$\varepsilon_{wp} = 0.8$$

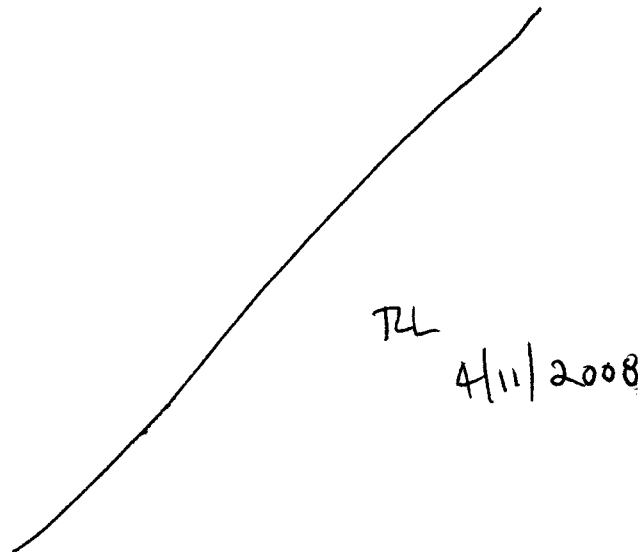
$$\varepsilon_{bf} = 0.8$$

Eqs. (12)-(16) are used for air properties

The values shown above for D_{wp} and $L_{wp} + 2\delta$ is used for all the waste packages even though the actual values are different. These are example calculations only for purposes of demonstrating the computation procedure results.

The results of these calculations for four typical waste packages are listed in Table 6. First, it is clear that thermal radiation is again the dominant heat transfer mode between the waste package and the drip shield and between the backfill and the tunnel wall. The values of G_{r3pd} and G_{r3bw} are much greater than G_{c3pd} , and G_{c3bw} even for low T_{rw} values. The overall thermal resistance, however, for this path is dominated by the backfill. As a result, the convection and radiation processes could likely be neglected for this Case. It would be a good approximation to simply consider the backfill as another conductive path between the waste package and the rock wall.

Second, the computed values of T_{wp} are much greater than the rock wall temperatures, because of the insulating effect of the backfill. Thus, the assumed values of the waste package and drip shield inner wall temperatures to start the solution procedure are severely in error. This error turns out to have little effect on the final result for the waste package temperature because the convection and radiation processes play a small role in the overall heat transfer process. So, the linearized solution is a good representation of the complete, but iterative, solution.



TL
4/11/2008

Table 6. Heat Transfer Analysis for Case 3 - Complete and Linearized Solutions

Waste Package	Q_{wp} watt	T_{rw} K	Complete (Iterative) Solution							Linearized Solution						
			G_{k3} watt/K	G_{c3pd} watt/K	G_{r3pd} watt/K	G_{bf3} watt/K	G_{c3bw} watt/K	G_{r3bw} watt/K	T_{wp} K	G_{k3} watt/K	G_{c3pd} watt/K	G_{r3pd} watt/K	G_{bf3} watt/K	G_{c3bw} watt/K	G_{r3bw} watt/K	T_{wp} K
		300	0.8	2.9	45.5	1.8	4.4	92.8	300.8	0.8	14.4	45.2	1.8	19.0	92.8	300.8
5-DHLW-Long	2	373	0.8	2.3	87.4	1.8	3.5	178.3	373.8	0.8	13.4	86.8	1.8	17.6	178.3	373.8
		473	0.8	1.8	177.9	1.8	2.7	363.5	473.8	0.8	12.5	177.0	1.8	16.3	363.5	473.8
		300	0.8	5.5	50.8	1.8	8.7	92.9	312.2	0.8	14.4	45.2	1.8	19.0	92.8	312.2
5-DHLW-Short	31	373	0.8	4.4	95.4	1.8	6.9	178.4	385.0	0.8	13.4	86.8	1.8	17.6	178.3	385.0
		473	0.8	3.4	190.7	1.8	5.4	363.6	484.9	0.8	12.5	177.0	1.8	16.3	363.5	484.9
		300	0.8	6.5	250.8	1.8	17.7	94.5	532.1	0.8	14.4	45.2	1.8	19.0	92.8	535.8
44-BWR	600	373	0.8	5.7	366.9	1.8	14.3	179.8	603.6	0.8	13.4	86.8	1.8	17.6	178.3	605.8
		473	0.8	4.9	579.4	1.8	11.2	364.8	702.6	0.8	12.5	177.0	1.8	16.3	363.5	703.7
		300	0.8	5.0	960.3	1.8	21.5	96.6	831.6	0.8	14.4	45.2	1.8	19.0	92.8	842.4
21-PWR	1380	373	0.8	4.6	1226.5	1.8	17.5	181.8	902.1	0.8	13.4	86.8	1.8	17.6	178.3	908.3
		473	0.8	4.2	1673.1	1.8	13.7	366.5	1000.3	0.8	12.5	177.0	1.8	16.3	363.5	1003.5

For Linearized Solution:

Air properties use the rock wall temp as reference.

G_{c3pd} and G_{c3bw} assume $T_{wp}=T_{rw}+20^{\circ}\text{C}$, $T_{dsf}=T_{rw}+10^{\circ}\text{C}$, and $T_{bfo}=T_{rw}+5^{\circ}\text{C}$.

G_{r3pd} and G_{r3bw} use $4T_{rw}^3$ instead of complete temperature term.

The calculations required for obtaining the results shown in Table 6 were performed in Excel. The Excel file is maintained in S. Green's desktop computer as C:\Projects\div20\Notebook\notebook_10-2-03\ WP_Drift_HT.xls.

=====
 Entries made into Scientific Notebook #536E for the period April 3, 2002 to September 30, 2003 have been made by Steven Green (October 2, 2003).

No original text or figures entered into this Scientific Notebook has been removed

STG 10/02/2003

=====
 10/21/03 STG

This entry is to record a derivation of a simple moisture evaporation and condensation model that can be used in CFD codes. If the CFD code can simulate the diffusion and advection of chemical species within the flow field, this model can be used to provide sources and sinks of the species at specific locations (e.g. walls) in the flow.

A complete description of the mass, momentum, and binary gas diffusion equations are described in the paper, "A Model for Moisture Transport in a High-Level Radioactive Waste Repository Drift," submitted to the SME Annual Meeting, February 2004.

The following overall assumptions are made for the entire flow field.

- The fluid is considered to be a binary mixture of water vapor and air, each of which are considered to be ideal gases. (Of course, the air is itself a mixture of many gases, but is considered here to be a single component).
- Temperatures are below the boiling point of the water at the mean drift pressure. This means that the evaporation/condensation is dictated solely by comparing the local vapor pressure to the saturation vapor pressure of water.
- Condensate layers are not thick enough to cause film flow on the walls. This is equivalent to the condensate being assumed to be adiabatically absorbed into the wall.

Additional assumptions for the evaporation/condensation model are described as needed

The binary species conservation equation for the water vapor is as follows (from Burmeister, Louis C., 1983, Convective Heat Transfer, John Wiley and Sons, New York,.)

$$\rho \left(\frac{\partial c_v}{\partial t} + u \frac{\partial c_v}{\partial x} + v \frac{\partial c_v}{\partial y} + w \frac{\partial c_v}{\partial z} \right) = \nabla \cdot (\rho D \nabla c_v) + \dot{m}_{source}^m \quad (1)$$

where ρ = bulk density of the air/vapor mixture

c_v = vapor mass concentration mass; i.e., ratio of vapor mass to total mass

\dot{m}_{source}^m = source of vapor as a result of mass transfer to or from liquid water at walls

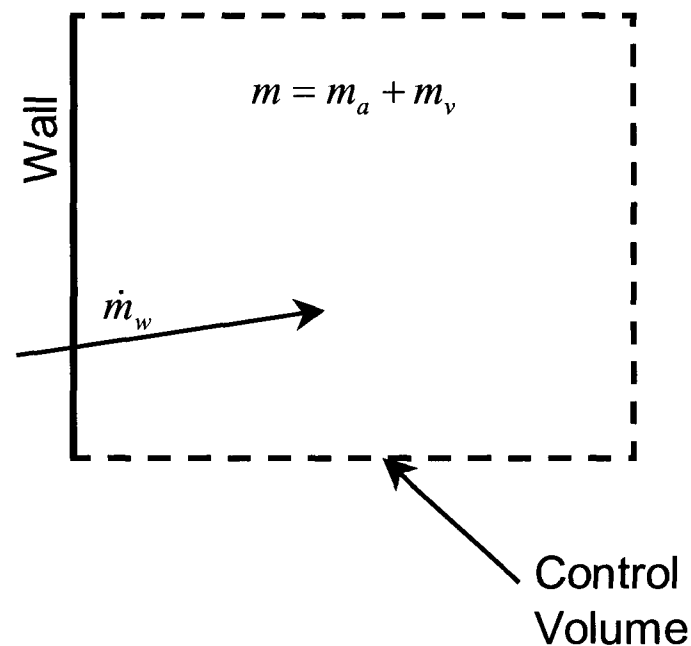
u, v, w = vector components of bulk fluid flow

x, y, z = coordinate directions

D = diffusion coefficient for water vapor/air

It is presumed that the CFD code provides the appropriate solution scheme for solving the species conservation equation if the spatially varying, temperature dependent source term is defined. The objective of this analysis is to prescribe a calculation scheme for the source term.

Consider a small control volume adjacent to a wall at which either evaporation or condensation can take place. During a calculation, the control volume will be a single computational cell or finite element in the discretized flow domain.



The following definitions are made:

m_1 = mass of air/vapor mixture in control at the beginning of a time step

m_2 = mass of air/vapor mixture in control at the end of a time step

m_w = mass of water evaporated/condensed in a time step

m_{a1}, m_{a2} = mass of dry air at beginning and end of time step, respectively

m_{v1}, m_{v2} = mass of water vapor at beginning and end of time step, respectively

e_1 = mass-specific thermodynamic energy of air/vapor mixture at beginning of time step

e_2 = mass-specific thermodynamic energy of air/vapor mixture at end of time step

h_{vap} = heat of vaporization

The conservation of energy is applied to the evaporation/condensation process that takes place in a time step. A major underlying assumption is that in a single time-step, the water vapor in the control volume adjust to be saturated (100% relative humidity) in that time step.

Evaporation or condensation will take place as necessary to satisfy this condition. Any heat transfer to/from the walls takes place via conduction/convection with the air/vapor mixture; the wall does not exchange energy directly with the liquid water.

Armed with these assumptions, the conservation of energy is expressed as

$$\{\text{Energy change in the air/vapor mixture}\} = \{\text{Energy of phase change}\} \quad (2)$$

$$m_1(e_2 - e_1) = m_w h_{vap}$$

The initial temperature and composition (i.e., vapor concentration) of the control volume are known. So, there are two unknowns in this equation, m_w and e_2 . These two quantities both depend on the air/vapor temperature at the end of the time step. So, a second equation relating the mass of water to the control volume initial composition (from the on-going CFD solution of Eq. (1)) and the control final composition (enforced saturation conditions) can be developed.

First, define some helpful equations from engineering psychrometrics. The air and vapor are assumed to be ideal gases; so the mole fraction of each is equal to their partial pressure fractions as

$$x_v = \frac{\text{moles of water vapor}}{\text{total moles}} = \frac{P_v}{P_{tot}} \quad (3)$$

$$x_a = \frac{\text{moles of air}}{\text{total moles}} = \frac{P_a}{P_{tot}} = \frac{P_{tot} - P_v}{P_{tot}} = 1 - x_v \quad (4)$$

The humidity ratio is defined as the ratio of the water vapor mass to the dry air mass,

$$W = \frac{m_v}{m_a} = \frac{x_v}{x_a} \frac{M_v}{M_a} = \frac{P_v}{P_a} \frac{M_v}{M_a} = \frac{P_v}{P_{tot} - P_v} \frac{M_v}{M_a} \quad (5)$$

It follows that humidity ratio for saturated air is

$$W_{sat} = \frac{P_{v,sat}}{P_a} \frac{M_v}{M_a} \quad (6)$$

The Keenan, Keyes, Hill, and Moore expression for estimating the saturation pressure of water is described on pages 2-3 of this notebook.

The mass fraction of water vapor, c_v , can now be defined in terms of humidity ratio,

$$c_v = \frac{\text{mass of water vapor}}{\text{total mass}} = \frac{m_v}{m_a + m_v} = \frac{W}{1 + W} = \frac{x_v \frac{M_v}{M_a}}{x_a + x_v \frac{M_v}{M_a}} \quad (7)$$

where M_v , M_a are the molecular weights of air and water respectively.

This can be solved for the humidity ratio in terms of the mass concentration:

$$W = \frac{c_v}{1 - c_v} \quad (8)$$

We can also solve for the mole fraction in terms of the concentration

$$x_v = \left(\frac{c_v}{\frac{M_v}{M_a} + c_v \left(1 - \frac{M_v}{M_a} \right)} \right) \quad (9)$$

Now we can return to the solution to Eq. (2). Solving for the energy (a thermodynamic property) at the end of the time step

$$e_2 = e_1 + h_{vap} \frac{m_w}{m_1} \quad (10)$$

The mass of water that has changed phase is

$$m_w = m_{v2} - m_{v1} \quad (11)$$

The mass, m_{v2} , is the mass of vapor in saturated air at the temperature T_2 . Substitute this into Eq. (10) rearrange with the psychrometric relations,

$$e_2 = e_1 + h_{vap} \frac{m_{v2} - m_{v1}}{m_1} = e_1 + h_{vap} \left(\frac{m_{v2}}{m_2 - (m_{v2} - m_{v1})} - c_{v1} \right) = e_1 + h_{vap} \left(\frac{1}{\frac{1}{c_{v2}} - 1 + \frac{W_1}{W_2}} - c_{v1} \right) \quad (12)$$

This can be further simplified to

$$e_2 = e_1 + h_{vap} \left(\frac{W_2 - W_1}{1 + W_1} \right) \quad (13)$$

where the humidity ratio, W_2 , and the concentration, c_{v2} , are for saturation conditions at the final control volume energy temperature, T_2 .

The thermodynamic property energy must include the composition effects,

$$e = e_a + e_v = (1 - c_v) \rho_a C_{va} T + c_v \rho_v C_{vv} T \quad (14)$$

where C_{va} and C_{vv} are the constant volume specific heats of air and water vapor, respectively.

Other, more accurate expressions for the constituent energy values can be used on the right side of Eq. (14). Care must be taken however, to ensure that the reference temperature for the properties is consistent.

Finally, the solution to Eq. (2) is obtained by finding the temperature that provides for the equality of Eq. (13). The mass source term can now be computed,

$$\dot{m}_{source}^m = \frac{m_w}{(\Delta t)(\Delta V)} \quad (15)$$

where Δt = the current time step

ΔV = volume of the computational unit (finite volume or finite element)

In the computer program, FLOW-3D, this is also accomplished by forcing the concentration for the cells next to the wall to be equal to the saturation concentration.

It is also important include the energy of the phase change as a source term in the conservation of energy equation:

$$\dot{q}_{source}^m = \frac{m_w h_{vap}}{(\Delta t)(\Delta V)} \quad (16)$$

Similarly, in FLOW-3D, this is accomplished by forcing the energy of the cell next to the wall to be the value, e_2 , in Eq. (13)

The moisture transport algorithm described above was incorporated into the FLOW-3D user-modifiable routine QSADD. QSADD is called at the end of the CFD calculations for the mass, momentum, energy, and diffusion equations. QSADD is a general purpose routine intended to provide a location for users to compute once-per-time-step parameters for outputs or for special source terms. QSADD is NOT called within the main iteration loops; so the calculation are suspect for source terms that are highly non-linear or strongly coupled to the field variable (temperature, density, velocity, etc.). This subroutine is part of the FLOW-3D software distribution and is intended to be modified by the code user as necessary; however, the program file header contains a statement that the file contains proprietary Flow Science information. The code listing will not be provided here until specific approval is received from Flow Science.

Instead, the moisture transport algorithm was built into a separate subroutine called by QSADD. This routine is called

C:\FLOW3D\source\hydr3d\qsadd_moist_stg.F

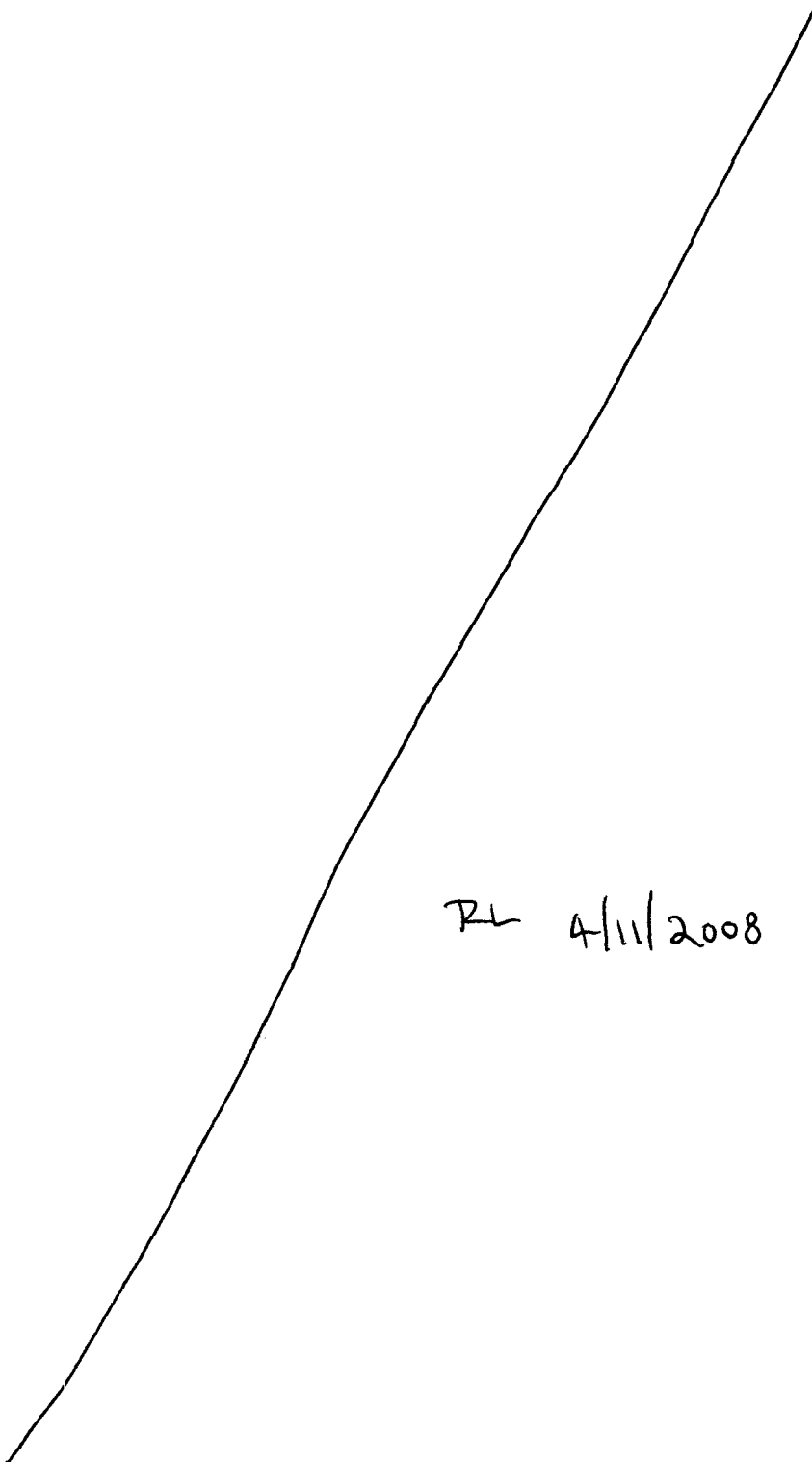

```

tnc = tinit-273.15
term1 = F0kkhm +
1      F1kkhm*(0.65-0.01*(tnc)) +
2      F2kkhm*(0.65-0.01*(tnc))**2 +
3      F3kkhm*(0.65-0.01*(tnc))**3 +
4      F4kkhm*(0.65-0.01*(tnc))**4 +
5      F5kkhm*(0.65-0.01*(tnc))**5 +
6      F6kkhm*(0.65-0.01*(tnc))**6 +
7      F7kkhm*(0.65-0.01*(tnc))**7
Pvsati=217.99*exp(0.01/tinit*(374.136-(tnc))*term1)
Pvsati = Pvsat * 101300.
c
c Saturation Molar concentration ..... moles of vapor per total moles
Xvsati = Pvsati/p(ijk)
c
c Saturation Humidity ratio .....mass of vapor to mass of dry air
Wvsati = Xvsati/(1.-Xvsati)*vapmw/airmw
c
c Saturation Mass Concentration .....mass of vapor to total mass
Yvsati = Wvsati/(1.+Wvsati)
c
c Current vapor mass concentration
Yvacti = sclr(ijk, isvap_stg)
Wvacti = Yvacti/(1.-Yvacti)
c
nitr_moist = 0
100 continue
tnc = tfinal-273.15
term1 = F0kkhm +
1      F1kkhm*(0.65-0.01*(tnc)) +
2      F2kkhm*(0.65-0.01*(tnc))**2 +
3      F3kkhm*(0.65-0.01*(tnc))**3 +
4      F4kkhm*(0.65-0.01*(tnc))**4 +
5      F5kkhm*(0.65-0.01*(tnc))**5 +
6      F6kkhm*(0.65-0.01*(tnc))**6 +
7      F7kkhm*(0.65-0.01*(tnc))**7
Pvsat=217.99*exp(0.01/tfinal*(374.136-(tnc))*term1)
Pvsat = Pvsat * 101300.
c
c Saturation Molar concentration ..... moles of vapor per total moles
Xvsat = Pvsat/p(ijk)
c
c Saturation Humidity ratio .....mass of vapor to mass of dry air
Wvsat = Xvsat/(1.-Xvsat)*vapmw/airmw
c
c Saturation Mass Concentration .....mass of vapor to total mass
Yvsat = Wvsat/(1.+Wvsat)
c
c Current vapor mass concentration
Yvact = sclr(ijk, isvap_stg)
Wvact = Yvact/(1.-Yvact)
c
c--- The mass that changes phase and the energy change of teh dray air must be solved
simultaneously
c This assumes that the phase change rate is high enough to bring the vapor to
saturation
c in a single time step.
c
c Consider changing this to a rate-based calculation in future modifications
c
c      deltmass = (Yvsat-Yvact)*rho(ijk)
deltmass = (Yvsat/(1.-Yvsat*(1.-Wvacti/Wvsat))
1      -Yvacti)*rho(ijk)
tfsave = tfinal
tfinal = tinit - hvvap_stg*deltmass/rho(ijk)/
1      ((1.-Yvact)*cvl+Yvact*cvvap_stg)
nitr_moist = nitr_moist +1
c
c write(51,*) ' i,j,k,p(ijk),tn(ijk),sclr(ijk,1),sclrn(ijk,1)'
c write(51,*) i,j,k,p(ijk),tn(ijk),sclr(ijk,1),sclrn(ijk,1)

```


C:\Projects\div20\moisture_transport\natconv_box\ Nat_Conv_Box.mcd

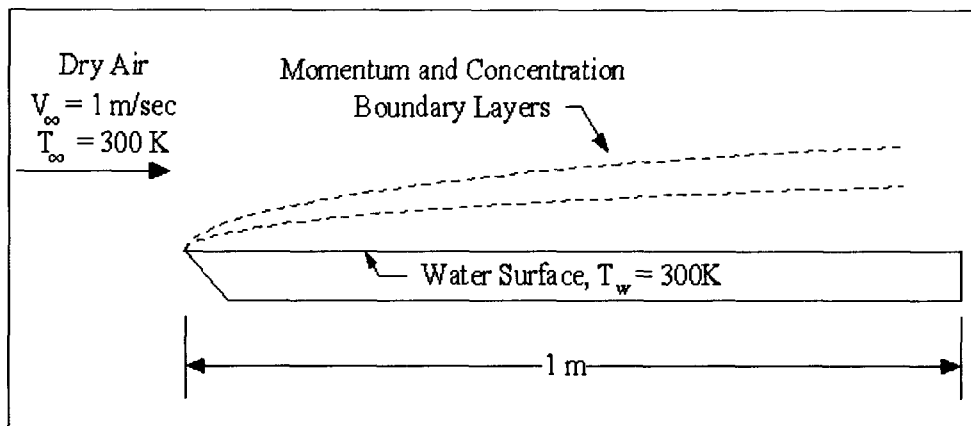
The Mathcad sheets are reproduced here in graphical form.



Heat and Mass Transfer for Laminar Flow over a Flat Plate

Air flowing over a water surface at 1 m/sec. The water surface is 1-m in the free stream flow direction. . Freestream air is dry at 300 K. Water is at 300K

Determine the evaporation rate from the water surface.



$$V_{a,f} := 1 \cdot \frac{\text{m}}{\text{sec}} \quad T_{a,f} := 300 \text{ K} \quad MW_w := 18 \cdot \frac{\text{gm}}{\text{mole}} \quad R_{\text{gas}} := 8.314 \frac{\text{joule}}{\text{mol} \cdot \text{K}}$$

$$L_w := 1 \cdot \text{m} \quad \phi_f := 0.5 \quad \text{Relative humidity of freestream}$$

Fluid Properties:

$$\rho_a := 1.18 \frac{\text{kg}}{\text{m}^3} \quad \text{Air density} \quad \rho_{w,l} := 1000 \frac{\text{kg}}{\text{m}^3} \quad \text{Liquid water density}$$

$$c_{p,a} := 1000 \frac{\text{joule}}{\text{kg} \cdot \text{K}}$$

$$\mu_a := 2 \cdot 10^{-5} \cdot \text{Pa} \cdot \text{sec} \quad \text{Air dynamic viscosity} \quad D_{wa} := 2.6 \cdot 10^{-5} \cdot \frac{\text{m}^2}{\text{sec}} \quad \text{Binary diffusion coefficient for water vapor into air}$$

$$k_a := 0.026 \frac{\text{watt}}{\text{m} \cdot \text{K}} \quad \text{Air thermal conductivity}$$

$$Pr_a := 0.7 \quad \text{Air Prandtl Number}$$

$$v_a := \frac{\mu_a}{\rho_a} \quad v_a = 1.695 \times 10^{-5} \frac{\text{m}^2}{\text{s}} \quad \text{Air kinematic viscosity} \quad Sc_{wa} := \frac{v_a}{D_{wa}} \quad Sc_{wa} = 0.652 \quad \text{Schmidt Number for water into air}$$

$$\alpha_a := \frac{k_a}{\rho_a \cdot c_{p,a}} \quad \alpha_a = 2.203 \times 10^{-5} \frac{\text{m}^2}{\text{s}} \quad \text{Air thermal diffusivity}$$

Flow regime

$$Re_{a,L} := \frac{\rho_a \cdot V_{a,f} \cdot L_w}{\mu_a} \quad Re_{a,L} = 5.9 \times 10^4 \quad \text{Flow is laminar over the entire length since } Re_{a,L} < 5 \cdot 10^5$$

Heat Transfer

$$Nu_L := 0.664 Re_{a,L}^{0.5} Pr_a^{\frac{1}{3}} \quad Nu_L = 143.206 \quad \text{Use laminar B.L. theory to define:}$$

$$h_L := \frac{Nu_L \cdot k_a}{L_w} \quad h_L = 3.723 \frac{\text{watt}}{\text{m}^2 \cdot \text{K}} \quad \text{Nusselt Number}$$

Average heat transfer coefficient over the water surface

Mass Transfer:

$$Sh_L := 0.664 Re_{a,L}^{0.5} Sc_{wa}^{\frac{1}{3}} \quad Sh_L = 139.847 \quad \text{Use laminar B.L. theory to define:}$$

Sherwood Number

$$h_{m,L} := \frac{Sh_L \cdot D_{wa}}{L_w} \quad h_{m,L} = 3.636 \times 10^{-3} \frac{\text{m}}{\text{s}} \quad \text{Average mass transfer coefficient over the water surface}$$

Saturation pressure of water vapor

$$\begin{aligned} F_0 &:= -741.9242 & F_4 &:= 0.1094098 \\ F_1 &:= -29.721 & F_5 &:= 0.439993 \\ F_2 &:= -11.5286 & F_6 &:= 0.2520658 \\ F_3 &:= -0.8685635 & F_7 &:= 0.05218684 \end{aligned}$$

$$FPvsat_{KKHM}(T) := 217.99 \exp \left[\frac{0.01}{T} \cdot [374.136 - (T - 273.15)] \cdot \sum_{k=0}^7 F_k \cdot [0.65 - 0.01 \cdot (T - 273.15)]^k \right] \text{atm}$$

$$P_{v,\text{sat},\text{surf}} := FPvsat_{KKHM} \left(\frac{T_{a,f}}{K} \right) \quad P_{v,\text{sat},\text{surf}} = 3.536 \times 10^3 \text{ Pa} \quad \text{Partial pressure of water vapor at liquid surface}$$

$$\rho_{v,\text{surf}} := \frac{P_{v,\text{sat},\text{surf}} \cdot MW_w}{R_{\text{gas}} \cdot T_{a,f}} \quad \rho_{v,\text{surf}} = 0.026 \frac{\text{kg}}{\text{m}^3} \quad \text{Bulk density of water vapor at surface assumed saturated}$$

$$P_{v,\text{sat},f} := FPvsat_{KKHM} \left(\frac{T_{a,f}}{K} \right) \quad P_{v,\text{sat},f} = 3.536 \times 10^3 \text{ Pa} \quad \text{Partial pressure of water vapor in freestream}$$

$$\rho_{v,f} := \phi_f P_{v,\text{sat},f} \quad \rho_{v,f} := 0 \frac{\text{kg}}{\text{m}^3} \quad \text{Bulk density of water vapor in freestream.}$$

$$m\dot{c}_w := h_{m,L} L_w (\rho_{v,\text{surf}} - \rho_{v,f}) \quad m\dot{c}_w = 9.278 \times 10^{-5} \frac{\text{kg}}{\text{ms}} \quad \text{Total evaporation rate of water per unit width of surface based on surface-average heat and mass transfer coefficients}$$

Lengthwise Distribution

Heat Transfer

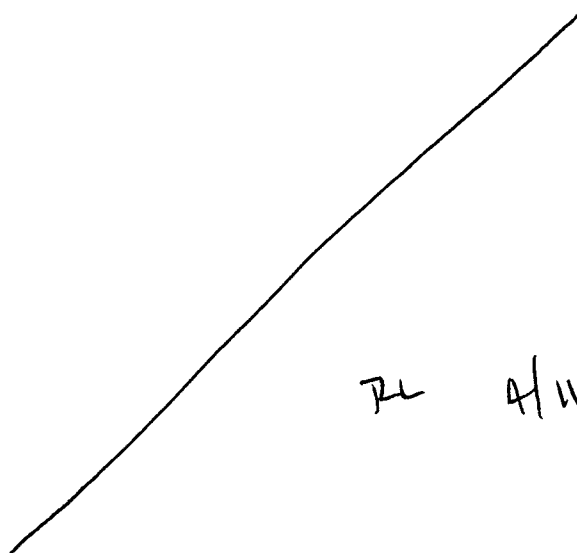
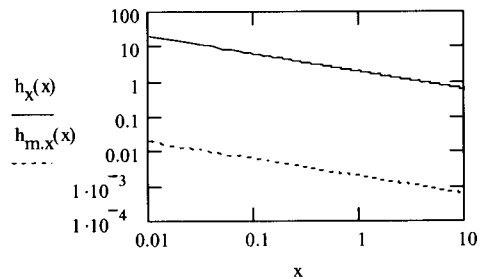
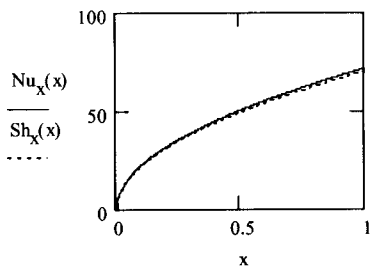
$$Nu_x(x) := 0.332 \left(\frac{\rho_a \cdot V_a \cdot f \cdot x}{\mu_a} \right)^{0.5} \cdot Pr_a^{-\frac{1}{3}} \quad Nu_x(0.02\text{m}) = 10.126$$

$$h_x(x) := \frac{Nu_x(x) \cdot k_a}{x} \quad h_x(0.02\text{m}) = 4.163 \frac{\text{watt}}{\text{m}^2 \cdot \text{K}} \quad \text{Local heat transfer coefficient over the water surface}$$

Mass Transfer:

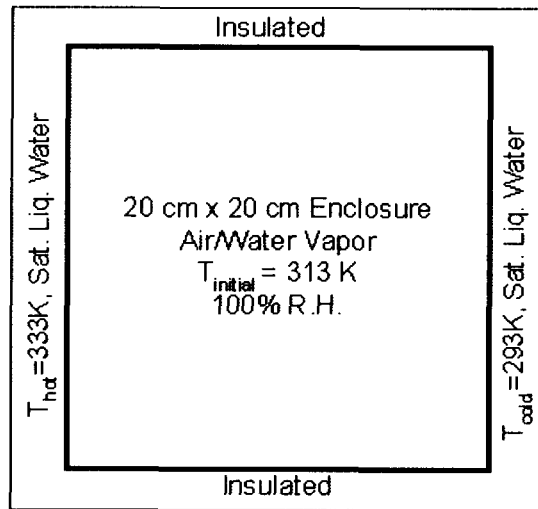
$$Sh_x(x) := 0.332 \left(\frac{\rho_a \cdot V_a \cdot f \cdot x}{\mu_a} \right)^{0.5} \cdot Sc_{wa}^{-\frac{1}{3}} \quad Sh_L = 139.847 \quad \text{Sherwood Number}$$

$$h_{m,x}(x) := \frac{Sh_x(x) \cdot D_{wa}}{x} \quad h_{m,x}(0.02\text{m}) = 4.065 \times 10^{-3} \frac{\text{m}}{\text{s}} \quad \text{Local mass transfer coefficient at water surface}$$



RL 4/11/2008

Heat and Mass Transfer for Natural Convection in a 2-D Square Cavity



Fluid Properties

$$R_{\text{gas}} := 8.314 \frac{\text{joule}}{\text{mol}\cdot\text{K}}$$

$$MW_a := 28.97 \frac{\text{gm}}{\text{mole}}$$

Air Mol. wt.

$$MW_w := 18 \frac{\text{gm}}{\text{mole}}$$

Water Mol. wt.

$$Pr_{a,\text{box}} := 0.709$$

Air Prandtl Number

$$Pr_{v,\text{box}} := 0.936$$

Water Prandtl Number

$$c_{p,a} := 1005 \frac{\text{joule}}{\text{kg}\cdot\text{K}}$$

Air constant pressure specific heat

$$c_{p,v} := 2017 \frac{\text{joule}}{\text{kg}\cdot\text{K}}$$

Water constant pressure specific heat

$$\mu_a := 1.911 \cdot 10^{-5} \text{ Pa}\cdot\text{sec}$$

Air dynamic viscosity

$$\mu_v := 20.8 \cdot 10^{-6} \text{ Pa}\cdot\text{sec}$$

Water dynamic viscosity

$$k_a := 0.02709 \frac{\text{watt}}{\text{m}\cdot\text{K}}$$

Air thermal conductivity

$$k_v := 44.9 \cdot 10^{-3} \frac{\text{watt}}{\text{m}\cdot\text{K}}$$

Water thermal conductivity

$$D_{wa} := 2.6 \cdot 10^{-5} \frac{\text{m}^2}{\text{sec}}$$

Binary diffusion coefficient for water vapor into air

Saturation pressure of water vapor

$$F_0 := -741.9242$$

$$F_4 := 0.1094098$$

$$F_1 := -29.721$$

$$F_5 := 0.439993$$

$$F_2 := -11.5286$$

$$F_6 := 0.2520658$$

$$F_3 := -0.8685635$$

$$F_7 := 0.05218684$$

$$FP_{\text{sat}}^{\text{KKHM}}(T) := 217.99 \exp \left[\frac{0.01}{T} \cdot [374.136 - (T - 273.15)] \cdot \sum_{k=0}^7 F_k \cdot [0.65 - 0.01 \cdot (T - 273.15)]^k \right] \text{ atm}$$

Square Box

$$T_{a.\text{box}} := 313\text{K} \quad \text{Average gas temperature}$$

$$P_{\text{tot.}\text{box}} := 1 \cdot \text{atm} \quad \text{Total pressure}$$

$$P_{v.\text{sat.}\text{box}} := \text{FPvsat}_{\text{KKHM}} \left(\frac{T_{a.\text{box}}}{\text{K}} \right)$$

$$P_{a.\text{box}} := P_{\text{tot.}\text{box}} - P_{v.\text{sat.}\text{box}} \quad \text{Partial pressures of air and vapor}$$

$$\rho_{v.\text{box}} := \frac{P_{v.\text{sat.}\text{box}} \cdot \text{MW}_w}{R_{\text{gas}} \cdot T_{a.\text{box}}}$$

$$\rho_{a.\text{box}} := \frac{P_{a.\text{box}} \cdot \text{MW}_a}{R_{\text{gas}} \cdot T_{a.\text{box}}} \quad \text{Partial densities of air and vapor}$$

$$c_{v.\text{box}} := \frac{\rho_{v.\text{box}}}{\rho_{v.\text{box}} + \rho_{a.\text{box}}}$$

Water vapor concentration

$$\rho_{\text{box}} := \rho_{v.\text{box}} + \rho_{a.\text{box}}$$

$$\rho_{\text{box}} = 1.097 \frac{\text{kg}}{\text{m}^3} \quad \text{Mixture density}$$

$$k_{\text{box}} := \frac{\rho_{v.\text{box}} \cdot k_v + \rho_{a.\text{box}} \cdot k_a}{\rho_{\text{box}}}$$

$$k_{\text{box}} = 0.028 \frac{\text{watt}}{\text{mK}} \quad \text{Mixture thermal conductivity}$$

$$c_{p.\text{box}} := \frac{\rho_{v.\text{box}} \cdot c_{p.v} + \rho_{a.\text{box}} \cdot c_{p.a}}{\rho_{\text{box}}}$$

$$c_{p.\text{box}} = 1.052 \times 10^3 \frac{\text{joule}}{\text{kg} \cdot \text{K}} \quad \text{Mixture specific heat}$$

$$\mu_{\text{box}} := \frac{\rho_{v.\text{box}} \cdot \mu_v + \rho_{a.\text{box}} \cdot \mu_a}{\rho_{\text{box}}}$$

$$\mu_{\text{box}} = 1.919 \times 10^{-5} \frac{\text{kg}}{\text{ms}} \quad \text{Mixture viscosity}$$

$$\alpha_{\text{box}} := \frac{k_{\text{box}}}{\rho_{\text{box}} \cdot c_{p.\text{box}}}$$

$$\alpha_{\text{box}} = 2.419 \times 10^{-5} \frac{\text{m}^2}{\text{s}} \quad \text{Mixture thermal diffusivity}$$

$$\nu_{\text{box}} := \frac{\mu_{\text{box}}}{\rho_{\text{box}}}$$

$$\nu_{\text{box}} = 1.749 \times 10^{-5} \frac{\text{m}^2}{\text{s}} \quad \text{Mixture kinematic viscosity}$$

$$\text{Pr}_{\text{box}} := \frac{\nu_{\text{box}}}{\alpha_{\text{box}}}$$

$$\text{Pr}_{\text{box}} = 0.723$$

Mixture Prandtl number

$$\text{Sc}_{\text{box}} := \frac{\nu_{\text{box}}}{D_{wa}}$$

$$\text{Sc}_{\text{box}} = 0.673$$

Mixture Schmidt Number

$$\beta_{\text{box}} := \frac{1}{T_{a.\text{box}}}$$

Ideal gas thermal expansion coefficient

$$L_{\text{box}} := 0.2 \text{ m} \quad \text{Length scale for box}$$

$$T_{\text{hot.box}} := 333 \text{ K} \quad T_{\text{cold.box}} := 293 \text{ K} \quad \text{Hot and cold side wall temperatures}$$

$$Gr_{\text{box}} := \frac{\rho_{\text{box}}^2 \cdot g \cdot \beta_{\text{box}}}{\mu_{\text{box}}} (T_{\text{hot.box}} - T_{\text{cold.box}}) \cdot L_{\text{box}}^3 \quad Gr_{\text{box}} = 3.278 \times 10^7 \quad \text{Grashof Number}$$

$$Ra_{\text{box}} := Gr_{\text{box}} \cdot Pr_{\text{box}} \quad Ra_{\text{box}} = 2.37 \times 10^7 \quad \text{Rayleigh Number}$$

$$Nu_{\text{box}} := 0.18 \left(\frac{Pr_{\text{a.box}} \cdot Ra_{\text{box}}}{0.2 + Pr_{\text{a.box}}} \right)^{0.29} \quad Nu_{\text{box}} = 23.049$$

$$h_{\text{box}} := \frac{Nu_{\text{box}} \cdot k_a}{L_{\text{box}}} \quad h_{\text{box}} = 3.122 \frac{\text{watt}}{\text{m}^2 \cdot \text{K}}$$

Correlation for heat transfer:

Incropera and Dewitt, 2nd ed., p. 440 calls this reference:

-> Catton, I., "Natural Convection in Enclosures," Proceedings of the 6th International Heat Transfer Conference, Toronto, Canada, 1978, Vol. 6, p. 13

Catton calls this reference:

-> Berkovsky and Plevnikov, "_____", Heat Transfer and Turbulent Convection, Spalding, D. B., Afgan. H. eds., Volumes I and II, Hemisphere Publishing, pp. 443-455

Use the analogy between heat and mass transfer to propose this correlation for mass transfer:

$$Sh_{\text{box}} := 0.18 \left(\frac{Sc_{\text{box}}}{0.2 + Sc_{\text{box}}} \cdot Ra_{\text{box}} \right)^{0.29} \quad Sh_{\text{box}} = 22.97$$

$$h_{\text{m.box}} := \frac{Sh_{\text{box}} \cdot D_{\text{wa}}}{L_{\text{box}}} \quad h_{\text{m.box}} = 2.986 \times 10^{-3} \frac{\text{m}}{\text{s}}$$

$$P_{\text{v.sat.hot}} := FP_{\text{v.sat}} \text{KKHM} \left(\frac{T_{\text{hot.box}}}{\text{K}} \right)$$

$$P_{\text{v.sat.cold}} := FP_{\text{v.sat}} \text{KKHM} \left(\frac{T_{\text{cold.box}}}{\text{K}} \right)$$

Water vapor partial pressures at the walls

$$\rho_{\text{v.sat.hot}} := \frac{P_{\text{v.sat.hot}} \cdot MW_{\text{w}}}{R_{\text{gas}} \cdot T_{\text{hot.box}}}$$

$$\rho_{\text{v.sat.cold}} := \frac{P_{\text{v.sat.cold}} \cdot MW_{\text{w}}}{R_{\text{gas}} \cdot T_{\text{cold.box}}}$$

Water vapor density

$$\rho_{\text{v.sat.hot}} = 0.129 \frac{\text{kg}}{\text{m}^3}$$

$$\rho_{\text{v.sat.cold}} = 0.017 \frac{\text{kg}}{\text{m}^3}$$

$$Le_{\text{box}} := \frac{\alpha_{\text{box}}}{D_{\text{wa}}} \quad Le_{\text{box}} = 0.93$$

Now define the Lewis Number for this situation

$$Sh_{\text{box},Le} := \frac{h_{\text{box}}}{Le_{\text{box}}^{0.667} \cdot \rho_{\text{box}} \cdot c_{p,\text{box}}} \cdot \frac{L_{\text{box}}}{D_{\text{wa}}}$$

Sherwood Number estimate using the heat/mass transfer analogy correlation described by:
Incropera and DeWitt, 2nd ed., p.285.

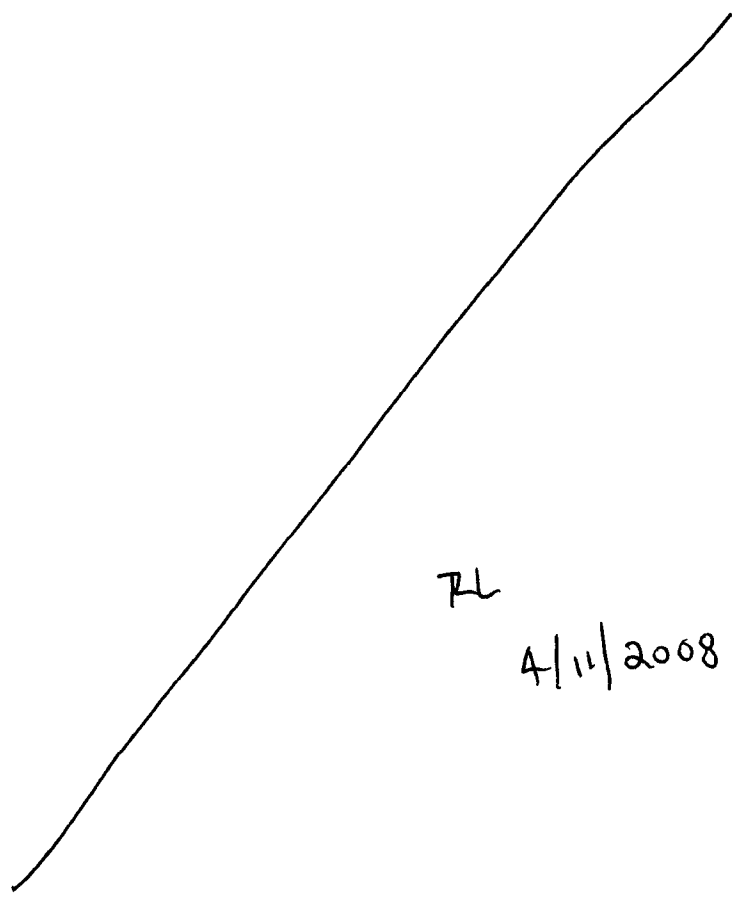
This value is close to the one above; so, just keep using the one above

$$Sh_{\text{box},Le} = 21.838$$

$$h_{m,\text{box},Le} := \frac{Sh_{\text{box},Le} \cdot D_{\text{wa}}}{L_{\text{box}}} \quad h_{m,\text{box},Le} = 2.839 \times 10^{-3} \frac{\text{m}}{\text{s}}$$

$$m\dot{f}_{w,\text{box}} := h_{m,\text{box}} \cdot L_{\text{box}} \cdot (\rho_{v,\text{sat},\text{hot}} - \rho_{v,\text{sat},\text{cold}}) \quad m\dot{f}_{w,\text{box}} = 6.666 \times 10^{-5} \frac{\text{kg}}{\text{ms}} \quad \text{Evaporation rate of water per unit depth of box}$$

$$m\dot{f}_{w,\text{box},Le} := h_{m,\text{box},Le} \cdot L_{\text{box}} \cdot (\rho_{v,\text{sat},\text{hot}} - \rho_{v,\text{sat},\text{cold}}) \quad m\dot{f}_{w,\text{box},Le} = 6.338 \times 10^{-5} \frac{\text{kg}}{\text{ms}} \quad \text{Evaporation rate of water per unit depth of box using Lewis number correlation}$$



RL
4/11/2008

The CFD calculations for the SME paper were performed with FLOW-3D, Version 8.1. The installation of this code for CNWRA purposes has been documented by David Walter in Scientific Notebook

The FLOW3D input file for the laminar boundary layer problem is as follows:

Evaporation from a flat plate with laminar air flow
Air at 0% R.H. flows at 1 m/sec over a 1 m long f; at plate
Re = 5e4 => laminar flow over entire length
Uses S.Green's phase change model and scalar tracking method

```
$xput
  remark='units are ...',
  itb=0, ifenrg=2, ifrho=1, ihtc=1, ifvis=0,
  iadiz=1, imphtc=1,
  iusrd = 1,
  twfin=20.,
$end

$limits
$end

$props
  rhof=1.177,
  mu1=2.e-05, units='si', cv1=717., thc1=0.026,
$end

$scalar
  nsc=2,
  isclr(1)=2, cmisc(1)=2.6e-05, scltit(1)='Vap.Wat',
  isclr(2)=2, cmisc(2)=0., scltit(2)='Liq.Water',
$end

$bcdata
  wl=6, wr=8,
  wf=1, wbk=1,
  wb=2, wt=6,
  ubc(1)=1., tbc(1)=300., sclbc(1,1)=0.,
  tbc(6)=300., ubc(6)=1., pbc(6)=101300., sclbc(6,1)=0.,
$end

$mesh
  px(1)=0.0,          px(1)=0.0, sizez(1)=4.e-04,
  px(2)=1.0,          pz(2)=0.05,
  nxcelt=20, nycelt=1, nzcelt=50,
$end

$obs
  avrck=-3.1,
  tobs(1)=0., tobs(2)=1000.,
  nob=1, iob(1)=1, ioh(1)=1, zh(1)=.0002,
  twobs(1,1)=300., twobs(2,1)=300.,
$end

$fl
  ui=1.,
```

576
576
4/2/08

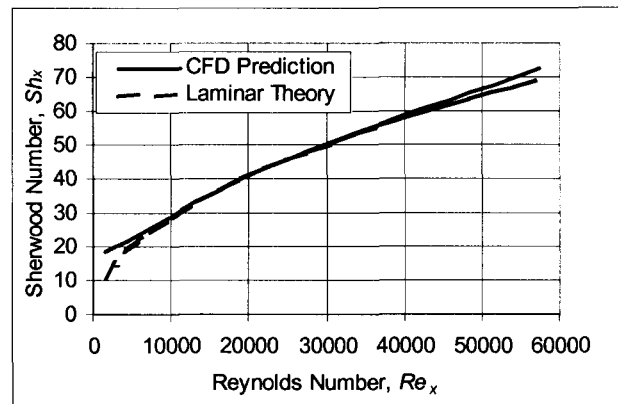
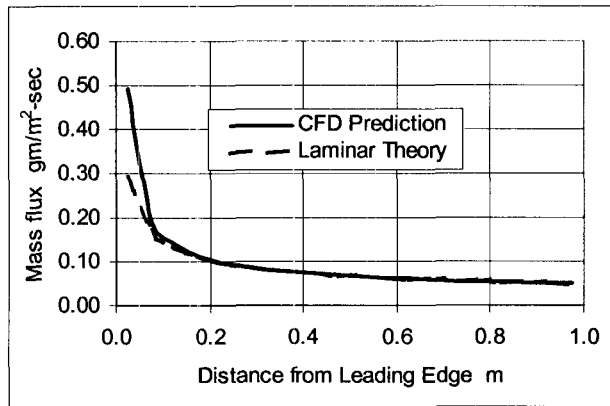
```
sclri(1)=0., sclri(2)=0.,  
presi=101300.,  
$end  
  
$bf  
$end  
  
$temp  
tempi=300.,  
$end  
  
$motn  
$end  
  
$grafic  
$end  
  
$parts  
$end  
  
$usrdat  
imoist_stg(1) = -1,  
isvap_stg = 1,  
isliq_stg = 2,  
hvvap_stg=2300.,  
cvvap_stg=1411.,  
rvap_stg=416.,  
rgas_stg=289.,  
$end
```

Documentation: general comments, background, expectations, etc.

The value of sclr(2) is equal to the mass flux in kg/sec/m². This value is extracted from the data files by using the FLOW3D GUI and saved to an ASCII test file. The values are then imported into the spreadsheet

C:\Projects\div20\moisture_transport\blayer.xls

This spreadsheet compares the FLOW-3D results to the predictions using laminar boundary layer theory. The graphs contained in the spreadsheet are reproduced here



The FLOW3D input file for the 2-D box problem is as follows:

```

Title
This is a sample input file

$xput
  remark='units are SI',
  itb=0, ifvis=3, ifenrg=2, ifrho=1, ihtc=2, ipdis=1,
  gz=-9.8,
  iadiz=1,
  iusrd=1,
  delt=1.e-4, pltdt=2.,
  twfin=50.0,
$end

$limits
$end

$props
  rhof=1.097,
  mu1=2.e-05, units='si',
  cv1=717., thc1=0.026,
$end

$scalar
  nsc=2,
  isclr(1)=2, cmisc(1)=0.26e-04, scltit(1)='Vap.Water', rmisc=0.5,
  isclr(2)=0, cmisc(2)=0., scltit(2)='Liq.Water',
$end

$bcdata
  wl=2, wr=2, wf=1, wbk=1,
  wb=2, wt=2,
$end

$mesh
  px(2)=0.20,      pz(2)=0.20,

```

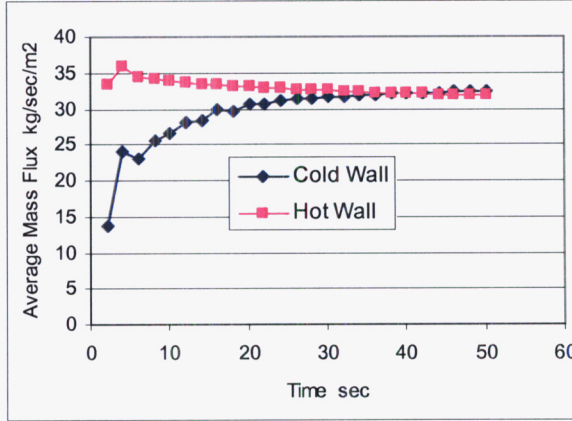
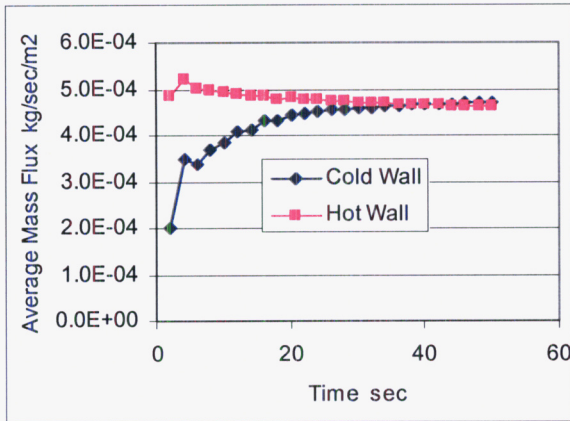
```
    nxcelt=40, nycelt=1, nzcelt=40,  
$end  
  
$obs  
    avrck=-3.1,  
    nobs = 2,  
    tobs(1)=0., tobs(2)=1000.,  
    xh(1)=0.0025,  
    twobs(1,1)=333., twobs(2,1)=333.,  
    xl(2)=0.1975,  
    twobs(1,2)=293., twobs(2,2)=293.,  
$end  
  
$fl  
    sclr(1)=0.046,  
    presi=101300.,  
$end  
  
$bf  
$end  
  
$temp  
    ntmp=1,  
    tempi=313.,  
$end  
  
$motn  
$end  
  
$grafic  
$end  
  
$parts  
$end  
  
$usrdat  
    imoist_stg(1) = -1,  
    imoist_stg(2) = -2,  
    isvap_stg = 1,  
    isliq_stg = 2,  
    hvvap_stg=2300.,  
    cvvap_stg=717.,  
    rvap_stg=416.,  
    rgas_stg=289.,  
$end
```

Documentation: general comments, background, expectations, etc.

The value of sclr(2) is equal to the mass flux in kg/sec/m². This value is extracted for each of the two side walls from the data file by using the FLOW3D GUI and saved to an ASCII test file. The values are then imported into the spreadsheet

C:\Projects\div20\moisture_transport\natconv_box\evap_box_hot2.xls

This spreadsheet computes the time-dependent mass flux and Sherwood numbers for the two walls. The values are plotted to show that the mass flux values at the two walls are within 1.5% of each other. The graph contained in the spreadsheet are reproduced here



END OF ENTRY FOR 10/21/03

STG

2/22/04

STG

This entry is to document an analysis to approximate the magnitude of the Soret effect (i.e., thermo-diffusion) on the transport of water vapor in a repository drift. One usually ignores the effects of temperature gradient on the diffusion of gases, because in many instances the effect is small. The purpose here is to prove that this assumption is valid in this case.

The so-called Soret effect is the concentration gradient that is produced in multicomponent substances if a temperature gradient is imposed through the mixture. Laboratory measurements of the thermo-diffusion effect exist, but reliable data for air and water vapor have not yet been found by me. We shall use kinetic theory to estimate magnitude of the effect.

A thorough coverage of the kinetic theory of gases is in

Hirshfelder, J. O., Curtiss, C. F., Bird, R. B., **Molecular Theory of Gases and Liquids**, John Wiley and Sons, Inc., New York, 1954

This source will be cited throughout this entry as HCB.

According to HCB, the static concentration difference created by the thermal gradient is given by

$$\Delta x_{thermal} = k_T \ln\left(\frac{T_{hot}}{T_{cold}}\right) \quad \text{(HCB Eq. 8.1-16)} \quad [1]$$

where $\Delta x_{thermal}$ = concentration difference between hot and cold region

k_T = thermodiffusion coefficient ratio

T_{hot} = temperature of hot region

T_{cold} = temperature of cold region

Another way of characterizing the Soret effect is that a thermal gradient can create a mass flux,

$$j_t \approx \frac{D_T}{T_{mean}} \left(\frac{T_{hot} - T_{cold}}{L_{surf}} \right) \quad (\text{HCB Eq. 8.1-7}) \quad [2]$$

where j_T = mass flux due to thermal gradient (e.g., $\text{kg}\cdot\text{m}^{-1}\cdot\text{sec}^{-2}$)

D_T = Soret diffusion coefficient

$$T_{mean} = \frac{T_{cold} T_{hot}}{T_{hot} - T_{cold}} \ln \left(\frac{T_{hot}}{T_{cold}} \right) = \text{mean temperature of gas mixture (see HCB, p. 520)} \quad [3]$$

T_{hot} = hot surface temperature

T_{cold} = cold surface temperature

L_{surf} = distance between the hot and cold surfaces

The Soret diffusion coefficient is given by

$$D_T = k_T \rho_{net} \frac{M_1 M_2}{(x_1 M_1 + x_2 M_2)^2} D_{12} \quad (\text{HCB Eq. 8.1-10}) \quad [4]$$

where k_T = thermodiffusion coefficient ratio

ρ_{net} = net density of gas mixture

x_1 = mole concentration of component 1

x_2 = mole concentration of component 2

M_1 = molecular weight of component 1

M_2 = molecular weight of component 2

D_{12} = binary isothermal diffusion, "Fickian", diffusion coefficient ratio

Clearly, the estimation of thermodiffusion effects hinges on the diffusion coefficient ratio, k_T .

According to HCB, the first order approximation to the thermo diffusion

$$k_T = \frac{x_1 x_2}{6 \lambda_{12}} \frac{S_1 x_1 - S_2 x_2}{X_\lambda + Y_\lambda} (6C_{12} - 5) \quad (\text{HCB Eq. 8.2-50}) \quad [5]$$

where k_T = thermodiffusion coefficient ratio, a positive value indicates that component 1 moves into the cooler region and component 2 moves into the warmer region

x_1 = mole concentration of component 1

x_2 = mole concentration of component 2

$$\lambda_{12} = \frac{15}{4} k_B \eta_{12} \left(\frac{m_2 - m_1}{2m_1 m_2} \right) = \text{thermal conductivity of a hypothetical pure substance with the mixture molecular weight} = 2M_1 M_2 / (M_1 + M_2) \quad (\text{HCB Eq. 8.2-35}) \quad [6]$$

M_1 = molecular weight of component 1

M_2 = molecular weight of component 2

m_1 = weight of a single molecule of component 1

m_2 = weight of a single molecule of component 2

k_B = Boltzmann constant

$$\eta_{12} = \frac{5}{16} \left(\frac{\sqrt{2\pi m_1 m_2 k_B T / (m_1 + m_2)}}{\pi \sigma_{12}^2 \Omega_{12}^{(2,2)}(T_{12}^*)} \right) = \text{dynamic viscosity of a hypothetical pure substance with the mixture molecular weight} = 2M_1 M_2 / (M_1 + M_2) \quad (\text{HCB Eq. 8.2-20}) \quad [6]$$

$$T_{12}^* = T \frac{k_B}{\epsilon_{12}} = \text{reduced temperature (defined in conjunction with HCB Eq. 8.2-6)} \quad [5]$$

$$\sigma_{12} = \frac{1}{2} (\sigma_1 + \sigma_2) = \text{combination of molecular collision diameters (HCB Eq. 8.4-8)} \quad [5]$$

$$\epsilon_{12} = \sqrt{\epsilon_1 \epsilon_2} = \text{combination of minimum intermolecular potential energies (HCB Eq. 8.4-9)} \quad [5]$$

The quantities σ_1 , σ_2 , ϵ_1 , ϵ_2 are tabulated from experimental data for various kinds of models for intermolecular interactions. The Lennard-Jones (6-12) model is commonly used and is used here as well.

$$S_1 = \frac{M_1 + M_2}{2M_2} \frac{\lambda_{12}}{\lambda_1} - \frac{15}{4A_{12}} \left(\frac{M_2 - M_1}{2M_1} \right) = \text{convenience factor from derivation} \quad [6]$$

$$S_2 = \frac{M_1 + M_2}{2M_1} \frac{\lambda_{12}}{\lambda_2} - \frac{15}{4A_{12}} \left(\frac{M_1 - M_2}{2M_2} \right) = \text{convenience factor from derivation} \quad [7]$$

$$\lambda_1 = \frac{15}{4} \frac{k_B}{m_1} \eta_1 = \text{thermal conductivity of component 1}$$

$$\lambda_2 = \frac{15}{4} \frac{k_B}{m_2} \eta_2 = \text{thermal conductivity of component 2}$$

$$\eta_1 = \frac{5}{16} \left(\frac{\sqrt{\pi m_1 k_B T}}{\pi \sigma_1^2 \Omega_1^{(2,2)}(T_1^*)} \right) = \text{dynamic viscosity of component 1}$$

$$\eta_2 = \frac{5}{16} \left(\frac{\sqrt{\pi m_2 k_B T}}{\pi \sigma_2^2 \Omega_2^{22}(T_2^*)} \right) = \text{dynamic viscosity of component 2}$$

$$X_\lambda = \frac{x_1^2}{\lambda_1} + \frac{2x_1x_2}{\lambda_{12}} + \frac{x_2^2}{\lambda_2} \quad (\text{HCB Eq. 8.2-36}) \quad [8]$$

$$Y_\lambda = \frac{x_1^2}{\lambda_1} U_1 + \frac{2x_1x_2}{\lambda_{12}} U_Y + \frac{x_2^2}{\lambda_2} U_2 \quad (\text{HCB Eq. 8.2-36}) \quad [9]$$

$$U_1 = \frac{4}{15} A_{12} - \frac{1}{12} \left(\frac{12}{5} B_{12} + 1 \right) \frac{M_1}{M_2} + \frac{1}{2} \frac{(M_1 - M_2)^2}{M_1 M_2} \quad (\text{HCB Eq. 8.2-36}) \quad [10]$$

$$U_2 = \frac{4}{15} A_{12} - \frac{1}{12} \left(\frac{12}{5} B_{12} + 1 \right) \frac{M_2}{M_1} + \frac{1}{2} \frac{(M_2 - M_1)^2}{M_1 M_2} \quad (\text{HCB Eq. 8.2-36}) \quad [11]$$

$$U_Y = \frac{4}{15} A_{12} \left(\frac{(M_1 + M_2)^2}{4M_1 M_2} \right) \frac{\lambda_{12}}{\lambda_1 \lambda_2} - \frac{1}{12} \left(\frac{12}{5} B_{12} + 1 \right) - \frac{5}{32 A_{12}} \left(\frac{12}{5} B_{12} - 5 \right) \frac{(M_1 - M_2)^2}{M_1 M_2} \quad (\text{HCB Eq. 8.2-36}) \quad [12]$$

$$A_{12} = \frac{\Omega_{12}^{22}}{\Omega_{12}^{11}} \quad (\text{HCB Eq. 8.2-15}) \quad [13]$$

$$B_{12} = \frac{5\Omega_{12}^{12} - 4\Omega_{12}^{13}}{\Omega_{12}^{11}} \quad (\text{HCB Eq. 8.2-16}) \quad [14]$$

$$C_{12} = \frac{\Omega_{12}^{12}}{\Omega_{12}^{11}} \quad (\text{HCB Eq. 8.2-17}) \quad [15]$$

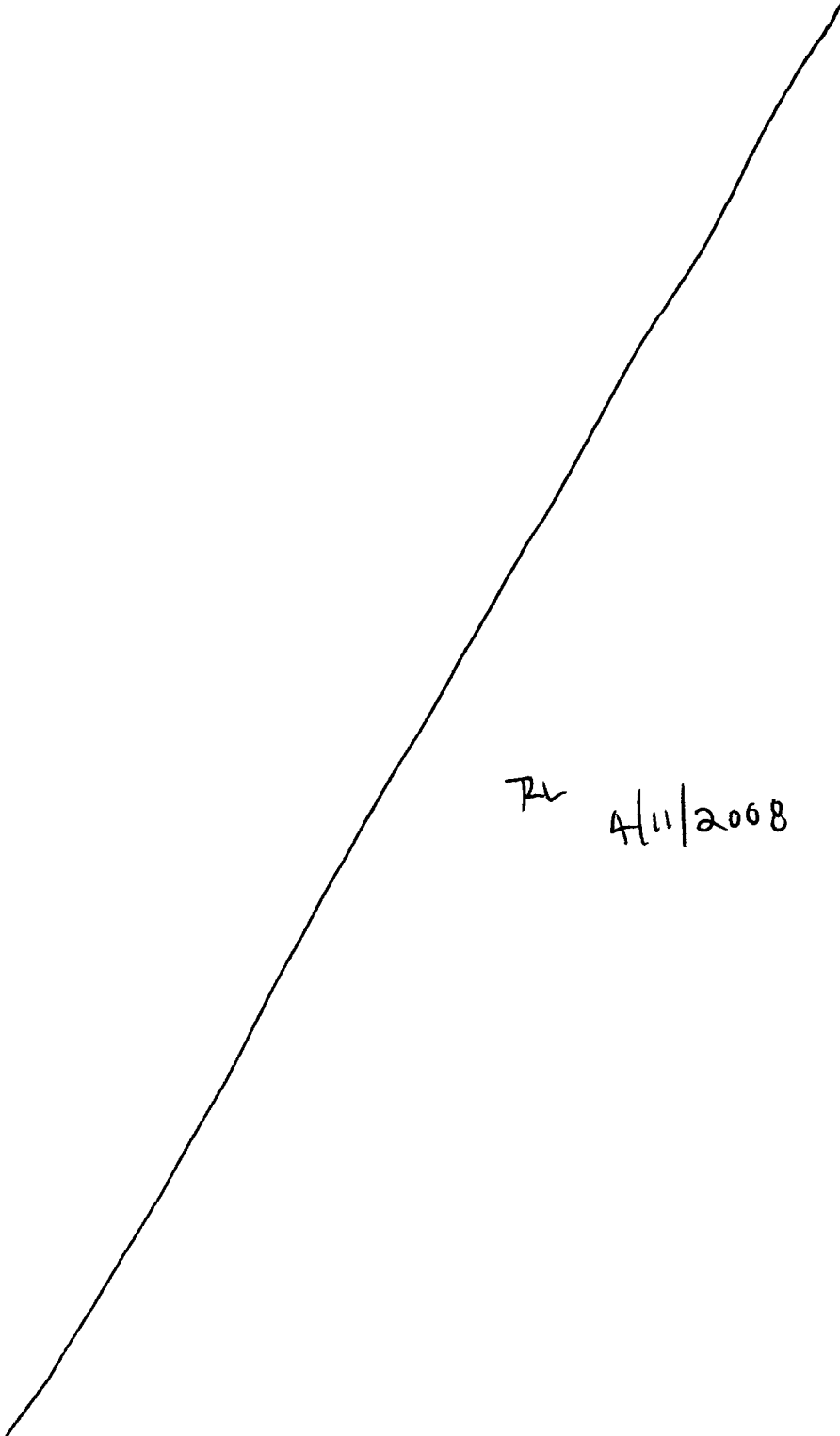
NOTE: the superscripts on the Ω terms are notation, not exponents. The Ω -terms, are integrals arriving from the statistical mechanics of kinetic theory (see HCB, pp.523-528). These integrals are functions of temperature, intermolecular energy, and intermolecular collision distance. These integrals are solved numerically and tabulated values are provided in HCB. The method of computation is described in the example problem presented below.

It should be noted that HCB refers to this approach as a "first approximation" to the calculation of the thermal diffusion coefficient and thermal diffusion coefficient ratio. This approximation arises from considering only the lowest order terms in the Sonine polynomial used to solve the integrals in the kinetic theory statistical mechanics equations (see HCB p. 475) The details of the analysis are omitted here.

The equations described above were programmed into Mathcad. The method was first applied to an example problem in HCB to verify that the equations had been properly interpreted and programmed. The Mathcad sheet is

C:\Projects\div20\moisture_transport\soret\soret.mcd

The pertinent parts of this Mathcad sheet are duplicated here. Note that, because of a nomenclature feature of Mathcad, the notation of the Ω -integrals is transformed from the form shown above. For example, Ω_{12}^{11} becomes $\Omega_{11.12}$ in the Mathcad sheet.



RV 4/11/2008

Example Problem from HCB:

Calculate k_T for 35.6% H_2 and 64.4% Ne for $T_{cold}=90.2K$, $T_{hot}=290.4K$

Define 'universal' constants

$$k_B := 1.38 \cdot 10^{-16} \frac{\text{erg}}{\text{K}} \quad \text{Boltzmann constant} \quad \text{angstrom} := 10^{-8} \cdot \text{cm} \quad \text{Define Angstrom units}$$

$$N_{av} := \frac{6.023 \cdot 10^{23}}{\text{mole}} \quad \text{Avogadro's Number} \quad R_{gas} := 8.314 \frac{\text{joule}}{\text{mol} \cdot \text{K}} \quad \text{Ideal gas constant}$$

Define problem conditions

$$T_{cold} := 90.2K \quad T_{hot} := 290.4K \quad \text{Temperatures}$$

$$x_1 := 0.356 \quad x_2 := 0.644 \quad \text{Mole Fractions}$$

Component 1 is H_2
Component 2 is Ne

Compute or define the remaining gas properties and mixture quantities

$$T_{mean} := \frac{T_{cold} \cdot T_{hot}}{T_{hot} - T_{cold}} \cdot \ln \left(\frac{T_{hot}}{T_{cold}} \right) \quad T_{mean} = 152.98K \quad \text{Mean temperature}$$

$$M_1 := 2.016 \frac{\text{gm}}{\text{mol}} \quad M_2 := 20.813 \frac{\text{gm}}{\text{mol}} \quad \text{Molecular weights}$$

$$\sigma_1 := 2.827 \text{angstrom} \quad \sigma_2 := 2.789 \text{angstrom} \quad \text{Collision diameter, from HCB, Table 1-A}$$

$$\epsilon_1 := 33.3K \cdot k_B \quad \epsilon_2 := 35.7K \cdot k_B \quad \text{Collision energy, from HCB, Table 1-A}$$

$$m_1 := \frac{M_1}{N_{av}} \quad m_2 := \frac{M_2}{N_{av}} \quad \text{Mass of molecule}$$

$$T'_1 := T_{mean} \cdot \frac{k_B}{\epsilon_1} \quad T'_2 := T_{mean} \cdot \frac{k_B}{\epsilon_2} \quad \text{Reduced Temperature}$$

$$T'_1 = 4.594 \quad T'_2 = 4.285$$

$$C_{v,1} := 10.0849 \frac{\text{joule}}{\text{gm} \cdot \text{K}} \cdot M_1 \quad C_{v,2} := 0.6179 \frac{\text{joule}}{\text{gm} \cdot \text{K}} \cdot M_2 \quad \text{Specific Heat}$$

$$\sigma_{12} := \frac{1}{2} \cdot (\sigma_1 + \sigma_2)$$

$$\epsilon_{12} := \sqrt{\epsilon_1 \cdot \epsilon_2} \quad T'_{12} := T_{mean} \cdot \frac{k_B}{\epsilon_{12}} \quad T'_{12} = 4.437$$

"Mixture" values for collision diameter and energy

Ω -integral values from Table I-M in HCB

Section of Table I-M from HCB for the H_2 -Ne example problem

T^*	$\Omega^{(1,1)*}$	$\Omega^{(1,2)*}$	$\Omega^{(1,3)*}$	$\Omega^{(2,2)*}$	$\Omega^{(2,3)*}$	$\Omega^{(2,4)*}$	$\Omega^{(3,3)*}$	$\Omega^{(3,4)*}$	$\Omega^{(4,4)*}$
4.1	0.6700	0.6167	0.7720	0.9097	0.9133	0.8805	0.8338	0.8311	0.9167
4.2	0.8740	0.8093	0.7727	0.9600	0.9093	0.8770	0.8533	0.8342	0.9125
4.3	0.8694	0.8060	0.7697	0.9553	0.9055	0.8735	0.8500	0.8312	0.9088
4.4	0.8652	0.8027	0.7668	0.9507	0.9018	0.8705	0.8467	0.8283	0.9054
4.5	0.8610	0.7993	0.7640	0.9464	0.8985	0.8670	0.8442	0.8256	0.9021
4.6	0.8568	0.7960	0.7613	0.9422	0.8950	0.8640	0.8408	0.8229	0.8988
4.7	0.8530	0.7933	0.7585	0.9382	0.8918	0.8610	0.8383	0.8202	0.8954
4.8	0.8492	0.7907	0.7560	0.9344	0.8885	0.8585	0.8358	0.8177	0.8925

$T^* = 4.285$ for Ne

$T^* = 4.437$ for Combined

$T^* = 4.594$ for H_2

$T_1 = 4.594$

$T_2 = 4.285$

Values needed for the pure individual components in the viscosity and thermal conductivity equations

$$\Omega_{22.1} := \frac{4.594 - 4.5}{4.6 - 4.5} \cdot (.9422 - .9464) + 0.9464$$

$$\Omega_{22.2} := \frac{(4.285 - 4.2)}{4.3 - 4.2} \cdot (.9553 - .9600) + .9600$$

$\Omega_{22.1} = 0.942$

$\Omega_{22.2} = 0.956$

$$\Omega_{11.12} := \frac{4.437 - 4.4}{4.5 - 4.4} \cdot (.8610 - .8652) + .8652$$

$\Omega_{11.12} = 0.864$

Values needed for the combined gas relations

$$\Omega_{12.12} := \frac{4.437 - 4.4}{4.5 - 4.4} \cdot (.7993 - .8027) + .8027$$

$\Omega_{12.12} = 0.801$

$$\Omega_{13.12} := \frac{4.437 - 4.4}{4.5 - 4.4} \cdot (.7640 - .7668) + .7668$$

$\Omega_{13.12} = 0.766$

$\Omega_{22.1} = 0.9424$ for the HCB textbook answer
 $\Omega_{22.2} = 0.9560$ for the HCB textbook answer
 $\Omega_{22.12} = 0.9492$ for the HCB textbook answer

$$\Omega_{22.12} := \frac{4.437 - 4.4}{4.5 - 4.4} \cdot (.9464 - .9507) + .9507$$

$\Omega_{22.12} = 0.949$

$$\Omega_{23.12} := \frac{4.437 - 4.4}{4.5 - 4.4} \cdot (.8985 - .9018) + .9018$$

$\Omega_{23.12} = 0.901$

$$A_{12} := \frac{\Omega_{22.12}}{\Omega_{11.12}}$$

$A_{12} = 1.099$

$A_{12} = 1.099$ for the HCB textbook answer
 $B_{12} = 1.093$ for the HCB textbook answer
 $C_{12} = 0.928$ for the HCB textbook answer

$$B_{12} := \frac{5 \cdot \Omega_{12.12} - 4 \cdot \Omega_{13.12}}{\Omega_{11.12}}$$

$B_{12} = 1.093$

$$C_{12} := \frac{\Omega_{12.12}}{\Omega_{11.12}}$$

$C_{12} = 0.928$

Component and combined viscosity and thermal conductivity

$$\eta_1 := \frac{5}{16} \cdot \frac{\sqrt{\pi \cdot m_1 \cdot k_B \cdot T_{\text{mean}}}}{\pi \cdot \sigma_1^2 \cdot \Omega_{22.1}}$$

$$\eta_1 = 6.222 \times 10^{-5} \frac{\text{gm}}{\text{cm} \cdot \text{sec}}$$

$$\lambda_1 := \frac{15}{4} \cdot \frac{k_B}{m_1} \cdot \eta_1$$

$$\lambda_1 = 2.298 \times 10^{-4} \frac{\text{cal}}{\text{sec} \cdot \text{cm} \cdot \text{K}}$$

$$\lambda_1 = 0.096 \frac{\text{watt}}{\text{m} \cdot \text{K}}$$

$$\lambda_{1.\text{Eucken}} := \frac{15}{4} \cdot \frac{R_{\text{gas}}}{M_1} \cdot \eta_1 \cdot \left(\frac{4}{15} \cdot \frac{C_{v,1}}{R_{\text{gas}}} + \frac{3}{5} \right)$$

$$\lambda_{1.\text{Eucken}} = 2.878 \times 10^{-4} \frac{\text{cal}}{\text{sec} \cdot \text{cm} \cdot \text{K}}$$

$$\eta_{12} := \frac{5}{16 \pi \sigma_{12}^2 \cdot \Omega_{22.12}} \cdot \sqrt{\frac{2 \cdot \pi \cdot m_1 \cdot m_2 \cdot k_B \cdot T_{\text{mean}}}{m_1 + m_2}}$$

$$\eta_{12} = 8.457 \times 10^{-6} \text{ Pa} \cdot \text{sec}$$

$$\lambda_{12} := \frac{15}{4} \cdot k_B \cdot \frac{m_1 + m_2}{2 \cdot m_1 \cdot m_2} \cdot \eta_{12}$$

$$\lambda_{12} = 1.713 \times 10^{-4} \frac{\text{cal}}{\text{sec} \cdot \text{cm} \cdot \text{K}}$$

$\lambda_1 = 2087 \times 10^7$ for the HCB textbook answer

$\lambda_2 = 737 \times 10^7$ for the HCB textbook answer

$\lambda_{12} = 1634 \times 10^7$ for the HCB textbook answer

TZL
4/11/2008

Final computation for thermal diffusion coefficient ratio

$$U_1 := \frac{4}{15} \cdot A_{12} - \frac{1}{12} \cdot \left(\frac{12}{5} \cdot B_{12} + 1 \right) \cdot \frac{M_1}{M_2} + \frac{1}{2} \cdot \frac{(M_1 - M_2)^2}{M_1 \cdot M_2} \quad U_1 = 4.474$$

$$U_2 := \frac{4}{15} \cdot A_{12} - \frac{1}{12} \cdot \left(\frac{12}{5} \cdot B_{12} + 1 \right) \cdot \frac{M_2}{M_1} + \frac{1}{2} \cdot \frac{(M_2 - M_1)^2}{M_1 \cdot M_2} \quad U_2 = 1.386$$

$$U_Y := \frac{4}{15} \cdot A_{12} \cdot \frac{(M_1 + M_2)^2}{4 \cdot M_1 \cdot M_2} \cdot \frac{\lambda_{12}^2}{\lambda_1 \cdot \lambda_2} - \frac{1}{12} \cdot \left(\frac{12}{5} \cdot B_{12} + 1 \right) - \frac{5}{32 \cdot A_{12}} \cdot \left(\frac{12}{5} \cdot B_{12} - 5 \right) \cdot \frac{(M_1 - M_2)^2}{M_1 \cdot M_2} \quad U_Y = 4.147$$

$$X_\lambda := \frac{x_1^2}{\lambda_1} + \frac{2 \cdot x_1 \cdot x_2}{\lambda_{12}} + \frac{x_2^2}{\lambda_2}$$

$$Y_\lambda := \frac{x_1^2}{\lambda_1} \cdot U_1 + \frac{2 \cdot x_1 \cdot x_2}{\lambda_{12}} \cdot U_Y + \frac{x_2^2}{\lambda_2} \cdot U_2$$

$$X_\lambda + Y_\lambda = 3.046 \times 10^4 \text{ sec} \cdot \text{cm} \cdot \frac{\text{K}}{\text{cal}}$$

$$X_\lambda + Y_\lambda = 3.030 \times 10^{-3} \text{ for the HCB textbook answer}$$

(the text retains a 10^7 factor for the units on λ)

$$S_1 := \frac{M_1 + M_2}{2 \cdot M_2} \cdot \frac{\lambda_{12}}{\lambda_1} - \frac{15}{4 \cdot A_{12}} \cdot \left(\frac{M_2 - M_1}{2 \cdot M_1} \right) - 1 \quad S_1 = -16.499 \quad S_1 = -15.94 \text{ for the HCB textbook answer}$$

$$S_2 := \frac{M_2 + M_1}{2 \cdot M_1} \cdot \frac{\lambda_{12}}{\lambda_2} - \frac{15}{4 \cdot A_{12}} \cdot \left(\frac{M_1 - M_2}{2 \cdot M_2} \right) - 1 \quad S_2 = 13.928 \quad S_2 = -12.75 \text{ for the HCB textbook answer}$$

$$k_T := \frac{x_1 \cdot x_2}{6 \cdot \lambda_{12}} \cdot \frac{S_1 \cdot x_1 - S_2 \cdot x_2}{X_\lambda + Y_\lambda} \cdot (6 \cdot C_{12} - 5) \quad k_T = -0.062 \quad k_T = -0.0607 \text{ for the HCB textbook answer}$$

This result agrees well enough with the value in HCB. The cause of the slight discrepancies are not known. They could be related to the fact that HCB might be using another approximation equation for the viscosity and thermal conductivity expressions.

Now that the method has been verified, turn to the problem of water vapor diffusion in air.

Compute k_T and thermo-diffusion rate for Air/Water Vapor mixture, 50% RH @ 300K
Assume a 100°C temperature difference over a 1 m distance

Specify mixture temperature and concentration conditions:

$$T_{\text{mean}} := 300 \text{ K}$$

$$\phi := 50\%$$

Approximate saturation pressure for water vapor/liquid interface

$$F_0 := -741.9242$$

$$F_4 := 0.1094098$$

$$F_1 := -29.721$$

$$F_5 := 0.439993$$

$$F_2 := -11.5286$$

$$F_6 := 0.2520658$$

$$F_3 := -0.8685635$$

$$F_7 := 0.05218684$$

This expression is given by Keenan, Keyes, Hill, and Moore in Steam Tables

$$FP_{\text{vsat}}_{\text{KKHM}}(T) := 217.99 \exp \left[\frac{0.01}{T} \cdot [374.136 - (T - 273.15)] \cdot \sum_{k=0}^7 \left[F_k \cdot [0.65 - 0.01 \cdot (T - 273.15)]^k \right] \right] \text{ atm}$$

Compute or define the remaining gas properties and mixture quantities

$$D_{\text{v,a}} := 0.026 \frac{\text{m}^2}{\text{sec}}$$

Coefficient of diffusion of water vapor into air. From heat transfer texts.

$$P_{\text{ref}} := 1 \cdot \text{atm}$$

$$P_{\text{s,H}_2\text{O}} := FP_{\text{vsat}}_{\text{KKHM}} \left(\frac{T_{\text{mean}}}{\text{K}} \right)$$

$$P_{\text{s,H}_2\text{O}} = 3.536 \times 10^3 \text{ Pa}$$

Saturation pressure of water at T_{mean}

$$x_1 := 1 - \frac{\phi \cdot P_{\text{s,H}_2\text{O}}}{1 \cdot \text{atm}}$$

$$x_2 := \frac{\phi \cdot P_{\text{s,H}_2\text{O}}}{1 \cdot \text{atm}}$$

Mole concentrations assuming ideal gas law

$$x_1 = 0.983$$

$$x_2 = 0.017$$

Component 1 is air
Component 2 is water vapor

$$M_1 := 28.97 \frac{\text{gm}}{\text{mol}}$$

$$M_2 := 18 \frac{\text{gm}}{\text{mol}}$$

Molecular weights

$$\sigma_1 := 3.617 \text{ angstrom}$$

$$\sigma_2 := 2.641 \text{ angstrom}$$

Collision diameter, from HCB, Table 1-A for Air
from RS, Appendix G for H2O

$$\epsilon_1 := 97.0 \text{ K} \cdot k_B$$

$$\epsilon_2 := 809.1 \text{ K} \cdot k_B$$

Collision energy

$$m_1 := \frac{M_1}{N_{\text{av}}}$$

$$m_2 := \frac{M_2}{N_{\text{av}}}$$

Mass of molecule

$$T_1 := T_{\text{mean}} \cdot \frac{k_B}{\epsilon_1} \quad T_1 = 3.093$$

$$T_2 := T_{\text{mean}} \cdot \frac{k_B}{\epsilon_2} \quad T_2 = 0.371 \quad \text{Reduced Temperature}$$

$$C_{\text{v},1} := 0.7165 \frac{\text{joule}}{\text{gm} \cdot \text{K}} \cdot M_1$$

$$C_{\text{v},2} := 1.4108 \frac{\text{joule}}{\text{gm} \cdot \text{K}} \cdot M_2 \quad \text{Specific Heat} \quad \text{From van Wylen and Sonntag}$$

$$\sigma_{12} := \frac{1}{2} (\sigma_1 + \sigma_2)$$

$$\epsilon_{12} := \sqrt{\epsilon_1 \cdot \epsilon_2}$$

"Mixture" values for collision diameter and energy

TABLE I-M

THE INTEGRALS $\Omega^{(l,s)*}$ FOR CALCULATING THE TRANSPORT COEFFICIENTS FOR THE LENNARD-JONES (6-12) POTENTIAL

T^*	$\Omega^{(1,1)*}$	$\Omega^{(1,2)*}$	$\Omega^{(1,3)*}$	$\Omega^{(2,2)*}$	$\Omega^{(2,3)*}$	$\Omega^{(2,4)*}$	$\Omega^{(3,3)*}$	$\Omega^{(3,4)*}$	$\Omega^{(3,5)*}$
0.30	2.662	2.256	1.962	2.785	2.535	2.333	2.152	1.990	2.557
0.35	2.476	2.078	1.795	2.628	2.375	2.163	1.978	1.819	2.378
0.40	2.318	1.931	1.663	2.492	2.232	2.016	1.833	1.682	2.223
0.45	2.184	1.808	1.556	2.368	2.105	1.889	1.713	1.574	2.090
0.95	1.476	1.231	1.096	1.629	1.422	1.286	1.194	1.131	1.410
1.00	1.439	1.204	1.076	1.587	1.388	1.258	1.172	1.113	1.377
1.05	1.406	1.179	1.058	1.549	1.357	1.234	1.152	1.097	1.347
1.10	1.375	1.157	1.041	1.514	1.329	1.212	1.135	1.082	1.319
1.15	1.346	1.137	1.027	1.482	1.304	1.192	1.119	1.068	1.294
2.8	0.9612	0.8767	0.8250	1.038	0.9855	0.9415	0.9117	0.8887	0.9863
2.9	0.9576	0.8700	0.8237	1.048	0.9780	0.9355	0.9058	0.8836	0.9792
3.0	0.9490	0.8640	0.8187	1.039	0.9708	0.9295	0.9008	0.8788	0.9721
3.1	0.9406	0.8580	0.8138	1.030	0.9643	0.9240	0.8958	0.8742	0.9658
3.2	0.9328	0.8520	0.8093	1.022	0.9578	0.9185	0.8908	0.8698	0.9596
3.3	0.9256	0.8473	0.8048	1.014	0.9519	0.9125	0.8847	0.8636	0.9528

$T^* = 0.371$ for Water Vapor

$T^* = 1.071$ for Combined

$T^* = 3.093$ for Air

$T_1 = 3.093$

$T_2 = 0.371$

Values needed for the pure individual components in the viscosity and thermal conductivity equations

$\Omega_{22.1} := \frac{3.093 - 3.0}{3.1 - 3.0} \cdot (1.030 - 1.039) + 1.039$

$\Omega_{22.2} := \frac{(0.371 - 0.35)}{0.40 - 0.35} \cdot (2.492 - 2.628) + 2.628$

$\Omega_{22.1} = 1.031$

$\Omega_{22.2} = 2.571$

$T_{12} := T_{\text{mean}} \cdot \frac{k_B}{\epsilon_{12}} \quad T_{12} = 1.071$

$\Omega_{11.12} := \frac{1.071 - 1.05}{1.10 - 1.05} \cdot (1.375 - 1.406) + 1.406 \quad \Omega_{11.12} = 1.393$

$\Omega_{12.12} := \frac{1.071 - 1.05}{1.10 - 1.05} \cdot (1.157 - 1.179) + 1.179 \quad \Omega_{12.12} = 1.17 \quad \Omega_{22.12} := \frac{1.071 - 1.05}{1.10 - 1.05} \cdot (1.514 - 1.549) + 1.549 \quad \Omega_{22.12} = 1.534$

$\Omega_{13.12} := \frac{1.071 - 1.05}{1.10 - 1.05} \cdot (1.041 - 1.058) + 1.058 \quad \Omega_{13.12} = 1.051 \quad \Omega_{23.12} := \frac{1.071 - 1.05}{1.10 - 1.05} \cdot (1.329 - 1.357) + 1.357 \quad \Omega_{23.12} = 1.345$

Values needed for the combined gas relations

$A_{12} := \frac{\Omega_{22.12}}{\Omega_{11.12}} \quad A_{12} = 1.101$

$B_{12} := \frac{5 \cdot \Omega_{12.12} - 4 \cdot \Omega_{13.12}}{\Omega_{11.12}} \quad B_{12} = 1.181$

$C_{12} := \frac{\Omega_{22.12}}{\Omega_{11.12}} \quad C_{12} = 0.84$

Component and combined viscosity and thermal conductivity

$$\eta_1 := \frac{5}{16} \cdot \frac{\sqrt{\pi \cdot m_1 \cdot k_B \cdot T_{\text{mean}}}}{\pi \cdot \sigma_1^2 \cdot \Omega_{22.1}}$$

$$\eta_1 = 1.845 \times 10^{-4} \frac{\text{gm}}{\text{cm} \cdot \text{sec}}$$

$$\lambda_1 := \frac{15}{4} \cdot \frac{k_B}{m_1} \cdot \eta_1$$

$$\lambda_1 = 4.742 \times 10^{-5} \frac{\text{cal}}{\text{sec} \cdot \text{cm} \cdot \text{K}}$$

$$\lambda_1 = 0.02 \frac{\text{watt}}{\text{m} \cdot \text{K}}$$

$$\lambda_{1.\text{Eucken}} := \frac{15}{4} \cdot \frac{R_{\text{gas}}}{M_1} \cdot \eta_1 \cdot \left(\frac{4}{15} \cdot \frac{C_{v,1}}{R_{\text{gas}}} + \frac{3}{5} \right)$$

$$\lambda_{1.\text{Eucken}} = 6.004 \times 10^{-5} \frac{\text{cal}}{\text{sec} \cdot \text{cm} \cdot \text{K}}$$

$$\eta_2 := \frac{5}{16} \cdot \frac{\sqrt{\pi \cdot m_2 \cdot k_B \cdot T_{\text{mean}}}}{\pi \cdot \sigma_2^2 \cdot \Omega_{22.2}}$$

$$\eta_2 = 1.094 \times 10^{-4} \frac{\text{gm}}{\text{cm} \cdot \text{sec}}$$

$$\lambda_2 := \frac{15}{4} \cdot \frac{k_B}{m_2} \cdot \eta_2$$

$$\lambda_2 = 4.523 \times 10^{-5} \frac{\text{cal}}{\text{sec} \cdot \text{cm} \cdot \text{K}}$$

$$\lambda_2 = 0.019 \frac{\text{watt}}{\text{m} \cdot \text{K}}$$

$$\frac{15}{4} \cdot \frac{R_{\text{gas}}}{M_1} \cdot \eta_1 = 4.743 \times 10^{-5} \frac{\text{cal}}{\text{sec} \cdot \text{cm} \cdot \text{K}}$$

$$\eta_{12} := \frac{5}{16 \pi \cdot \sigma_{12}^2 \cdot \Omega_{22.12}} \cdot \sqrt{\frac{2 \cdot \pi \cdot m_1 \cdot m_2 \cdot k_B \cdot T_{\text{mean}}}{m_1 + m_2}}$$

$$\eta_{12} = 1.45 \times 10^{-5} \text{Pa} \cdot \text{sec}$$

$$\lambda_{12} := \frac{15}{4} \cdot k_B \cdot \frac{m_1 + m_2}{2 \cdot m_1 \cdot m_2} \cdot \eta_{12}$$

$$\lambda_{12} = 4.862 \times 10^{-5} \frac{\text{cal}}{\text{sec} \cdot \text{cm} \cdot \text{K}}$$

RL
4/11/2008

Final computation for thermal diffusion coefficient ratio

$$U_1 := \frac{4}{15} \cdot A_{12} - \frac{1}{12} \cdot \left(\frac{12}{5} \cdot B_{12} + 1 \right) \cdot \frac{M_1}{M_2} + \frac{1}{2} \cdot \frac{(M_1 - M_2)^2}{M_1 \cdot M_2} \quad U_1 = -0.105$$

$$U_2 := \frac{4}{15} \cdot A_{12} - \frac{1}{12} \cdot \left(\frac{12}{5} \cdot B_{12} + 1 \right) \cdot \frac{M_2}{M_1} + \frac{1}{2} \cdot \frac{(M_2 - M_1)^2}{M_1 \cdot M_2} \quad U_2 = 0.211$$

$$U_Y := \frac{4}{15} \cdot A_{12} \cdot \frac{(M_1 + M_2)^2}{4 M_1 \cdot M_2} \cdot \frac{\lambda_{12}^2}{\lambda_1 \cdot \lambda_2} - \frac{1}{12} \cdot \left(\frac{12}{5} \cdot B_{12} + 1 \right) - \frac{5}{32 A_{12}} \cdot \left(\frac{12}{5} \cdot B_{12} - 5 \right) \cdot \frac{(M_1 - M_2)^2}{M_1 \cdot M_2} \quad U_Y = 0.094$$

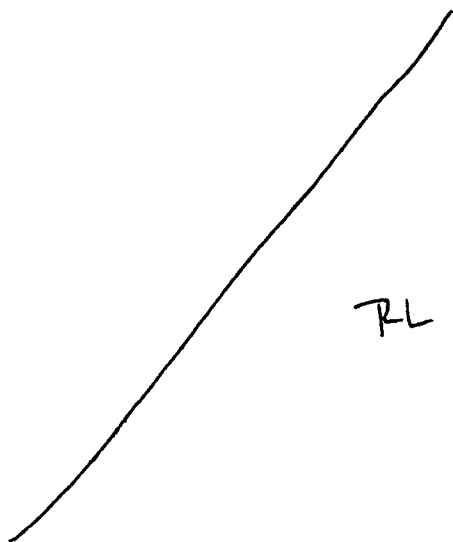
$$X_\lambda := \frac{x_1^2}{\lambda_1} + \frac{2 \cdot x_1 \cdot x_2}{\lambda_{12}} + \frac{x_2^2}{\lambda_2} \quad Y_\lambda := \frac{x_1^2}{\lambda_1} \cdot U_1 + \frac{2 \cdot x_1 \cdot x_2}{\lambda_{12}} \cdot U_Y + \frac{x_2^2}{\lambda_2} \cdot U_2 \quad X_\lambda + Y_\lambda = 1.9 \times 10^4 \text{ sec} \cdot \text{cm} \cdot \frac{\text{K}}{\text{cal}}$$

$$S_1 := \frac{M_1 + M_2}{2 \cdot M_2} \cdot \frac{\lambda_{12}}{\lambda_1} - \frac{15}{4 A_{12}} \cdot \left(\frac{M_2 - M_1}{2 \cdot M_1} \right) - 1 \quad S_1 = 0.982$$

$$S_2 := \frac{M_2 + M_1}{2 \cdot M_1} \cdot \frac{\lambda_{12}}{\lambda_2} - \frac{15}{4 A_{12}} \cdot \left(\frac{M_1 - M_2}{2 \cdot M_2} \right) - 1 \quad S_2 = -1.166$$

$$k_T := \frac{x_1 \cdot x_2}{6 \cdot \lambda_{12}} \cdot \frac{S_1 \cdot x_1 - S_2 \cdot x_2}{X_\lambda + Y_\lambda} \cdot (6 \cdot C_{12} - 5) \quad k_T = 1.175 \times 10^{-4}$$

The positive value means that component 2 will move toward the warmer region. This is against the concentration gradient dictated by the saturation pressure which prescribes a higher concentration at the higher temperature.



RL
4/11/2008

Diffusion fluxes

$$T_{\text{hot}} := T_{\text{mean}} + 50 \cdot \text{K} \quad P_{\text{s.hot}} := \text{FPvsat}_{\text{KKHM}} \left(\frac{T_{\text{hot}}}{\text{K}} \right) \quad x_{2,\text{hot}} := \frac{P_{\text{s.hot}}}{P_{\text{ref}}} \quad \text{Conditions at hot surface}$$

$$T_{\text{cold}} := T_{\text{mean}} - 50 \cdot \text{K} \quad P_{\text{s.cold}} := \text{FPvsat}_{\text{KKHM}} \left(\frac{T_{\text{cold}}}{\text{K}} \right) \quad x_{2,\text{cold}} := \frac{P_{\text{s.cold}}}{P_{\text{ref}}} \quad \text{Conditions at cold surface}$$

$$L_{\text{surf}} := 1 \cdot \text{m} \quad \text{Separation distance of hot and cold surfaces (from assumed problem conditions)}$$

$$\Delta x_{\text{thermal}} := k_T \cdot \ln \left(\frac{T_{\text{hot}}}{T_{\text{cold}}} \right) \quad \Delta x_{\text{thermal}} = 3.952 \times 10^{-5} \quad \text{Static concentration difference due to temperature difference. This would be the concentration difference when there is no net flow of species 2.}$$

$$\rho_{\text{net}} := [x_2 \cdot M_2 + (1 - x_2) \cdot M_1] \cdot \frac{P_{\text{ref}}}{R_{\text{gas}} \cdot T_{\text{mean}}} \quad \text{Net density at mean temperature}$$

$$D_T := k_T \cdot \rho_{\text{net}} \cdot \frac{M_1 \cdot M_2}{(x_1 \cdot M_1 + x_2 \cdot M_2)^2} \cdot D_{\text{v.a}} \quad D_T = 2.248 \times 10^{-6} \frac{\text{kg}}{\text{ms}} \quad \text{Thermal diffusion coefficient for these conditions}$$

$$j_t := \frac{D_T}{T_{\text{mean}}} \cdot \frac{(T_{\text{hot}} - T_{\text{cold}})}{L_{\text{surf}}} \quad j_t = 7.493 \times 10^{-7} \frac{\text{kg}}{\text{m}^2 \cdot \text{s}} \quad \text{Mass flux due to thermal (Soret) diffusion}$$

$$j := \rho_{\text{net}} \cdot D_{\text{v.a}} \cdot \frac{(x_{2,\text{hot}} - x_{2,\text{cold}})}{L_{\text{surf}}} \quad j = 0.012 \frac{\text{kg}}{\text{m}^2 \cdot \text{s}} \quad \text{Fickian ('normal') diffusion}$$

$$\frac{j_t}{j} = 6.009 \times 10^{-3} \%$$

The diffusion due to the concentration gradient is >16,600 times the diffusion in the opposite direction due to the thermal gradient.

CONCLUSION:

Thermo-diffusion effects are negligible compared to Fickian diffusion

END OF ENTRY FOR 2/22/04

STG

due to the temperature dependence of density. The pertinent material properties are listed in the following table

Property	Units	Air	Water Vapor
Density	kg/m ³	0.84638	0.5247
Specific Heat	Joule/kg/K	728.7	1497.9
Viscosity	Pa-sec	2.3543×10 ⁻⁵	1.394×10 ⁻⁵
Thermal expansion coefficient	K ⁻¹	2.432×10 ⁻³	2.489×10 ⁻³
Reference temperature for fluid density	K	417	417

Boundary Conditions

The boundary conditions are the waste package power dissipation and the temperature of the rock at a distance of 1 m from the drift wall surface. The waste packages are assigned a heat generation rate of 1075 watts each. The long cylinder over the rightmost 133 m of drift represents 22.5 waste packages; so, the power generation rate is 24,200 watts.

The outer surface of the 1-m layer of simulated rock was defined by an axially varying temperature profile as predicted by the mountain-scale heat transfer model in the TPA code by Randy Fedors. The temperature profile, representing the rock wall temperature at a time of 109.1 yr after drift closure, is shown in Figure 2.

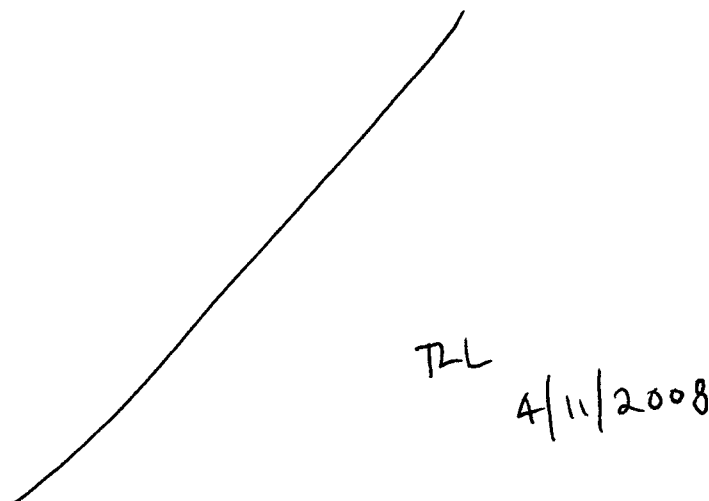
An equation was fitted to the rock temperature values for use in FLOW-3D to define the temperature at the model boundary. A reasonable curve fit for this model is given by

$$T = \frac{76.04796 + 8.4226972x}{1 + 0.062212946x + 9.2009395 \times 10^{-6} x^2} \quad (T \text{ is in } ^\circ\text{C})$$

The curve fit was produced by the commercial software package Table Curve 2D (Version 5.0). The rock wall temperatures and the curve fit coefficients are defined in the Excel spread sheet:

C:\Projects\div20\moisture_transport\Air-Water-Compare \rocktemps.xls

The temperature at the rock wall boundary is assumed to be constant around the circumference at each axial location.



3/12/04 *STG*

This entry is to document the work done to compare the predicted fluid velocity and temperature profiles in a full-scale drift when either pure air or pure water vapor is the gas in the drift. The intent is to give insight into whether there is a strong effect of fluid properties on the gas temperature and circulation rates. If there is a strong effect, then it will be important to accurately model the mixture properties of the actual case of combined air and water vapor.

Model Geometry Description

The schematic of a drift shown in Figure 1 forms the basis of the model used in this computational analysis. A 200 m section of drift from the closed end is simulated. The drift is 5.5 m in diameter and the invert surface is 2.03 m from the drift centerline. Waste packages are simulated by cylinders that are 1.8 m in diameter and 5.6 m in length. The waste packages are placed on 6.1 m intervals so that there is a 0.5 m gap between packages. The line of waste packages start at a distance of 5 m from the closed end of the drift. Ten distinct waste packages are included in the model covering. Starting at a position of 67 m from the closed end, the remainder of the waste packages are simulated by a long cylinder with no gaps. A 1-m thick layer of rock surrounding the drift is simulated.

Material Properties

The thermal conductivity of the rock surrounding the drift was specified as a uniform 1.6 W/m/K over its entire extent. This value was provided by Randy Fedors as being typical of a part of the strata surrounding a proposed drift in Yucca Mountain. The product of density and specific heat of the rock was given a value of 3 joule/m³/K. This value is not realistic, but by specifying this value the thermal response of the rock does not dictate the time step of the CFD simulation in converging to a steady state solution.

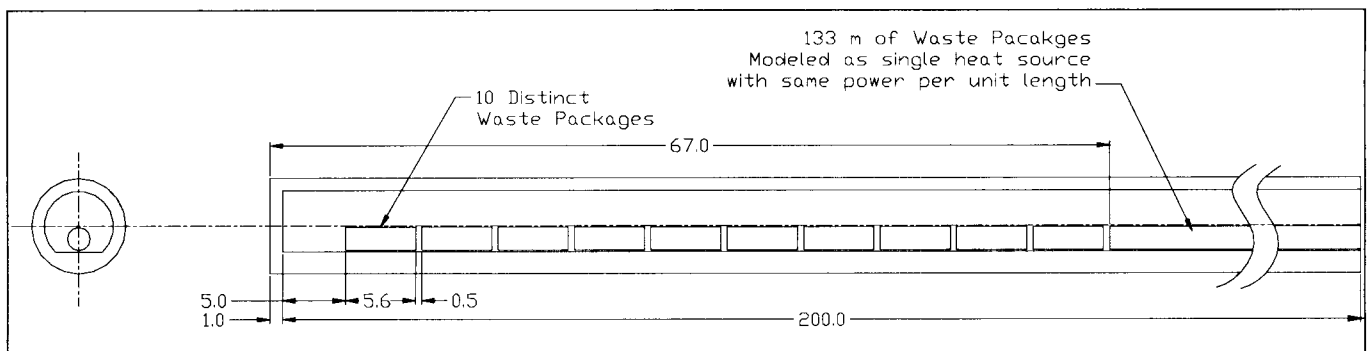


Figure 1. Drift and Waste Package Model for Comparing the Thermal Response of Air and Water Vapor

The waste packages are specified as having a thermal conductivity of 10 W/m/K which is considered to be typical of the overall waste package construction. Similar to the rock wall, the product of density and specific heat of the waste package material is set to a non-realistic value of 30 joule/m³/K.

The gas in the drift is either air or water vapor. The Boussinesq assumption is made for this simulation. The fluid is considered to be nominally incompressible except for a buoyancy force

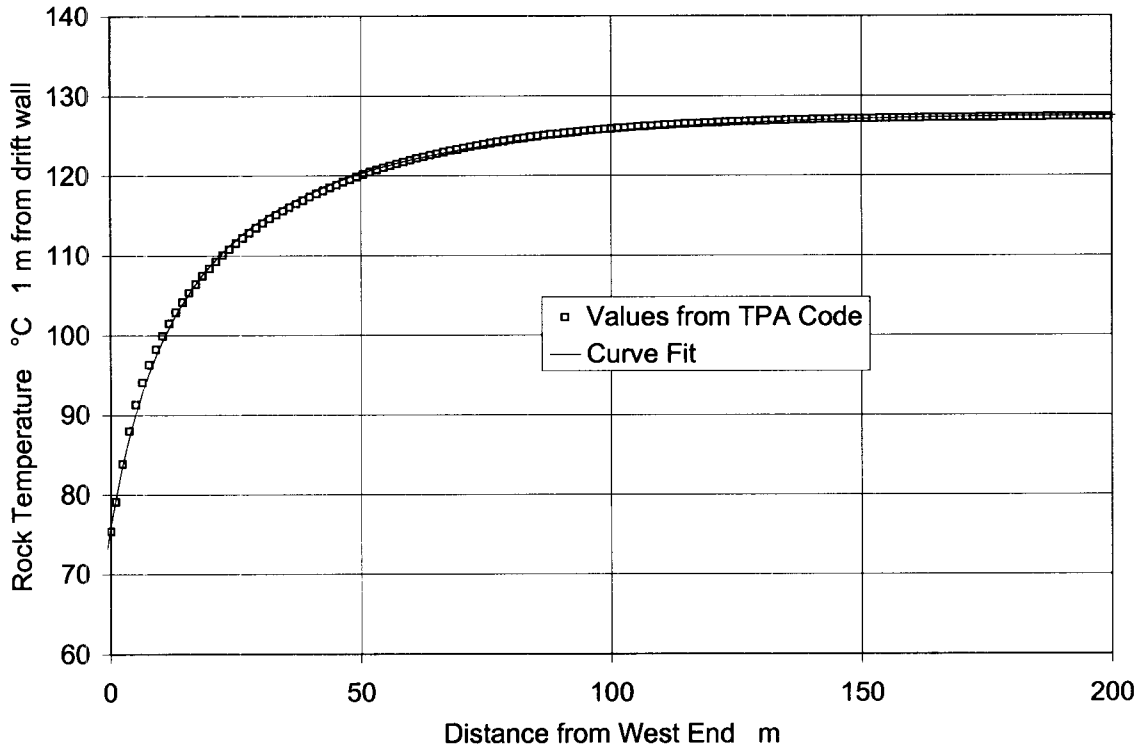


Figure 2. Rock Wall Boundary Temperature for Simulations
 Graph created in Excel spreadsheet rocktemps.xls

FLOW-3D Input Files

The CFD calculations for the SME paper were performed with FLOW-3D, Version 8.2. The installation of this code for CNWRA purposes has been documented by David Walter in Scientific Notebook

The input file (prepinr.Full-Scale-3D-1-r3c-air) for the air simulation is as follows.

576
 (576)
 4/17/08

Cold Trap - Full Scale 3D - No Vapor Transport, Temp. Gradient Boundary

12/12/03

Boundary Temperature set to match data at 1 m from drift wall from Randy Fedors' Data (see grid.xls)

Drift wall thermal conductivity set to constant value (does not vary with axial location)

(Filename = prepinr.Full-Scale-3D-1)

12/15/03

Last run took 32,000 CPU time for 1200 sec simulation. Not to steady state. Refined mesh in the y and z directions (mainly in fluid region). First attempt at GO restart.

Restart at 1200 sec with finish time of 2400 sec.

(Filename = prepinr.Full-Scale-3D-1)

12/16/03

Lost network connection last night at 21:43 and the run terminated.
Restarted at 1650 secs.
Renamed flsgrfr.Full-Scale-3D-1 to flsgrf.Full-Scale-3D-1-r2.
(Filename = prepinr.Full-Scale-3D-1-r2)

12/17/03

Run completed to 2400 sec of simulation time. Still not at steady state.
Reduced rcobs term for drift and invert from 7 to 3 to get to steady state quicker.
Restarted at 2400 sec with finish time of 3600 sec.
Renamed flsgrfr.Full-Scale-3D-1-r2 to flsgrf.Full-Scale-3D-1-r3.
(Filename = prepinr.Full-Scale-3D-1-r3)

12/18/03

Run completed to 3600 sec of simulation time. Still not at steady state.
Restarted at 3600 sec with finish time of 3600 sec.
Renamed flsgrfr.Full-Scale-3D-1-r3 to flsgrf.Full-Scale-3D-1-r4.
(Filename = prepinr.Full-Scale-3D-1-r4)

12/23/03

Run completed to 7200 sec of simulation time. Still not at steady state.
Restarted at 7200 sec with finish time of 14400 sec.
Renamed flsgrfr.Full-Scale-3D-1-r4 to flsgrf.Full-Scale-3D-1-r5.
(Filename = prepinr.Full-Scale-3D-1-r5)

12/29/03

Run not quite complete, but reviewed results and input file. Discovered that the power for teh heaters was not specified correctly.
The power was specified a 1075 watts at time 1 and 2151 at time 2. This was an mistake made when the the power was cut in half.
Will restart from restart #2. Restart time=2400 sec. Finish time=4800 sec.
Renamed flsgrf.Full-Scale-3D-1-r3 to flsgrf.Full-Scale-3D-1-r3b.
(Filename = prepinr.Full-Scale-3D-1-r3b)

12/31/03

Results nearly reached steady state.
Calculated the average fluid temperature to be 417K. Fluid properties were intially set for a reference temperature of 395K.
Will update fluid properties for more accurate reference temperature and restart.
This is an identical run to prepinr.Full-Scale-3D-1-r3c-h2o execept with air not water vapor.
Restart time=4800 sec. Finish time=5200 sec.
Renamed flsgrfr.Full-Scale-3D-1-r3b to flsgrf.Full-Scale-3D-1-r3c-air.
(Filename = prepinr.Full-Scale-3D-1-r3c-air)

\$xput

```
    remark='units are mks',  
    twfin=5200., remark='finish time (sec)',  
    itb=0,    remark='no free surface',  
    gz=-9.8, remark='gravity',  
    ifenrg=3, remark='solve energy transport equation using monotonicity  
preserving',  
    ifrho=1, remark='evaluate density as function of fluid fraction and  
local temperature',
```

```
ihct=2, remark='evaluate heat transfer and solve the obstacle
conduction equation',
ifvis=-1, remark='LES Turbulence',
ipdis=1, remark='hydrostatic pressure in z direction',
imphtc=1, remark='ADI fully implicit evaluation of temperature terms',
irstoe=1, isolid=0, iorder=1, delt=.01,
iadiy=1, iadiz=1,
iwsh=1,
iusrd=1,
trest=4800.,
$end

$limits
$end

$props
remark=' equation of state parameters for air @ 417K (average rock wall
temperature from grid.xls',
remark=' Handbook of tables for Applied Engineering Science, 2nd edition,
Table 1-2 (See AirProperties.pdf)',
cv1=728.7, remark=' specific heat ',
rhof=.84638, remark=' density',
thc1=0.03484, remark=' conductivity',
thexf1=2.432e-03, remark=' thermal expansion coefficient ',
tstar=417., remark=' reference temperature for thermal',
mul=2.3543e-05, remark=' viscosity',
$end

$scalar
$end

$bcdata
wl=1, Remark='Left boundary - wall, constant temp',
wr=1, Remark='Right boundary - wall, constant temp (cold wall)',
wf=1, Remark='Front boundary - Symmetry',
wbk=1, Remark='Back boundary - Symmetry',
wb=1, Remark='Bottom boundary - Symmetry',
wt=1, Remark='Top boundary - Symmetry',
$end

$mesh
nxcelt=244,
px(1)=-1.25, nxcell(1)=1,
px(2)=-1.0, nxcell(2)=3,
px(3)=0.0, nxcell(3)=140,
px(4)=40., nxcell(4)=70,
px(5)=80., nxcell(5)=10,
px(6)=120., nxcell(6)=10,
px(7)=160., nxcell(7)=10,
px(8)=199.,
nycelt=32,
py(1)=0., nycell(1)=28,
py(2)=2.75, nycell(2)=3,
py(3)=3.75, nycell(3)=1,
py(4)=4.25,
nzcelt=58,
pz(1)=-4.25, nzcell(1)=1,
```

```
pz(2)=-3.75, nzcell(2)=5,  
pz(3)=-2.03, nzcell(3)=48,  
pz(4)=2.75,  nzcell(4)=3,  
pz(5)=3.75,  nzcell(5)=1,  
pz(6)=4.25,
```

```
$end
```

```
$obs
```

```
avrck=-3.1,  
nobs=14,  
tobs(1)=0., tobs(2)=100000.,  
Remark='Obstacle 1 - Drift Wall (1m rock)',  
  iob(1)=1, ioh(1)=1,  
    rah(1)=3.75, zl(1)=-1., roty(1)=90.,  
  iob(2)=1, ioh(2)=0,  
    rah(2)=2.75, zl(2)=0., roty(2)=90.,  
  kobs(1)=1.61, Remark='From Fedor e-mail 12-9-03',  
  rcobs(1)=3.,  
  twobs(1,1)=395.,  
Remark='Obstacle 2 - Phantom Boundary',  
  iob(3)=2, ioh(3)=1,  
  iob(4)=2, ioh(4)=0,  
    rah(4)=3.75, zl(4)=-1., roty(4)=90.,  
  twobs(1,2)=395.,  
Remark='Obstacle 3 - Invert',  
  iob(5)=3, ioh(5)=1,  
    rah(5)=2.75, zl(5)=0., roty(5)=90.,  
  iob(6)=3, ioh(6)=0,  
    zl(6)=-2.03, Remark='From SK-0154 Rev02 1-28-00',  
  kobs(3)=1.61, Remark='From Fedor e-mail 12-9-03',  
  rcobs(3)=3.,  
  twobs(1,3)=395.,  
Remark='Obstacle 4 - Heater 1',  
  iob(7)=4, ioh(7)=1,  
    rah(7)=.9, zl(7)=-2.8, zh(7)=2.8, roty(7)=90.,  
    trnx(7)=7.8, trnz(7)=-1., Remark='From SK-0154 Rev02 1-28-00',  
  twobs(1,4)=395., kobs(4)=10., rcobs(4)=30.,  
  pobs(1,4)=1075., pobs(2,4)=1075.,  
Remark='Obstacle 5 - Heater 2',  
  iob(8)=5, ioh(8)=1,  
    rah(8)=.9, zl(8)=-2.8, zh(8)=2.8, roty(8)=90.,  
    trnx(8)=13.9, trnz(8)=-1., Remark='From SK-0154 Rev02 1-28-00',  
  twobs(1,5)=395., kobs(5)=10., rcobs(5)=30.,  
  pobs(1,5)=1075., pobs(2,5)=1075.,  
Remark='Obstacle 6 - Heater 3',  
  iob(9)=6, ioh(9)=1,  
    rah(9)=.9, zl(9)=-2.8, zh(9)=2.8, roty(9)=90.,  
    trnx(9)=20., trnz(9)=-1., Remark='From SK-0154 Rev02 1-28-00',  
  twobs(1,6)=395., kobs(6)=10., rcobs(6)=30.,  
  pobs(1,6)=1075., pobs(2,6)=1075.,  
Remark='Obstacle 7 - Heater 4',  
  iob(10)=7, ioh(10)=1,  
    rah(10)=.9, zl(10)=-2.8, zh(10)=2.8, roty(10)=90.,  
    trnx(10)=26.1, trnz(10)=-1., Remark='From SK-0154 Rev02 1-28-00',  
  twobs(1,7)=395., kobs(7)=10., rcobs(7)=30.,  
  pobs(1,7)=1075., pobs(2,7)=1075.,  
Remark='Obstacle 8 - Heater 5',
```

```
iob(11)=8, ioh(11)=1,
  rah(11)=.9, zl(11)=-2.8, zh(11)=2.8, roty(11)=90.,
  trnx(11)=32.2, trnz(11)=-1., Remark='From SK-0154 Rev02 1-28-00',
  twobs(1,8)=395., kobs(8)=10., rcobs(8)=30.,
  pobs(1,8)=1075., pobs(2,8)=1075.,
Remark='Obstacle 9 - Heater 6',
iob(12)=9, ioh(12)=1,
  rah(12)=.9, zl(12)=-2.8, zh(12)=2.8, roty(12)=90.,
  trnx(12)=38.3, trnz(12)=-1., Remark='From SK-0154 Rev02 1-28-00',
  twobs(1,9)=395., kobs(9)=10., rcobs(9)=30.,
  pobs(1,9)=1075., pobs(2,9)=1075.,
Remark='Obstacle 10 - Heater 7',
iob(13)=10, ioh(13)=1,
  rah(13)=.9, zl(13)=-2.8, zh(13)=2.8, roty(13)=90.,
  trnx(13)=44.4, trnz(13)=-1., Remark='From SK-0154 Rev02 1-28-00',
  twobs(1,10)=395., kobs(10)=10., rcobs(10)=30.,
  pobs(1,10)=1075., pobs(2,10)=1075.,
Remark='Obstacle 11 - Heater 8',
iob(14)=11, ioh(14)=1,
  rah(14)=.9, zl(14)=-2.8, zh(14)=2.8, roty(14)=90.,
  trnx(14)=50.5, trnz(14)=-1., Remark='From SK-0154 Rev02 1-28-00',
  twobs(1,11)=395., kobs(11)=10., rcobs(11)=30.,
  pobs(1,11)=1075., pobs(2,11)=1075.,
Remark='Obstacle 12 - Heater 9',
iob(15)=12, ioh(15)=1,
  rah(15)=.9, zl(15)=-2.8, zh(15)=2.8, roty(15)=90.,
  trnx(15)=56.6, trnz(15)=-1., Remark='From SK-0154 Rev02 1-28-00',
  twobs(1,12)=395., kobs(12)=10., rcobs(12)=30.,
  pobs(1,12)=1075., pobs(2,12)=1075.,
Remark='Obstacle 13 - Heater 10',
iob(16)=13, ioh(16)=1,
  rah(16)=.9, zl(16)=-2.8, zh(16)=2.8, roty(16)=90.,
  trnx(16)=62.7, trnz(16)=-1., Remark='From SK-0154 Rev02 1-28-00',
  twobs(1,13)=395., kobs(13)=10., rcobs(13)=30.,
  pobs(1,13)=1075., pobs(2,13)=1075.,
Remark='Obstacle 14 - Heater 11 (Long Heater - 22.5 Heaters)',
iob(17)=14, ioh(17)=1,
  rah(17)=.9, zl(17)=-2.8, roty(17)=90.,
  trnx(17)=68.8, trnz(17)=-1., Remark='From SK-0154 Rev02 1-28-00',
  twobs(1,14)=395., kobs(14)=10., rcobs(14)=30.,
  pobs(1,14)=24200., pobs(2,14)=24200.,
```

\$end

\$fl
\$end

\$bf
\$end

\$temp
 tempi=395.,
\$end

\$motn

```
$end

$grafic
$end
  jobsf=1,
  jobsbk=2,
$parts
$end
$usrdat
  idrftw_stg(2)=-2,
$end
```

The input file (prepinr.Full-Scale-3D-1-h2o-r2) for the water vapor simulation is as follows.

Cold Trap - Full Scale 3D - Phase Change, Temp. Gradient Boundary, Water Vapor

12/12/03

Boundary Temperature set to match data at 1 m from drift wall from Randy Fedors' Data (see grid.xls)
Drift wall thermal conductivity set to constant value (does not vary with axial location)
(Filename = prepinr.Full-Scale-3D-1)

12/15/03

Last run took 32,000 CPU time for 1200 sec simulation. Not to steady state. Refined mesh in the y and z directions (mainly in fluid region). First attempt at GO restart.
Restart at 1200 sec with finish time of 2400 sec.
(Filename = prepinr.Full-Scale-3D-1)

12/16/03

Lost network connection last night at 21:43 and the run terminated.
Restarted at 1650 secs.
Renamed flsgrfr.Full-Scale-3D-1 to flsgrf.Full-Scale-3D-1-r2.
(Filename = prepinr.Full-Scale-3D-1-r2)

12/17/03

Run completed to 2400 sec of simulation time. Still not at steady state. Reduced rcobs term for drift and invert from 7 to 3 to get to steady state quicker.
Restarted at 2400 sec with finish time of 3600 sec.
Renamed flsgrfr.Full-Scale-3D-1-r2 to flsgrf.Full-Scale-3D-1-r3.
(Filename = prepinr.Full-Scale-3D-1-r3)

12/18/03

Run completed to 3600 sec of simulation time. Still not at steady state. Restarted at 3600 sec with finish time of 3600 sec.
Renamed flsgrfr.Full-Scale-3D-1-r3 to flsgrf.Full-Scale-3D-1-r4.
(Filename = prepinr.Full-Scale-3D-1-r4)

12/23/03

Run completed to 7200 sec of simulation time. Still not at steady state.

Restarted at 7200 sec with finish time of 14400 sec.
Renamed flsgrfr.Full-Scale-3D-1-r4 to flsgrf.Full-Scale-3D-1-r5.
(Filename = prepnr.Full-Scale-3D-1-r5)

12/29/03

Run not quite complete, but reviewed results and input file. Discovered that the power for teh heaters was not specified correctly. The power was specified a 1075 watts at time 1 and 2151 at time 2. This was an mistake made when the the power was cut in half. Will restart from restart #2. Restart time=2400 sec. Finish time=4800 sec. Renamed flsgrf.Full-Scale-3D-1-r3 to flsgrf.Full-Scale-3D-1-r3b.
(Filename = prepnr.Full-Scale-3D-1-r3b)

12/31/03

Results nearly reached steady state. Calculated the average fluid temperature to be 417K. Fluid properties were intially set for a reference temperature of 395K. Will update fluid properties for more accurate reference temperature and restart. Also will cahnge fluid to water vapor. This is an identical run to prepnr.Full-Scale-3D-1-r3c-air execept with water vapor not air. Restart time=4800 sec. Finish time=5200 sec. Renamed flsgrfr.Full-Scale-3D-1-r3b to flsgrf.Full-Scale-3D-1-r3c-h2o.
(Filename = prepnr.Full-Scale-3D-1-r3c-h2o)

1/5/03

Previous run terminated due to excessive pressure iterations. Will start model from time zero with 2000sec finish time.
(Filename = prepnr.Full-Scale-3D-1-h20)

1/7/03

Previous run finished but not quite to steady state. Restart at t=2000 with finish of 4000 sec.
(Filename = prepnr.Full-Scale-3D-1-h20)

1/9/03

Still not at steady state. Restart at t=3964 sec with finish of 7000 sec. Renamed flsgrfr.Full-Scale-3D-1-h20 to flsgrf.Full-Scale-3D-1-h20-r2.
(Filename = prepnr.Full-Scale-3D-1-h20-r2)

\$xput

```
    remark='units are mks',
    twfin=7000., remark='finish time (sec)',
    itb=0,    remark='no free surface',
    gz=-9.8, remark='gravity',
    ifenrg=3, remark='solve energy transport equation using monotonicity
preserving',
    ifrho=1, remark='evaluate density as function of fluid fraction and
local temperature',
    ihtc=2,  remark='evaluate heat transfer and solve the obstacle
conduction equation',
    ifvis=-1, remark='LES Turbulence',
    ipdis=1, remark='hydrostatic pressure in z direction',
    imphtc=1, remark='ADI fully implicit evaluation of temperature terms',
    irstoe=1, isolid=0, iorder=1, delt=.01,
    iadiy=1, iadiz=1,
```

```
iwsh=1,  
iusrd=1,  
trest=3964.,  
$end
```

```
$limits  
$end
```

```
$props  
remark=' equation of state parameters for water vapor @ 417K',  
remark=' Data from NIST Standard Reference Database 69 - March 2003: NIST  
Chemistry WebBook (http://webbook.nist.gov)',  
cvl=1497.9,      remark=' specific heat ',  
rhof=.52427,    remark=' density',  
thc1=0.028351,  remark=' conductivity',  
thexf1=2.489e-03, remark=' thermal expansion coefficient ',  
tstar=417.,     remark=' reference temperature for thermal',  
mul=1.394e-05,  remark=' viscosity',  
$end
```

```
$scalar  
$end
```

```
$bcdata  
wl=1, Remark='Left boundary - wall, constant temp',  
wr=1, Remark='Right boundary - wall, constant temp (cold wall)',  
wf=1, Remark='Front boundary - Symmetry',  
wbk=1, Remark='Back boundary - Symmetry',  
wb=1, Remark='Bottom boundary - Symmetry',  
wt=1, Remark='Top boundary - Symmetry',  
$end
```

```
$mesh  
nxcelt=244,  
px(1)=-1.25, nxcell(1)=1,  
px(2)=-1.0,  nxcell(2)=3,  
px(3)=0.0,   nxcell(3)=140,  
px(4)=40.,   nxcell(4)=70,  
px(5)=80.,   nxcell(5)=10,  
px(6)=120.,  nxcell(6)=10,  
px(7)=160.,  nxcell(7)=10,  
px(8)=199.,  
nycelt=32,  
py(1)=0.,    nycell(1)=28,  
py(2)=2.75,  nycell(2)=3,  
py(3)=3.75,  nycell(3)=1,  
py(4)=4.25,  
nzcelt=58,  
pz(1)=-4.25, nzcell(1)=1,  
pz(2)=-3.75, nzcell(2)=5,  
pz(3)=-2.03, nzcell(3)=48,  
pz(4)=2.75,  nzcell(4)=3,  
pz(5)=3.75,  nzcell(5)=1,  
pz(6)=4.25,  
$end
```

```
$obs
```

```
avrck=-3.1,
nobs=14,
tobs(1)=0., tobs(2)=100000.,
Remark='Obstacle 1 - Drift Wall (1m rock)',
  iob(1)=1, ioh(1)=1,
    rah(1)=3.75, z1(1)=-1., roty(1)=90.,
  iob(2)=1, ioh(2)=0,
    rah(2)=2.75, z1(2)=0., roty(2)=90.,
kobs(1)=1.61, Remark='From Fedor e-mail 12-9-03',
rcobs(1)=3.,
twobs(1,1)=395.,
Remark='Obstacle 2 - Phantom Boundary',
  iob(3)=2, ioh(3)=1,
  iob(4)=2, ioh(4)=0,
    rah(4)=3.75, z1(4)=-1., roty(4)=90.,
  twobs(1,2)=395.,
Remark='Obstacle 3 - Invert',
  iob(5)=3, ioh(5)=1,
    rah(5)=2.75, z1(5)=0., roty(5)=90.,
  iob(6)=3, ioh(6)=0,
    z1(6)=-2.03, Remark='From SK-0154 Rev02 1-28-00',
kobs(3)=1.61, Remark='From Fedor e-mail 12-9-03',
rcobs(3)=3.,
twobs(1,3)=395.,
Remark='Obstacle 4 - Heater 1',
  iob(7)=4, ioh(7)=1,
    rah(7)=.9, z1(7)=-2.8, zh(7)=2.8, roty(7)=90.,
    trnx(7)=7.8, trnz(7)=-1., Remark='From SK-0154 Rev02 1-28-00',
  twobs(1,4)=395., kobs(4)=10., rcobs(4)=30.,
  pobs(1,4)=1075., pobs(2,4)=1075.,
Remark='Obstacle 5 - Heater 2',
  iob(8)=5, ioh(8)=1,
    rah(8)=.9, z1(8)=-2.8, zh(8)=2.8, roty(8)=90.,
    trnx(8)=13.9, trnz(8)=-1., Remark='From SK-0154 Rev02 1-28-00',
  twobs(1,5)=395., kobs(5)=10., rcobs(5)=30.,
  pobs(1,5)=1075., pobs(2,5)=1075.,
Remark='Obstacle 6 - Heater 3',
  iob(9)=6, ioh(9)=1,
    rah(9)=.9, z1(9)=-2.8, zh(9)=2.8, roty(9)=90.,
    trnx(9)=20., trnz(9)=-1., Remark='From SK-0154 Rev02 1-28-00',
  twobs(1,6)=395., kobs(6)=10., rcobs(6)=30.,
  pobs(1,6)=1075., pobs(2,6)=1075.,
Remark='Obstacle 7 - Heater 4',
  iob(10)=7, ioh(10)=1,
    rah(10)=.9, z1(10)=-2.8, zh(10)=2.8, roty(10)=90.,
    trnx(10)=26.1, trnz(10)=-1., Remark='From SK-0154 Rev02 1-28-00',
  twobs(1,7)=395., kobs(7)=10., rcobs(7)=30.,
  pobs(1,7)=1075., pobs(2,7)=1075.,
Remark='Obstacle 8 - Heater 5',
  iob(11)=8, ioh(11)=1,
    rah(11)=.9, z1(11)=-2.8, zh(11)=2.8, roty(11)=90.,
    trnx(11)=32.2, trnz(11)=-1., Remark='From SK-0154 Rev02 1-28-00',
  twobs(1,8)=395., kobs(8)=10., rcobs(8)=30.,
  pobs(1,8)=1075., pobs(2,8)=1075.,
Remark='Obstacle 9 - Heater 6',
  iob(12)=9, ioh(12)=1,
    rah(12)=.9, z1(12)=-2.8, zh(12)=2.8, roty(12)=90.,
```

```
    trnx(12)=38.3, trnz(12)=-1., Remark='From SK-0154 Rev02 1-28-00',
    twobs(1,9)=395., kobs(9)=10., rcobs(9)=30.,
    pobs(1,9)=1075., pobs(2,9)=1075.,
Remark='Obstacle 10 - Heater 7',
    iob(13)=10, ioh(13)=1,
    rah(13)=.9, zl(13)=-2.8, zh(13)=2.8, roty(13)=90.,
    trnx(13)=44.4, trnz(13)=-1., Remark='From SK-0154 Rev02 1-28-00',
    twobs(1,10)=395., kobs(10)=10., rcobs(10)=30.,
    pobs(1,10)=1075., pobs(2,10)=1075.,
Remark='Obstacle 11 - Heater 8',
    iob(14)=11, ioh(14)=1,
    rah(14)=.9, zl(14)=-2.8, zh(14)=2.8, roty(14)=90.,
    trnx(14)=50.5, trnz(14)=-1., Remark='From SK-0154 Rev02 1-28-00',
    twobs(1,11)=395., kobs(11)=10., rcobs(11)=30.,
    pobs(1,11)=1075., pobs(2,11)=1075.,
Remark='Obstacle 12 - Heater 9',
    iob(15)=12, ioh(15)=1,
    rah(15)=.9, zl(15)=-2.8, zh(15)=2.8, roty(15)=90.,
    trnx(15)=56.6, trnz(15)=-1., Remark='From SK-0154 Rev02 1-28-00',
    twobs(1,12)=395., kobs(12)=10., rcobs(12)=30.,
    pobs(1,12)=1075., pobs(2,12)=1075.,
Remark='Obstacle 13 - Heater 10',
    iob(16)=13, ioh(16)=1,
    rah(16)=.9, zl(16)=-2.8, zh(16)=2.8, roty(16)=90.,
    trnx(16)=62.7, trnz(16)=-1., Remark='From SK-0154 Rev02 1-28-00',
    twobs(1,13)=395., kobs(13)=10., rcobs(13)=30.,
    pobs(1,13)=1075., pobs(2,13)=1075.,
Remark='Obstacle 14 - Heater 11 (Long Heater - 22.5 Heaters)',
    iob(17)=14, ioh(17)=1,
    rah(17)=.9, zl(17)=-2.8, roty(17)=90.,
    trnx(17)=68.8, trnz(17)=-1., Remark='From SK-0154 Rev02 1-28-00',
    twobs(1,14)=395., kobs(14)=10., rcobs(14)=30.,
    pobs(1,14)=24200., pobs(2,14)=24200.,
$end
```

```
$fl
$end
```

```
$bf
$end
```

```
$temp
    tempi=395.,
$end
```

```
$motn
$end
```

```
$grafic
$end
    jobsf=1,
    jobsbk=2,
$parts
$end
```

```
$usrdat  
  idrftw_stg(2)=-2,  
$end
```

Comparison of Results

The gas circulation rate is computed by integrating the fluid velocity over the cross section for all locations where the gas is moving away from the closed end of the drift. A closed boundary was assumed for these simulations; therefore, at any given cross section along the drift axis, the flow of gas away from the closed end of the drift is balanced by flow toward the closed end. So, the gas circulation rate is volumetric flow of gas that is being exchanged between volumes on either side of a plane at the specified axial.

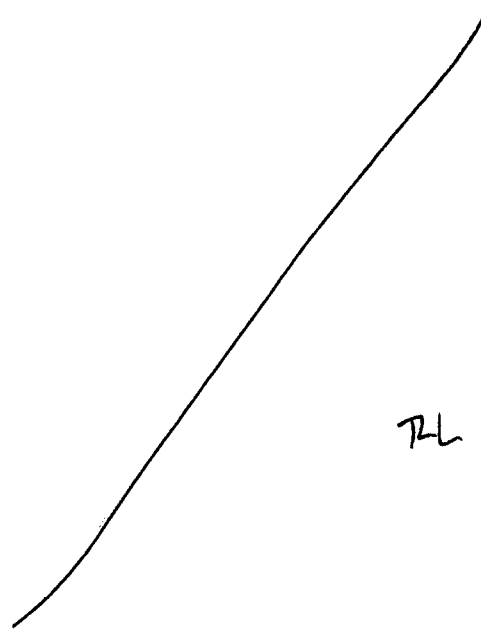
4/12/08
573
6/3E

These calculations are performed in a special post-processing computer program written by Robert Hart (see Scientific Notebook _____). This special program reads the text output from the FLOW-3D post processing program for the cell-by-cell temperature, flow and geometry factors and computes the cross-section averaged quantities presented here. These processed results are summarized in the Excel spreadsheet

C:\Projects\div20\moisture_transport\Air-Water-Compare\ullscale_Air-Water Comparison.xls

This spreadsheet was used to generate the graphs in Figure 3 and Figure 4.

The predicted gas circulation rates for dry air and pure water vapor are compared in Figure 3. There are some slight differences between the two sets of results, but the gas circulation rates for the two gas compositions are in close agreement. The circulation rate is strongest at the closed end of the drift where the gas circulates between the hot waste package and the relatively cooler end wall. The circulation rate decreases with the distance, but the circulation rate does not decrease to an insignificant value until the no-flow end is reached.



RL
4/11/2008

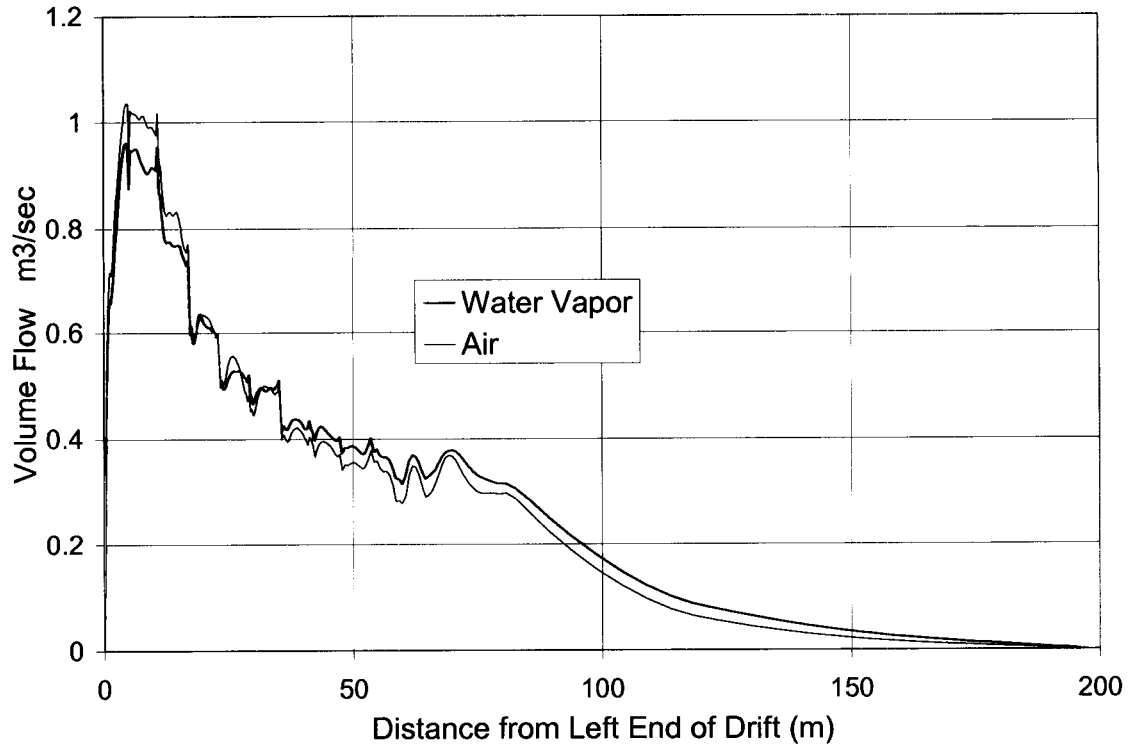


Figure 3. Predicted Axial Circulation Rate

The axial fluid temperature profile is shown in Figure 4. Similar to the gas circulation rates, this graph shows that the average temperature in the drift cross section is virtually identical for both dry air and pure water vapor. The cross-section mean temperature varies by only 5°C along the drift, while the rock temperature increases about 47°C along the drift. This indicated that the gas circulation is tending to mix the gas and decrease the effects of the axial variation in rock temperature.

TL 4/11/2008

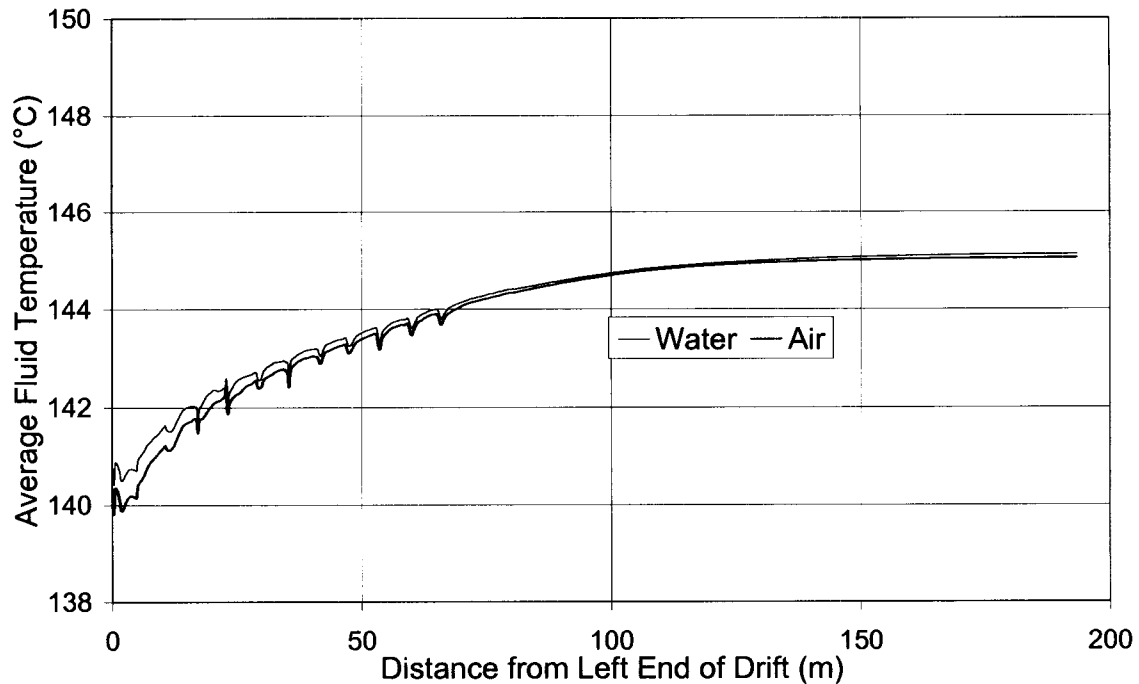


Figure 4. Predicted Axial Fluid Temperature Profile

There are axial variations in both the circulation rate and fluid temperature for locations less than about 60 meters from the closed end that are not present from 60 to 200 meters. This is indicative of the mesh expanding in the axial direction away from the closed end. The coarser mesh cannot resolve the geometric details around the waste packages that are greater than 60 meters from the closed end. The CFD model in these locations is essentially for a 140-m long cylinder with a heat generation rate per unit length consistent with locations that are closer than 60 m from the closed end.

Conclusion

From these CFD predictions, it is clear that the temperature and circulation rates for pure air and water vapor are approximately equal. This implies that the details of the gas composition do not strongly affect the overall simulation of fluid dynamics and heat transfer in the drift. While the water vapor concentration will strongly impact the corrosion rates of metallic components, the overall temperature and overall gas flow rates do not depend on the precision with which the composition is known.

The axial flow decreases slightly more strongly than linearly but is significant enough far away from the drift end to modulate the axial gas temperature variation. This is unfortunate from the standpoint that two-dimensional simulations can be performed much more quickly than three-dimensional simulations. Because of this advantage, it is recommended that additional work be conducted to determine whether some way of using two-dimensional simulations can be warranted. It is not clear at this time that this approach will be acceptable.

END OF ENTRY FOR 3/12/04

STG

4/17/08

523

3/20/04

STG

576

3/18/04

This entry is to describe the modifications to the phase change and moisture transport model described in the entry on 10/21/03. After making several comparisons to the benchtop drift model experiment (see David Walter, Scientific Notebook # , Entry for / / for the comparison) and the moisture transport experiment (described by Steve Svedeman, Scientific Notebook # , entry for / /) it was clear that the original phase change model was not accurate. These issues did not arise in the simple verification tests described on 10/21/03.

Unfortunately, the earlier version of the model was also published in the paper, "A Model for Moisture Transport in a High-Level Radioactive Waste Repository Drift," submitted to the SME Annual Meeting, February 2004.

A summary of the change to the model is as follows:

1. In the original model, it was assumed that all of the energy exchange associated with the phase change was between evaporating/condensing water and the air/vapor mixture. In the version described here, the energy exchange is between the evaporating/condensing water and the wall. The energy of the air/vapor mixture is altered indirectly via convection/conduction with the wall.
2. In the original model, it was assumed that the temperature of the air/vapor was below the saturation temperature at the drift pressure. This restriction is no longer in place. The temperature can be any value above the freezing point of the water.

The phase change model is replaced entirely by the following description. In addition to correcting the model

The following overall assumptions are made for the entire flow field.

- The fluid is considered to be a binary mixture of water vapor and air, each of which are considered to be ideal gases. (Of course, the air is itself a mixture of many gases, but is considered here to be a single component).
- The energy of phase change is provided to/from the wall.
- Condensate layers are not thick enough to cause film flow on the walls.
- Currently, it is assumed that the CFD grid structure is such that the surfaces of solid walls at which phase change takes place are contained within the grid structure. That is, a computation grid volume is split between fluid material and wall material. This assumption is a convenience for FLOW-3D, but can be relaxed in the future with additional coding to locate walls that are coincident with mesh lines (as is done in other codes such as FLUENT)

Additional assumptions for the evaporation/condensation model are described as needed

The binary species conservation equation for the water vapor is as follows (from Burmeister, Louis C., 1983, Convective Heat Transfer, John Wiley and Sons, New York,.)

643
2/20/04
to 5/26/04
523
4/17/08

$$\rho \left(\frac{\partial c_v}{\partial t} + u \frac{\partial c_v}{\partial x} + v \frac{\partial c_v}{\partial y} + w \frac{\partial c_v}{\partial z} \right) = \nabla \cdot (\rho D \nabla c_v) + \dot{m}_{source}^m \tag{1}$$

where ρ = bulk density of the air/vapor mixture

c_v = vapor mass concentration mass; i.e., ratio of vapor mass to total mass

\dot{m}_{source}^m = source of vapor as a result of mass transfer to/from liquid water at walls

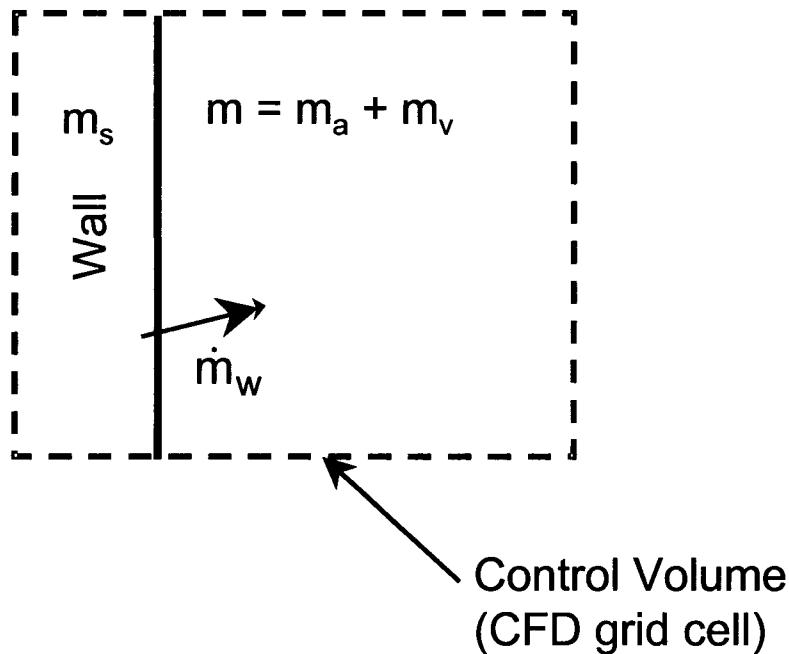
u, v, w = vector components of bulk fluid flow

x, y, z = coordinate directions

D = diffusion coefficient for water vapor/air

It is presumed that the CFD code provides the appropriate solution scheme for solving the species conservation equation if the spatially varying, temperature dependent source term is defined. The objective of this analysis is to prescribe a calculation scheme for the source term.

Consider a small control volume adjacent to a wall at which either evaporation or condensation can take place. During a calculation, the control volume will be a single computational cell or finite element in the discretized flow domain.



The conservation of energy is applied to the solid wall and the liquid film on the wall over a single time step in the calculation. Evaporation or condensation will take place as necessary to satisfy the energy change of the solid material. Any heat transfer to/from the air/vapor mixture takes place via conduction/convection with the wall; the air/vapor mixture wall does not exchange energy directly with the water that is undergoing the phase change..

Armed with these assumptions, the conservation of energy is expressed as

{Energy change in the solid wall material} = {Energy of phase change}

$$m_s \frac{(e_{s,2} - e_{s,1})}{\Delta t} = \dot{m}_w h_{vap} \quad (2)$$

$$\rho_s C_s V_s \frac{(T_{s,2} - T_{s,1})}{\Delta t} = \dot{m}_w h_{vap} \quad (3)$$

where m_s = mass of solid wall inside the control volume

\dot{m}_w = mass flow rate of water evaporating/condensing

$e_{s,1}$ = mass-specific energy of solid material at the beginning of the time step

$e_{s,2}$ = mass-specific energy of solid material at the end of the time step

ρ_s = solid material density

C_s = solid material specific heat

V_s = solid material volume

h_{vap} = heat of vaporization

Δt = time step

The two unknowns in Eq. (1) are the final wall energy (or wall temperature) and the mass flow rate of water undergoing phase change. The second of the two required equations is an expression for the mass flow rate of water.

First, define some helpful equations from engineering psychrometrics. The air and vapor are assumed to be ideal gases; so the mole fraction of each is equal to their partial pressure fractions as

$$x_v = \frac{\text{moles of water vapor}}{\text{total moles}} = \frac{P_v}{P_{tot}} \quad (4)$$

$$x_a = \frac{\text{moles of air}}{\text{total moles}} = \frac{P_a}{P_{tot}} = \frac{P_{tot} - P_v}{P_{tot}} = 1 - x_v \quad (5)$$

The humidity ratio is defined as the ratio of the water vapor mass to the dry air mass,

$$W = \frac{m_v}{m_a} = \frac{x_v M_v}{x_a M_a} = \frac{P_v M_v}{P_a M_a} = \frac{P_v M_v}{P_{tot} - P_v M_a} \quad (6)$$

The mass fraction of water vapor, c_v , can now be defined in terms of mole fraction ratio,

$$c_v = \frac{\text{mass of water vapor}}{\text{total mass}} = \frac{m_v}{m_a + m_v} = \frac{W}{1 + W} = \frac{x_v \frac{M_v}{M_a}}{x_a + x_v \frac{M_v}{M_a}} \quad (7)$$

where M_v , M_a are the molecular weights of air and water respectively. We can also solve for the mole fraction in terms of the concentration

$$x_v = \left(\frac{c_v}{\frac{M_v}{M_a} + c_v \left(1 - \frac{M_v}{M_a} \right)} \right) \quad (8)$$

The maximum allowable concentration of the water vapor is obtained when the partial pressure is equal to the water vapor saturation pressure at the temperature of interest. The saturation vapor of water is estimated from the Keenan, Keyes, Hill, and Moore expression (Keenan, J. H., Keyes, F. G., Hill, P. G., Moore, J. G., **Steam Tables: Thermodynamic Properties of Water, Including Vapor, Liquid, and Solid Phases**, John Wiley and Sons, Inc, 1969.),

$$\ln \left(\frac{P_{v,sat}}{217.99} \right) = \frac{0.01}{T} (374.136 - t) \left[-741.9242 + \sum_{i=1}^7 F_i (0.65 - 0.01t)^i \right]$$

(applicable temperature range is 0°C to 374°C)

$$F_1 = -29.72100$$

$$F_5 = +0.439993$$

$$F_2 = -11.55286$$

$$F_6 = +0.2520658$$

$$F_3 = -0.8685635$$

$$F_7 = +0.05218684$$

$$F_4 = +0.1094098$$

$$t = T - 273.15K = \text{degreed Celsius}$$

$$T = \text{absolute temperature, Kelvin}$$

$$P_{v,sat} = \text{water liquid - vapor saturation pressure, atmospheres}$$

For cases in which the vapor pressure is greater than the local total pressure (i.e., the temperature is greater than the boiling point of water) the vapor pressure is set equal to the total pressure such that $x_{v,sat} = c_{v,sat} = 1$.

With these fundamental concepts, we can now turn to estimating the phase change rate. One estimate for the mass flow rate of water evaporating from or condensing on the wall is to assume that the phase change rate is high enough to maintain the control volume at saturated conditions. The rate that is required to fully saturate the entire control volume in the time step is

$$\dot{m}_{w1} = (\rho_{sat} c_{v,sat} - \rho_i c_{v,i}) \frac{V_f}{\Delta t} \quad (9)$$

where \dot{m}_{w1} = mass flow rate to provide vapor-saturated fluid in the cell in the current time step

ρ_i = current fluid density in the cell

$c_{v,i}$ = current mass concentration of water vapor in the cell

V_f = volume of fluid in the cell

Δt = time step

ρ_{sat} = fluid density if saturated at the current fluid temperature

$$= \frac{P_i}{T_i} \left(\frac{x_{v,sat}}{R_v} + \frac{1 - x_{v,sat}}{R_a} \right) \quad (10)$$

$$c_{v,sat} = \text{mass concentration of water vapor at saturation at the current fluid temperature}$$

$$= \frac{x_{v,sat}}{(1-x_{v,sat})\frac{M_v}{M_a} + x_{v,sat}} \quad (11)$$

$$x_{v,sat} = \text{mole concentration of water vapor at saturation at the current fluid temperature}$$

$$= \frac{P_{v,sat}}{P_i} \quad (12)$$

The second estimate of the phase change rate is based on the time for vapor to move across the computational cell based on Fickian diffusion. The concentration gradient is estimated as the difference between the saturation concentration at the wall surface temperature and the current cell vapor concentration divided by the distance across the cell normal to the wall. This results in the following relation,

$$\dot{m}_{w2} \approx \rho_i D \frac{(c_{w,sat} - c_{v,i})}{L_{normal}} A_w = \rho_i D (c_{w,sat} - c_{v,i}) \frac{A_w^2}{V_f} \quad (13)$$

where \dot{m}_{w2} = mass flow rate based on diffusion normal to the wall

D = diffusion coefficient for water vapor/air

$c_{w,sat}$ = mass concentration of water vapor at saturation at the current fluid temperature

$$= \frac{x_{w,sat}}{(1-x_{w,sat})\frac{M_v}{M_a} + x_{w,sat}} \quad (14)$$

$x_{w,sat}$ = mole concentration of water vapor at saturation at the current wall temperature

$$= \frac{P_{w,sat}}{P_i} \quad (15)$$

A_w = wall surface area inside the cell

L_{normal} = length scale for diffusion normal to the wall, estimated as $\frac{A_w}{V_f}$

V_f = volume of fluid in the cell

The water vapor flow rate to/from the wall is taken to be the minimum of these two estimates

$$\dot{m}_w = \text{MIN}[\dot{m}_{w1}, \dot{m}_{w2}] \quad (16)$$

The final value for the vapor concentration is obtained from the following derivation,

$$m_{v,f} - m_{v,i} = \dot{m}_w \Delta t = \Delta m$$

$$c_{v,f} m_f - c_{v,i} m_i = \dot{m}_w \Delta t \quad m_f, m_i \text{ are the initial and final mixture mass}$$

$$c_{v,f} (m_i + \dot{m}_w \Delta t) - c_{v,i} m_i = \dot{m}_w \Delta t$$

$$c_{v,f} \left(1 + \frac{\dot{m}_w \Delta t}{m_i} \right) - c_{v,i} = \frac{\dot{m}_w \Delta t}{m_i}$$

$$c_{v,f} = \frac{c_{v,i} + \frac{\dot{m}_w \Delta t}{\rho_i V_f}}{1 + \frac{\dot{m}_w \Delta t}{\rho_i V_f}} \quad (17)$$

Equations (3) and (16) form a set of two equations that are solved simultaneously for $T_{s,2}$ and \dot{m}_w . A calculation procedure for implementing this model is as follows,

1. At the beginning of the procedure, the initial values are known: $T_{s,i}$, $T_{f,i}$, ρ_i , $c_{v,i}$, P_i .
2. Compute the saturation pressure at the fluid temperature, $P_{v,sat}(T_{f,i})$. Also the other saturation quantities, $X_{v,sat}$, $C_{v,sat}$.
3. Assume a value for the final wall temperature, $T_{w,f}=T_{w,i}$ to begin the convergence iteration loop.
4. Compute the saturation pressure at the final wall temperature, $P_{w,sat}(T_{w,i})$. Also the other saturation quantities, $X_{w,sat}$, $C_{w,sat}$, ρ_{sat} .
5. Compute the mass flow rate required to bring the control volume to saturation conditions, \dot{m}_{w1} , from Eq. (9). A positive value indicates evaporation.
6. Compute the mass flow rate to match the diffusion velocity across the control volume, \dot{m}_{w2} , from Eq. (13.) A positive value indicates evaporation.
7. Use the minimum of the two mass flow rate estimates, \dot{m}_w , from Eq. (16)
8. Compute a new value for the final wall temperature using a relaxation factor,

$$T_{s,2} = T_{s,1} + F_{relax} \frac{\dot{m}_w h_{vap}}{\rho_s C_s V_s} \Delta t \quad (18)$$

(During the initial implementation of the model, it was discovered that a relaxation factor was required to keep the algorithm stable)

9. Repeat steps 4-8 until converged to an acceptable tolerance.
10. Update the vapor mass concentration according to Eq. (17)

The moisture transport algorithm described above was incorporated into the FLOW-3D user-modifiable routine QSADD. QSADD is called at the end of the CFD calculations for the mass, momentum, energy, and diffusion equations. QSADD is a general purpose routine intended to provide a location for users to compute once-per-time-step parameters for outputs or for special source terms. QSADD is NOT called within the main iteration loops; so the calculation are suspect for source terms that are highly non-linear or strongly coupled to the field variable (temperature, density, velocity, etc.). This subroutine is part of the FLOW-3D software distribution and is intended to be modified by the code user as necessary; however, the program file header contains a statement that the file contains proprietary Flow Science information. The code listing will not be provided here until specific approval is received from Flow Science.

Instead, the moisture transport algorithm was built into a separate subroutine called by QSADD. This routine is called

C:\FLOW3D\source\hydr3d\qsadd_moist_stg.F


```

      tfinal= teval(ijk)
      tinit= tfinal
      twalli = tw(ijk)
      twallf = twalli
      tnk = tfinal
      tnc = tnk-273.15
c
c Compute the initial concentration before phase change
c Define 1 atmosphere as 101300 Pascal
c
      term1 = F0kkhm +
1          F1kkhm*(0.65-0.01*(tnc)) +
2          F2kkhm*(0.65-0.01*(tnc))**2 +
3          F3kkhm*(0.65-0.01*(tnc))**3 +
4          F4kkhm*(0.65-0.01*(tnc))**4 +
5          F5kkhm*(0.65-0.01*(tnc))**5 +
6          F6kkhm*(0.65-0.01*(tnc))**6 +
7          F7kkhm*(0.65-0.01*(tnc))**7
      Pvsati=217.99*exp(0.01/tnk*(374.136-(tnc))*term1)
      Pvsati = Pvsati * 101300.
c
c Saturation Molar concentration ..... moles of vapor per total moles
c If Pvsati > p, the saturation values will be invalid, but invalid values are trapped
below
      Xvsati = Pvsati/p(ijk)
c
c Saturation Mass Concentration .....mass of vapor to total mass
      Yvsati = Xvsati/((1.-Xvsati)*airmw/vapmw+Xvsati)
c
c Current vapor mass concentration
      Yvacti = sclr(ijk, isvap_stg)
c
c Begin the loop to balance the energy and evaporated/condensed mass
c
      nitr_moist = 0
100      continue
c
c Compute the saturation pressure at the final fluid film temperature.
c Assume this is the wall temperature.
c
c PATCH - If there is not a wall temperature, this means the volume fraction is 1 (no
wall)
c but the cell is next to an obstacle. Need to fix this later so that the
obstacle
c and mesh lines can coincide an the code will recognize that an adjacent
obstacle needs
c to be included in the energy balance.
c
      if (twalli .le. 0.) go to 1950
      tnk = twallf
      tnc = tnk-273.15
      term1 = F0kkhm +
1          F1kkhm*(0.65-0.01*(tnc)) +
2          F2kkhm*(0.65-0.01*(tnc))**2 +
3          F3kkhm*(0.65-0.01*(tnc))**3 +
4          F4kkhm*(0.65-0.01*(tnc))**4 +
5          F5kkhm*(0.65-0.01*(tnc))**5 +
6          F6kkhm*(0.65-0.01*(tnc))**6 +
7          F7kkhm*(0.65-0.01*(tnc))**7
      Pvsat=217.99*exp(0.01/tnk*(374.136-(tnc))*term1)
      Pvsat = Pvsat * 101300.
c
c Saturation Molar concentration ..... moles of vapor per total moles
c Limit the value to its maximum of Xvsat=1 if Pvsat > P(ijk)
      Xvsat = Pvsat/p(ijk)
      if (Xvsat .gt. 1.) Xvsat = 1.
c Saturation Mass Concentration .....mass of vapor to total mass
      Yvsat = Xvsat/((1.-Xvsat)*airmw/vapmw+Xvsat)
c
c Total density of cell mixture at saturation conditions at final temperature

```

```

c Same calculation as in RHOCAL_STG
      rhosat = p(ijk)/tfinal*
      1      (xvsat/rvap_stg+(1.-xvsat)/rgas_stg)
c
c Evaporated mass if entire cell goes to saturation condition
      delmmax = (rhosat*Yvsat - rho(ijk)*Yvacti)*vcell
c
c Evaporated mass based on diffusion rate from the surface across the cell
c diffusion mass flux = rho * diff.coeff * (Yvsat@Tfinal - Yvacti)/(distance normal to
cell)
c distance normal =~ open volume of cell divided by wall surface area
      delmdif = rho(ijk)*cmisc(isvap_stg)*delt*
      1      (Yvsat-Yvacti)*sa*sa/vcell
c
c Mass flow into cell is the minimum of the two delta-mass estimates
      delm = delmmax
      if (abs(delmdif) .lt. abs(delmmax)) delm=delmdif
c
c New estimate of final temperature
      tfsave = tfinal
c
c Solid wall energy change based on energy balance with the mass undergoing ophase
change
      twfsave = twallf
      vwall = vcell/vf(ijk)*(1.-vf(ijk))
      if (rcobs(nob) .gt. 0.) then
          twallf = twalli-delm*hvvap_stg/rcobs(nob)/vwall
      endif
      twallf = twfsave + vaprlx_stg*(twallf-twfsave)
      nitr_moist = nitr_moist+1
c
c Check for convergence
      if (abs(twallf-twfsave) .gt. .001 .and.
      1      nitr_moist .lt. 25) go to 100
c
c New value of concentration
      delmrat = delm/rho(ijk)/vcell
      sclr(ijk,isvap_stg) = (Yvacti + delmrat)/(1.+delmrat)
c
c Liquid mass flux at wall
c positive for condensation, negative for evaporation
      sclr(ijk,isliq_stg) = -delm/delt/sa
cc
cc Update the energy to account only for the vapor phase entering or leaving the cell
c PATCH - Do not execute the following three lines until the FLOW-3D energy/temp calc's
are resolved
cc
c      tvap = tfinal
c      if (delm .gt. 0) tvap=tw(ijk)
c      rhoe(ijk) = rhoe(ijk) + delm/vcell*cvvap_stg*tvap
c
c
c Change the wall temperature according to the energy balance above.
      if (rcobs(nob) .gt. 0) then
          tw(ijk) = twallf
      endif
c
c Auxiliary scalar quantities
      sclr(ijk,4) = -444.
      sclr(ijk,5) = -555.
1950      continue
2000      continue
c
c Loop over all real cells to compute the relative humidity
c
      do 3000 k=2,km1
          do 3000 j=2,jm1
              do 3000 i=2,im1
c ----- calculate current cell index
                  include './comdeck/ijk.f'
c ----- skip calculation for completely blocked cells

```



```

c is to be included in evap/condensation
c
      if(imoist_stg(nob) .ne. -nob .and.
1      ilqonly_stg(nob) .ne. -nob) go to 2000      !=====
c
      mincel=kajk(nob,nbl)
      maxcel=kajk(nob+1,nbl)-1
      if(maxcel.lt.mincel) go to 2000
      do 1950 m=mincel,maxcel
        ijk=ijkobs(m)
        call inijk(ijk,i,j,k)
        if(ijk.lt.1) go to 1950
        if(vf(ijk).lt.em6) go to 1950
        include '../comdeck/mijk.f'
        include '../comdeck/pijk.f'
c
c Retrieve the cell surface area and fluid volume
c
      vcell=vf(ijk)*delx(i)*dely(j)/rri(i)*delz(k)
      sa=waobs(m)
c
c
c Compute the concentration at saturation as follows:
c
c----- CODE MUST BE RUN WITH SI UNITS FOR THIS MODEL TO WORK!!!!!!!!!!!!
c
c   a. Guess the final temperature
c   b. Compute the saturation vapor pressure
c       Use the Keenan, Keyes, Hill, and Moore equation
c   c. Compute the saturation molar concentration (moles of vapor per total moles)
c       as the ratio of saturation vapor pressure to total pressure
c   d. Compute the mass concentration of vapor using the respective molecular weights
c   e. Compute the final temperature resulting from the phase change
c   f. Repeat steps b-e as needed.
c
c
c Get the current fluid temperature in the cell
c Save the initial temperature
c
      tfinal= teval(ijk)
      tinit= tfinal
      twalli = tw(ijk)
      twallf = twalli
          tnk = tfinal
      tnc = tnk-273.15
c
c Compute the initial concentration before phase change
c Define 1 atmosphere as 101300 Pascal
c
      term1 = F0kkhm +
1          F1kkhm*(0.65-0.01*(tnc)) +
2          F2kkhm*(0.65-0.01*(tnc))**2 +
3          F3kkhm*(0.65-0.01*(tnc))**3 +
4          F4kkhm*(0.65-0.01*(tnc))**4 +
5          F5kkhm*(0.65-0.01*(tnc))**5 +
6          F6kkhm*(0.65-0.01*(tnc))**6 +
7          F7kkhm*(0.65-0.01*(tnc))**7
      Pvsati=217.99*exp(0.01/tnk*(374.136-(tnc))*term1)
      Pvsati = Pvsati * 101300.
c
c Saturation Molar concentration ..... moles of vapor per total moles
c If Pvsati > p, the saturation values will be invalid, but invalid values are trapped below
      Xvsati = Pvsati/p(ijk)
c
c Saturation Mass Concentration .....mass of vapor to total mass
      Yvsati = Xvsati/((1.-Xvsati)*airmw/vapmw+Xvsati)
c
c Current vapor mass concentration
      Yvacti = sclr(ijk, isvap_stg)
c
c Begin the loop to balance the energy and evaporated/condensed mass

```

```

c
c      nitr_moist = 0
100      continue

c
c Compute the saturation pressure at the final fluid film temperature.
c Assume this is the wall temperature.
c
c PATCH - If there is not a wall temperature, this means the volume fraction is 1 (no wall)
c but the cell is next to an obstacle. Need to fix this later so that the obstacle
c and mesh lines can coincide an the code will recognize that an adjacent obstacle needs
c to be included in the energy balance.
c
      if (twalli .le. 0.) go to 1950
      tnk = twallf
      tnc = tnk-273.15
      term1 = F0kkhm +
1         F1kkhm*(0.65-0.01*(tnc)) +
2         F2kkhm*(0.65-0.01*(tnc))**2 +
3         F3kkhm*(0.65-0.01*(tnc))**3 +
4         F4kkhm*(0.65-0.01*(tnc))**4 +
5         F5kkhm*(0.65-0.01*(tnc))**5 +
6         F6kkhm*(0.65-0.01*(tnc))**6 +
7         F7kkhm*(0.65-0.01*(tnc))**7
      Pvsat=217.99*exp(0.01/tnk*(374.136-(tnc))*term1)
      Pvsat = Pvsat * 101300.

c
c Saturation Molar concentration ..... moles of vapor per total moles
c Limit the value to its maximum of Xvsat=1 if Pvsat > P(ijk)
      Xvsat = Pvsat/p(ijk)
      if (Xvsat .gt. 1.) Xvsat = 1.
c Saturation Mass Concentration .....mass of vapor to total mass
      Yvsat = Xvsat/((1.-Xvsat)*airmw/vapmw+Xvsat)

c
c Total density of cell mixture at saturation conditions at final temperature
c Same calculation as in RHOCAL_STG
      rhosat = p(ijk)/tfinal*
1         (xvsat/rvap_stg+(1.-xvsat)/rgas_stg)

c
c Evaporated mass if entire cell goes to saturation condition
      delmmax = (rhosat*Yvsat - rho(ijk)*Yvacti)*vcell

c
c Evaporated mass based on diffusion rate from the surface across the cell
c diffusion mass flux = rho * diff.coeff * (Yvsat@Tfinal - Yvacti)/(distance normal to cell)
c distance normal =~ open volume of cell divided by wall surface area
      delmdif = rho(ijk)*cmsc(isvap_stg)*delt*
1         (Yvsat-Yvacti)*sa*sa/vcell/0.5

c
c Mass flow into cell is the minimum of the two delta-mass estimates
      delm = delmmax
      if (abs(delmdif) .lt. abs(delmmax)) delm=delmdif

c
c New estimate of final temperature
      tfsave = tfinal

c
c Solid wall energy change based on energy balance with the mass undergoing ophase change
      twfsave = twallf
      vwall = vcell/vf(ijk)*(1.-vf(ijk))
      if (rcobs(nob) .gt. 0.) then
          twallf = twalli-delm*hvvap_stg/rcobs(nob)/vwall
      endif
      twallf = twfsave + vaprlx_stg*(twallf-twfsave)
      nitr_moist = nitr_moist+1

c
c
c For walls that have limited water available, check to be sure there is water.
c Bypass remaining calcs if there is no water to evaporate.
      if (ilqonly_stg(nob) .eq. -nob .and.
1         sclr(ijk,istlq_stg) .le. 0. .and.
2         delm .gt. 0.) then
          delm = 0.

```

```

        sclr(ijk,istlq_stg) = 0.
        twallf = twalli
        twfsave=twallf
    endif
c
c
c
c
c
c Check for convergence
        if (abs(twallf-twfsave) .gt. .001 .and.
            1          nitr_moist .lt. 25) go to 100
c
c New value of concentration
        delmrat = delm/rho(ijk)/vcell
        sclr(ijk,isvap_stg) = (Yvacti + delmrat)/(1.+delmrat)
c
c Liquid mass flux at wall
c positive for condensation, negative for evaporation
        sclr(ijk,isliq_stg) = -delm/delt/sa
c
c Total net liquid mass exchanged since beginning of simulation.
        sclr(ijk,istlq_stg) = sclr(ijk,istlq_stg) - delm

cc
cc Update the energy to account only for the vapor phase entering or leaving the cell
c PATCH - Do not execute the following three lines until the FLOW-3D energy/temp calc's are
resolved
cc
        tvap = tfinal
        if (delm .gt. 0) tvap=tw(ijk)
c
        rhoe(ijk) = rhoe(ijk) + delm/vcell*cvvap_stg*tvap
c Update the energy in the cell for the new concentration. Use TN for the temperature in RHOCAL
c
        rhoe(ijk) = rhoecl(ijk)
c
c
c Change the wall temperature according to the energy balance above.
        if (rcobs(nob) .gt. 0) then
            tw(ijk) = twallf
        endif
c
c Auxiliary scalar quantities
c
        sclr(ijk,4) = -444.
        sclr(ijk,5) = -555.
1950    continue
2000    continue
c
c Loop over all real cells to compute the relative humidity
c
        do 3000 k=2,km1
            do 3000 j=2,jm1
                do 3000 i=2,im1
c ----- calculate current cell index
                    include './comdeck/ijk.f'
c ----- skip calculation for completely blocked cells
                    if(vf(ijk).lt.em6) goto 3000

                    )
                    tnk = teval(ijk)
                    tnc = tnk-273.15
                    term1 = F0kkm +
1                      F1kkm*(0.65-0.01*(tnc)) +
2                      F2kkm*(0.65-0.01*(tnc))**2 +
3                      F3kkm*(0.65-0.01*(tnc))**3 +
4                      F4kkm*(0.65-0.01*(tnc))**4 +

```

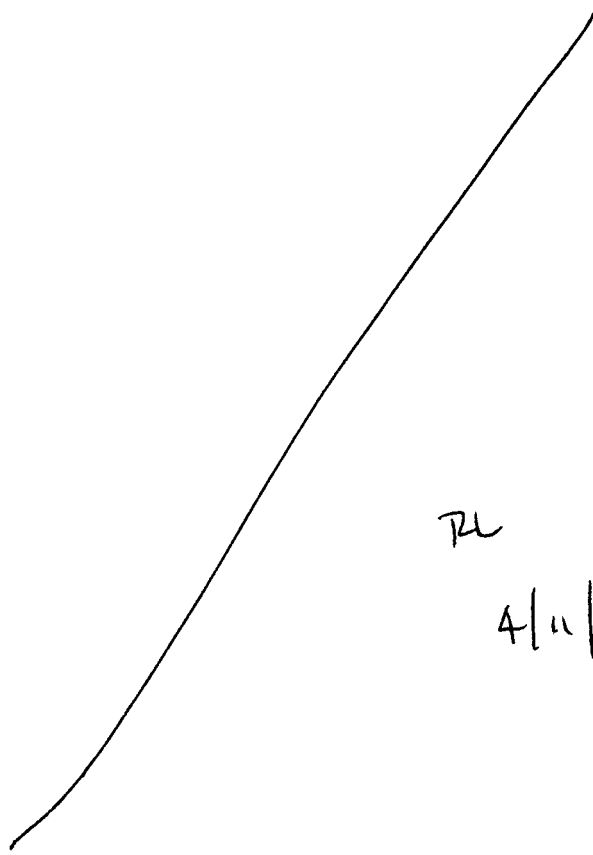
```

5          F5kkm*(0.65-0.01*(tnc))**5 +
6          F6kkm*(0.65-0.01*(tnc))**6 +
7          F7kkm*(0.65-0.01*(tnc))**7
          Pvsat=217.99*exp(0.01/tnk*(374.136-(tnc))*term1)
          Pvsat = Pvsat * 101300.
c
c Relatiuve Humidity ..... moles of vapor per moles of vapor at saturation
          Yvact = sclr(ijk, isvap_stg)
          Xvact = Yvact/(Yvact+(1.-Yvact)*vapmw/airmw)
          sclr(ijk, isrh_stg) = p(ijk)*Xvact/Pvsat
c
c
c Auxiliary scalar quantities
c          sclr(ijk,4) = tnk
c          sclr(ijk,5) = tn(ijk)
c          sclr(ijk,6) = rhoe(ijk)
c          sclr(ijk,7) = rho(ijk)
3000 continue
5000 continue
      return
      end

```

END OF ENTRY FOR 4/14/04

STG



RL

4/11/2008

3/30/05

STG

A document entitled "Software Validation Test Plan for FLOW-3D® Version 9.0" was written. This document outlines the plan for validating FLOW-3D® Version 9.0 for natural convection flows and combined forced and natural convection flows. Steve Green and David Walter are responsible for three test cases involving natural convection (laminar flow along a vertical flat plate, flow in a heated square cavity with isothermal side walls, and flow between two concentric isothermal spheres). MaryAnn Clarke is responsible for two test cases (combined forced and natural convection through an open cavity, and forced flow through an open box).

The document reviewer (Doug Gute) questioned whether the acceptance criteria of $\pm 25\%$ for the match between the measured and predicted Nusselt Numbers in the natural convection flows was typical and asked us to estimate the effect of this uncertainty on predicting the temperatures in the full scale Yucca Mountain drifts.

This entry documents the response to that query.

An two-dimensional engineering model of the heat transfer processes within a post-closure drift was developed by S. Green (Scientific Notebook 536E, entry for 9/30/03). One of the sample calculation cases in that analysis; namely, the case for the 21-PWR waste package with a rock temperature of 100°C and no drip shield. The basis for this selection is as follows:

- This waste package has the greatest decay heat of the four considered. Presumably this will lead to the highest cask temperatures of the four sample cases.
- Fedors has shown that rock wall temperatures in the range of 100°C are expected for a duration of many years
- The analysis below is simplest if the drip shield is not considered. The sensitivity of the predicted temperatures to the uncertainty in Nusselt numbers is assumed to be approximately consistent regardless of the presence of the drip shield.

The analysis is fully contained in the Mathcad file `Nu_tolerance.mcd`

A listing of this file is given in the following 3 pages.

Effects of Nusselt Number Variation on Predicting Temperature

Problem:

FLOW-3D is being validated for use on the Yucca Mountain Project in the area of free convection heat transfer. The basic approach to the validation exercise is to compare the results of free convection experiments to CFD simulations of the experiments. One of the important acceptance criteria is to match the predicted value for the Nusselt number to the measured value within a specific tolerance.

Churchill and Chu [Churchill, S.W. and H.S. Chu. "Correlating Equations for Laminar and Turbulent Free Convection from a Vertical Plate." International Journal of Heat and Mass Transfer. Volume 18, pp. 1323-1329. Pergamon Press, 1975] show Nusselt Number measurements for flow along a vertical flat plate which are spread about $\pm 25\%$ about the mean value for a Rayleigh Number of about $Ra=109$. This is somewhat larger, but still consistent with the general statement of Incropera and DeWitt [Incropera, F. P. and Dewitt, D. P. Fundamentals of Heat and Mass Transfer. Fourth Edition. pp. 487-490. John Wiley & Sons, New York. 1996] that one should expect uncertainties for Nusselt Number measurements in the range $\pm 15\%$.

Required:

Determine the effect of this range of uncertainty in Nusselt Numbers on predicting the temperature difference between the waste package and the rock wall of the YMP drifts.

Solution:

There is a wide range of decay heat rates from the waste packages that have been used in analyses of the heat transfer in the drifts. Likewise there is a wide range of rock temperatures near the drifts as the mountain responds to the transient waste package decay heat. In Scientific Notebook #536E, S. Green used an electric circuit analogy to estimate the waste package temperature under several scenarios assuming a radial 2-D geometry for a drift cross section. For the case of the heat transfer directly from the waste package to the rock wall via conduction, convection and radiation, (Case #1 in SN#536E) the heat transfer rate is given by

$$Q_{wp} = (G_c + G_r + G_k) \cdot \Delta T$$

<i>where</i>	$Q_{wp} := 1380 \cdot W$	<i>Decay heat transfer rate for the 21-PWR waste package</i>
	$G_c := 15.8 \cdot \frac{W}{K}$	<i>Thermal conductance for heat transfer by convection Value computed for this scenario.</i>
	$G_r := 98.8 \cdot \frac{W}{K}$	<i>Thermal conductance for heat transfer by radiation Value computed for this scenario.</i>
	$G_k := 0.8 \cdot \frac{W}{K}$	<i>Thermal conductance for heat transfer by conduction Value computed for this scenario.</i>

The derivation for G_c in S. Green SN #536E can be rearranged to yield

$$G_c = Nu_{gap} \frac{k_{gap} \cdot A_{wp} \cdot f_c}{0.5 \cdot (D_{rw} - D_{wp})}$$

For this case, the following geometry and fluid properties are assumed or computed:

$D_{rw} := 5 \cdot m$	Assumed rock wall inner diameter
$D_{wp} := 1.5 \cdot m$	Assumed waste package
$L_{wp} := 3 \cdot m$	Assumed effective length of the waste package
$A_{wp} := \pi \cdot D_{wp} \cdot L_{wp}$	Effective area of the waste package
$f_c := 0.75$	Assumed fraction of waste package exposed for convection and radiation
$k_{gap} := 0.031 \cdot \frac{W}{m \cdot K}$	Thermal conductivity of air at median temperature
$Pr := 0.702$	Prandtl No. for air from Tables, constant within 0.2% over temperature range.
$T_{wp} := 385 \cdot K$	Waste package temperature computed for this scenario
$T_{rw} := 373 \cdot K$	Rock wall temperature assumed for this scenario
$\rho := 0.932 \cdot \frac{kg}{m^3}$	Air density from ideal gas assumption at rock wall temperature
$\beta := 0.002639 \cdot \frac{1}{K}$	Thermal expansion coefficient for air, ideal gas assumption
$\mu := 2.32 \cdot 10^{-5} \cdot Pa \cdot sec$	Air dynamic viscosity, linear curve fit to data

An expression can be derived from the information provided by Green in SN#536E for the Nusselt Number in this scenario,

$$B_{conc.cyl} := \frac{0.386 \cdot (D_{rw} - D_{wp})}{D_{wp} \left(\frac{D_{rw} - D_{wp}}{2} \right)^{0.75} \cdot (D_{rw}^{-0.6} + D_{wp}^{-0.6})^{1.25}} \cdot \left(\frac{Pr}{0.861 + Pr} \right)^{0.25} \quad B_{conc.cyl} = 0.4$$

$$Ra_{gap} := \frac{\rho^2 \cdot g \cdot \beta}{\mu} \cdot Pr \cdot (T_{wp} - T_{rw}) \cdot \left(\frac{D_{rw} - D_{wp}}{2} \right)^3 \quad Ra_{gap} = 1.886 \times 10^9$$

$$Nu_{gap} := B_{conc.cyl} Ra_{gap}^{\frac{1}{4}}$$

$$Nu_{gap} = 83.452$$

Now we can express the sensitivity of the predicted temperature difference to the uncertainty in only the Nusselt Number

$$d\Delta T dNu = \frac{d}{dNu} \Delta T = \frac{Q_{wp}}{(G_c + G_r + G_k)^2} \frac{d}{dNu} (G_c) = \frac{Q_{wp}}{(G_c + G_r + G_k)^2} \cdot \frac{k_{gap} \cdot A_{wp} \cdot f_c}{0.5 \cdot (D_{rw} - D_{wp})}$$

where

$$d\Delta T dNu := \frac{Q_{wp}}{(G_c + G_r + G_k)^2} \cdot \frac{k_{gap} \cdot A_{wp} \cdot f_c}{0.5 \cdot (D_{rw} - D_{wp})}$$

$$d\Delta T dNu = 0.019 \text{ K}$$

If the uncertainty in Nusselt Number is $\pm 25\%$,

$$\delta_{Nu} := 0.25 \cdot Nu_{gap} \quad \delta_{Nu} = 20.863$$

Then the associated uncertainty in temperature difference is

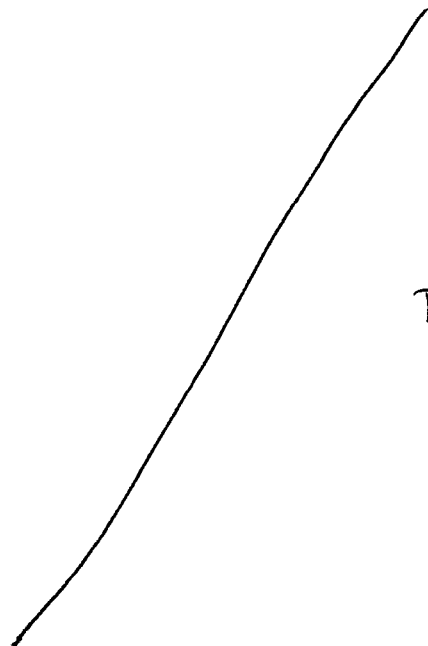
$$\delta_{\Delta T} := d\Delta T dNu \cdot \delta_{Nu}$$

$$\delta_{\Delta T} = 0.406 \text{ K}$$

This shows that if the Nusselt Number is known to within 25% of the value computed above, the associated temperature difference between the waste package and the rock wall will be known to within about 0.4 K.

Note that this analysis focuses only on the indirect correlation of Nusselt Number to the temperature difference driving the overall heat transfer. We have not investigated the possible underlying causes of the Nusselt Number uncertainty - all these underlying effects are lumped into a single expression for the Nusselt Number uncertainty. Other effects (e.g., temperature dependent properties, geometric uncertainty, and heat rate uncertainty) have all been neglected.

RL
4/11/2008



This analysis shows that the sensitivity of the predicted waste package to rock wall temperature difference to only Nusselt Number is mitigated by the strong effect of thermal radiation in the drift. The acceptance criteria of 25% for a Nusselt Number variance between FLOW-3D and the benchmark cases will attribute for approximately a 0.4 K uncertainty.

It should be noted that this analysis was based on many assumptions and was limited to a single sample calculation

END OF ENTRY FOR 3/30/05

STG

4/10/05

STG

This entry describes the work performed to prepare a validation test report for FLOW-3D Version 9.0 as described in the document "Software Validation Test Plan for FLOW-3D® Version 9.0". The particular test case discussed in this entry is that of laminar and transitional turbulent flow between two concentric isothermal cylinders in which the inner cylinder is at a higher temperature than the outer cylinder.

This work was performed primarily by S. Green in the January-March 2005 time period. This task was performed in parallel with the other similar validation work performed by David Walter

Experiments

This validation case is based on experiments reported in

Kuehn, T.H. and R.J. Goldstein. "An Experimental Study of Natural Convection Heat Transfer in Concentric and Eccentric Horizontal Cylindrical Annuli." *ASME Journal of Heat Transfer*. Volume 100, pp. 635-640. 1978.

The test apparatus is described more fully in an earlier paper,

Kuehn, T.H. and R.J. Goldstein. "An Experimental Study and Theoretical Study of Natural Convection in the Annulus Between Horizontal Concentric Cylinders," *Journal of Fluid Mechanics*, Volume 74, Part 4, pp. 695-719, 1976.

The experiment facility consisted of two concentric cylinders sealed in a pressure vessel. The outer diameter of the inner cylinder was 3.56 cm and the inner diameter of the outer cylinder was 9.25 cm. The annular gap between the cylinders was 2.845 cm. The cylinders were 20.8 cm in length. The inner cylinder was electrically heated while the outer cylinder was cooled with

a chilled water loop. The test chamber was filled with nitrogen as the test fluid. The nitrogen pressure was varied between 0.071 atm and 35.2 atm and the temperature difference between the two cylinders was varied between 0.83 K and 60.1 K. This provided for a Rayleigh Number range of 2.2×10^2 to 7.74×10^7 . Temperatures in the annulus were measured via Mach-Zender interferometer and surface temperatures were measured with thermocouples.

This range of Rayleigh Number values does not represent the expected Rayleigh number range of the Yucca Mountain drifts when there is no drip shield. For the case in which a drip shield is used, the range of Rayleigh Number values covered by the experiments covers the expected range of Rayleigh numbers for convection heat transfer between the waste package and the drip shield. The calculations supporting this statement are found in the Excel file:

WP_Drift_HT.xls

described in the entry for 9/30/03 in this Scientific Notebook (#536E).

Keuhn and Goldstein report the experiment results for the heat transfer across the annulus in terms of an effective thermal conductivity that is used in an expression of conduction heat transfer across a quiescent fluid (or solid object for that matter). The effective thermal conductivity is defined as follows.

The one-dimensional radial heat flux at the inner surface transfer across an annular material is defined as

$$q_i'' = \frac{2k_{eff}}{D_i \ln\left(\frac{D_o}{D_i}\right)} (T_i - T_o) \quad (\text{Eq. 1})$$

- where q_i'' = heat flux at inner cylindrical surface [e.g., W/m²]
 k_{eff} = effective thermal conductivity or material [e.g., W/(m×K)]
 D_i = inner surface diameter (e.g., m)
 D_o = outer surface diameter (e.g., m)
 T_i = inner surface temperature (e.g., K)
 T_o = outer surface temperature (e.g., K)

This expression is rearranged to yield

$$k_{eff} = q_i'' \frac{D_i \ln\left(\frac{D_o}{D_i}\right)}{2(T_i - T_o)} \quad (\text{Eq. 2})$$

The value of k_{eff} can be either a local value or a net value for a large surface depending on whether the value of q_i'' is a local value or the net value for the surface.

Keuhn and Goldstein do not describe the measurement uncertainty for temperature or the derived values of k_{eff} in the 1978 paper reporting the test values used here. In the 1976 paper reporting results for air in low Rayleigh Number flows, however, they state that the variance between values of k_{eff} derived from interferogram contours and those obtained from overall

heat transfer rates was less than 3%. The difference between the derived value of the Rayleigh Number was about 7%.

For nitrogen, the a single fringe shift in the interferogram corresponds to about 35 K at a pressure of 0.15 atm and about 0.1 K at a pressure of 35 atm.

FLOW-3D cases

Six of the reported 40 sets of test measurements were selected for simulation with FLOW-3D. These six cases are described in Table 4/12/05-1. A seventh case was selected for a simulation with a fine resolution mesh at $Ra=2.51 \times 10^6$ since Keuhn and Goldstein provide some details of the temperature profiles along the cylinder surfaces and between the cylinders for this case. The conditions used for the seven CFD simulations are listed in Table 4/12/05-2

Table 4/12/05-1. Experiments Selected for FLOW-3D Simulations

Ra_{gap}	P atm	ΔT °C	$\frac{1}{2}(T_i+T_o)$ °C
1.31×10^3	0.110	53.5	51.1
6.19×10^4	0.977	38.0	44.4
6.81×10^5	8.46	4.29	27.3
2.51×10^6	34.6	0.91	27.7
1.90×10^7	34.7	7.01	29.1
6.60×10^7	35.0	28.7	40.8

Table 4/12/05-2. FLOW-3D Simulation Conditions

Ra_{gap}	Mesh (Uniform)	ρ kg/m ³	β 1/K	μ Pa×sec	C_v J/(kg×K)	k W/(m×K)	FLOW-3D Input File Name
1.31×10^3	72×72	0.1158	3.08×10^{-3}	1.903×10^{-5}	742.6	0.0274	prepin.K-G_Validation_Ra1-3e03
6.19×10^4	72×72	1.051	3.15×10^{-3}	1.875×10^{-5}	742.6	0.0270	prepin.K-G_Validation_Ra6-2e04
6.81×10^5	72×72	9.627	3.32×10^{-3}	1.810×10^{-5}	744.2	0.02627	prepin.K-G_Validation_Ra6-8e05
2.51×10^6	72×72	39.40	3.323×10^{-3}	1.859×10^{-5}	750.3	0.02793	prepin.K-G_Validation_Ra2-5e06
2.51×10^6 (Fine Mesh)	144×144						prepin.K-G_Validation_Ra2-5e06_fine
1.90×10^7	72×72	39.32	3.309×10^{-3}	1.865×10^{-5}	750.3	0.02802	prepin.K-G_Validation_Ra1-9e07
6.60×10^7	72×72	38.07	3.185×10^{-3}	1.916×10^{-5}	749.9	0.02874	prepin.K-G_Validation_Ra6-6e07

The properties of nitrogen at the selected test conditions were provided from the computer program NIST12. This program is equivalent to the web-based property information software available at NIST.

FLOW-3D uses a structured Cartesian orthogonal mesh and the VOF method to define cells blocked by solid obstacles. Because the cylinder surfaces are curved, the fractional blockage of cells containing the solid surface varies greatly. Grid refinement in the boundary layers is of limited use; consequently, a uniform mesh was selected. The mesh resolution was chosen to adequately capture the expected temperature and velocity distributions for $Ra < 1 \times 10^5$ (i.e. truly

laminar flow throughout the entire flow domain). Keuhn and Goldstein report that turbulent eddies are observed at the top of the inner cylinder for $Ra \approx 2 \times 10^5$. The LES turbulence model was used for simulations of the higher Rayleigh number flows and a consistent mesh was used under the assumption that the selected mesh adequately captures the flow structures of interest. At increasing Rayleigh Numbers more and more of the flow is turbulent until at $Ra \approx 4 \times 10^8$ the upper half of the annulus is clearly in turbulent flow, but the lower half is in laminar flow.

The grid resolution was refined by a factor of 2 for the case of $Ra = 2.5 \times 10^6$

The FLOW-3D input file for the case of $Ra = 1.3 \times 10^3$ is listed below. The other input files are similar with the changes to cylinder temperatures, fluid properties and grid definition indicated in Table 4/12/05-2.

Listing of file prepin.K-G_Validation_Ra1-3e03

```
Nat. Conv. in conc. cyl. annulus, Ra=1.31x10^3, P=0.110 atm, e=0, DT=53.5'C
This is a simulation of a test reported in
  Kuehn, T. H., Goldstein, R. J., "An Experimental Study of Natural Convection
  in Concentric and Eccentric Horizontal Cylindrical Annuli," ASME Journal
  of Heat Transfer, Vol. 100, pp. 635-640.
The objective is to verify the the FLOW-3D simulation of this type of
flow from the standpoint of temperature distribution, Rayleigh Number, effective
conductivity, and the onset of turbulent flow.
A uniform mesh is used here with 72 cells across the diameter of the outer cylinder.
A similar simulation with a water vapor and air mixture with and without phase
change at the outer walls will be conducted to investigate the effects of phase change
on the overall heat transfer and flow processes.
The geometry of the Kuehn and Goldstein test setup is modeled here. Full scale
drift geometry will be compared on a dimensionless basis to test the Rayleigh scaling
hypothesis.
  Inner cylinder (isothermal) = 3.56 cm O.D.
  Outer cylinder (isothermal) = 9.25 cm I.D.
This particular case is for (see Table 1 of Kuehn and Goldstein)
Pressure = 0.110 atm
DT = 53.5'C
T-mean = 51.1'C
Ra-L = 1.31e+03
Pr = 0.717
Nitrogen
k-equivalent = 1.14 (measured)

Modified from prepin.uniform_K-G_Ra6e04
```

```
$xput
  remark='units are SI',
  twfin=30.,
  itb=0,          remark='No free surface',
  gz=-9.8,       remark='Gravity in -z direction',
  ifvis=0,       remark='Laminar',
  ifenrg=3,      remark='Second-order energy equation',
  ifrho=1,       remark='Boussinesq assumption',
  ihtc=1,        remark='Evaluate heat transfer at walls - no conduction solution',
  ipdis=1,       remark='Hydrostatic pressure gradient allowed',
  imphtc=1,      remark='Implicit heat transfer solution',
  iadix=1,       remark='Implicit line-solver for momentum',
  iadiz=1,
  iwsh=1,        remark='Evaluate wall shear stress',
  deltt=1.e-3,
  pltdt=10.,
$end

$limits
$end
```

```
$props
  units='si',
  rhof=0.1158,   remark='Nitrogen at 0.110 atm, 51.1 deg.C',
  mu1=1.903e-05,
  cv1=742.6,
  thc1=0.0274,
  tstar = 324.25, remark='Average temp of two surfaces is Boussinesq reference',
  thexf1 = 3.08e-03, remark='Nitrogen as ideal gas, beta=1/T',
$end

$scalar
$end

$bcdata
  wl=1, wr=1,   remark='All faces are either symmetry or obstacle-blocked',
  wf=1, wbk=1,
  wb=1, wt=1,
$end

$mesh
  py(1)=-0.0475,   px(1)=0.,   pz(1)=-0.0475,
  py(2)=-0.04625, px(2)=0.00128, pz(2)=-0.04625,
  py(3)= 0.04625,   px(3)=0.,   pz(3)= 0.04625,
  py(4)= 0.0475,   px(4)=0.,   pz(4)= 0.0475,
  nycell(1)=1,      nzcell(1)=1,
  nycell(2)=72,     nzcell(2)=72,
  nycell(3)=1,      nzcell(3)=1,
  nycelt=74,        nxcelt=1,   nzcelt=74,
$end

$obs
  avrck=-3.,
  nobs = 2,
  tobs(1)=0., tobs(2)=1000.,
  remark='Outer cylinder',
  ral(1)=0.04625, roty(1)=90.,
  twobs(1,1)=297.50, twobs(2,1)=297.50,
  remark='Inner cylinder',
  rah(2)=0.0178, roty(2)=90.,
  twobs(1,2)=351.00, twobs(2,2)=351.00,
$end

$f1
  presi=0.,
$end

$bf
$end

$temp
  ntmp=1,
  tempi=324.25,
$end

$motn
$end

$grafic
$end

$parts
$end

$surdat
$end
```

End of listing of file prepin.K-G_Validation_Ra1-3e03

The FLOW-3D postprocessor will provide the user with the total heat transfer rate from solid objects to the fluid. This output was transferred to an Excel file to execute the calculation indicated by Eq. 2. The following Excel file contains all the necessary FLOW-3D text output and post-processing calculations for the this validation test

[K-G_FLOW3D_Compare.xls](#)

The convection heat transfer can also be expressed in terms of a Nusselt number. First, the heat flux at the inner surface can be also expressed as

$$q_i'' = h_i(T_i - T_o) = \frac{Nu k_f}{D_i}(T_i - T_o) \quad (\text{Eq. 3})$$

where h_i = heat transfer coefficient [e.g., W/(m²×K)]

Nu = Nusselt number

k_f = fluid material thermal conductivity

Comparing Eq. 3 can be rearranged to yield the expression

$$Nu = q_i'' \frac{D_i}{k_f(T_i - T_o)} = 2 \frac{k_{eff}}{k_f} \frac{D_i}{\ln\left(\frac{D_o}{D_i}\right)} \quad (\text{Eq. 4})$$

The Nusselt Number, Nu , is described in terms of the computed or measured value of k_{eff} (which varies as a function of test conditions) a material property that is temperature dependent but is not affected by the flow field, and geometric parameters that are constant. Eq. 4 is not used in the post-processing of these data. It is shown here to demonstrate that relative variances (i.e. percent difference) between the computed and measured Nusselt numbers will be the same as the relative variances (i.e. percent difference) between the computed and measured values of k_{eff} , assuming one neglects the uncertainty of the fluid thermal conductivity, k_f . This particular uncertainty is indeed small compared to the variance between the measured and computed values for k_{eff} shown below.

The acceptance criterion for the variance between the measured and computed values of k_{eff} was established as $\pm 25\%$. This acceptance requirement is established in the "Software Validation Test Plan for FLOW-3D® Version 9.0" and is discussed in the entry for 4/11/05 of this notebook.

Comparison of Predicted and Measured Values

The measured values of k_{eff} reported by Kuehn and Goldstein are compared to the values predicted by FLOW-3D in Table 4/12-05-3

Table 4/12/05-2. FLOW-3D Simulation Conditions

Ra_{gap}	k_{eq} experiment	k_{eq} FLOW-3D	Deviation %
1.31×10^3	1.14	1.04	-9.0
6.19×10^4	3.32	2.90	-12.7
6.81×10^5	5.6	5.27	-5.8
2.51×10^6	7.88	7.87	-0.1
2.51×10^6 (Fine Mesh)		6.63	-15.9
1.90×10^7	13.27	14.52	9.5
6.60×10^7	18.65	20.83	11.7

For the nominal grid resolution it is seen that the variance ranges from -12.7% at low Ra to +11.7%. The variance is -15.7% for the refined grid resolution. All of these values are within the established acceptance criterion.

The surface heat flux variations over the inner and outer cylinders are presented in terms of the local value of k_{eff} in Figure

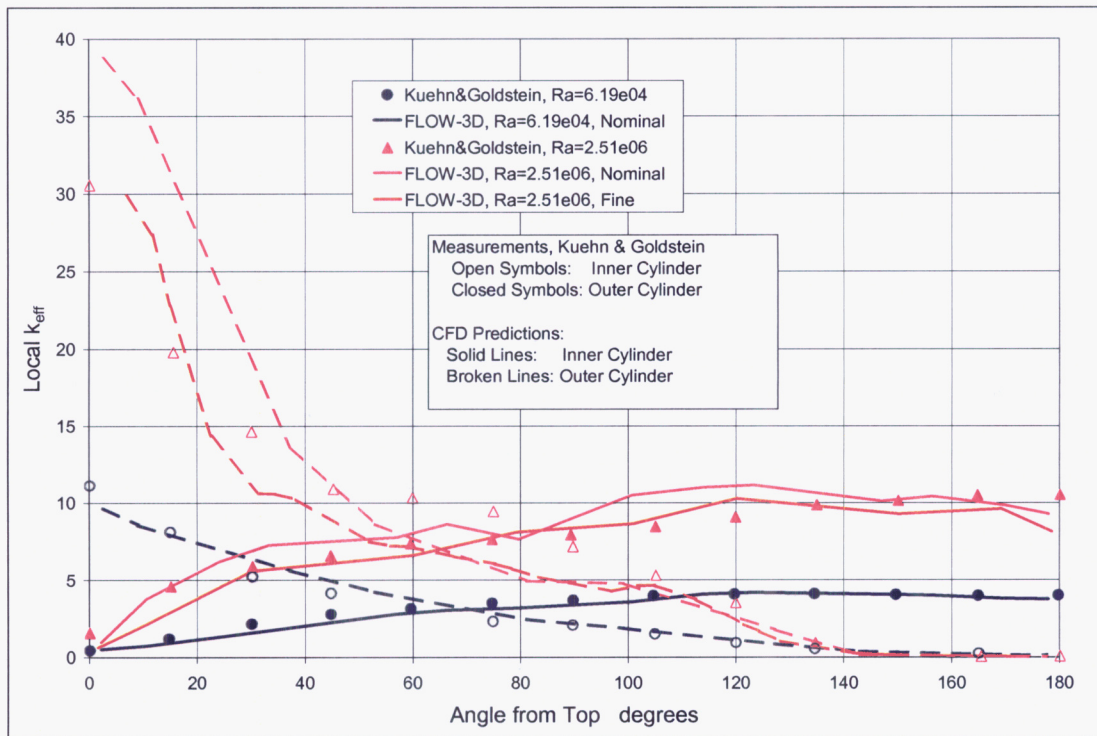


Figure 4/12/15-1. Local Value of k_{eff}

There is excellent agreement between the predicted and measured values of local k_{eff} for $Ra=6.19 \times 10^4$ on both the inner and outer cylinders. The agreement is also good at $Ra=2.51 \times 10^6$ for the outer surface. At the inner surface for $Ra=2.51 \times 10^6$ there are regions where the agreement is poor; however, the general trend of the measured values is matched by the CFD results.

With the nominal mesh for $Ra=2.51 \times 10^6$ the predicted values of k_{eff} near the top of the inner cylinder are greater than the measured values, but the predicted values are less than the measured values between about 50° and 100° from the top. From 100° to 180° the agreement is good, but this is a much less important area than the upper parts of the cylinder. With the refined mesh, the predicted values of k_{eff} near the top of the inner cylinder are in closer agreement with the measured values than for the nominal mesh. In the area of 50° and 180° from the results from the nominal and refined meshes are almost identical. This trend explains the decrease in the overall value of k_{eff} for the refined mesh compared to the nominal mesh. Nevertheless, the refined mesh gave only slightly different local values of k_{eff} ; so, the nominal mesh is seen as being adequate for this flow.

The predicted fluid temperature profiles for the case of $Ra=2.51 \times 10^6$ are compared to the measured values along selected radial lines around the annulus in Figure 4/12/05-2. First, it is seen that the results for the nominal mesh and the refined mesh are not significantly different. This is further evidence that the nominal mesh is adequately resolving the calculated flow characteristics. The general trends of the measured temperature profiles are observed in the predicted temperature profiles except at an angle of 0° .

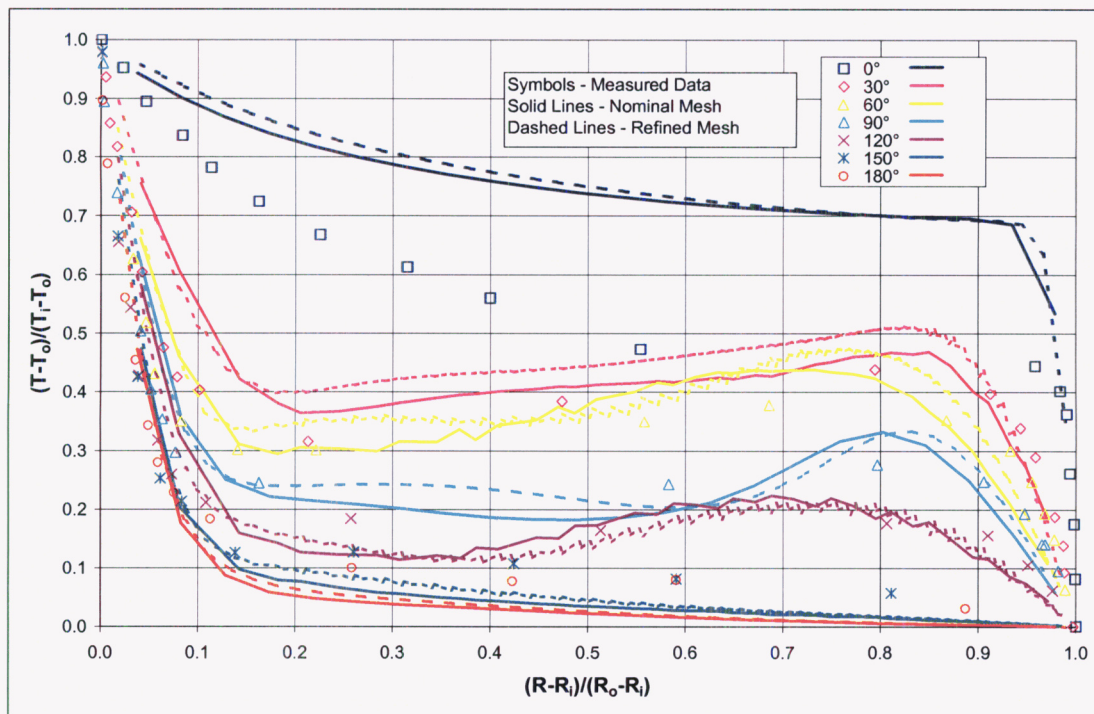
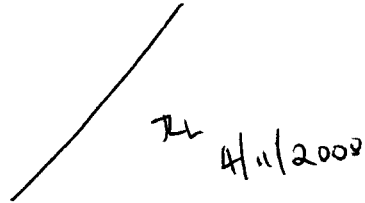


Figure 4/12/15-2. Fluid Temperature Profiles

It should be noted, however, that the temperature difference between the inner and outer cylinders for this case is only 0.91 K. The temperature difference between fringes on the

interferogram for this case (i.e. at a pressure of 34.6 atm) is about 0.1 K. So there are only about nine fringe contours across the annulus gap. The uncertainty in obtaining temperature values from such an interferogram are not discussed in the paper so we cannot assess this impact on the agreement between the measured temperature profiles and the predicted temperature profiles.



TL 4/11/2008

END OF ENTRY FOR 4/10/05 *STG*

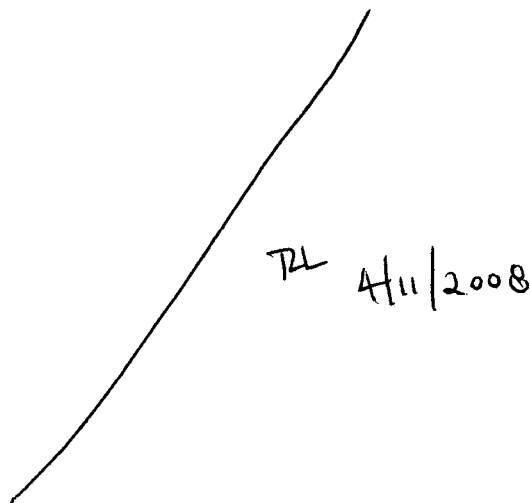
=====

Entries made into Scientific Notebook #536E for the period October 2004, to April 10, 2005, have been made by Steven Green (April 10, 2005).

No original text or figures entered into this Scientific Notebook has been removed

STG 04/10/2005

=====



TL 4/11/2008

5/16/05 STG

Candidate test cases with which to validate the FLOW-3D vapor transport model were reviewed. It was decided to use two tests cases for this validation effort and to continue the scoping activity for the software. The two test cases will be:

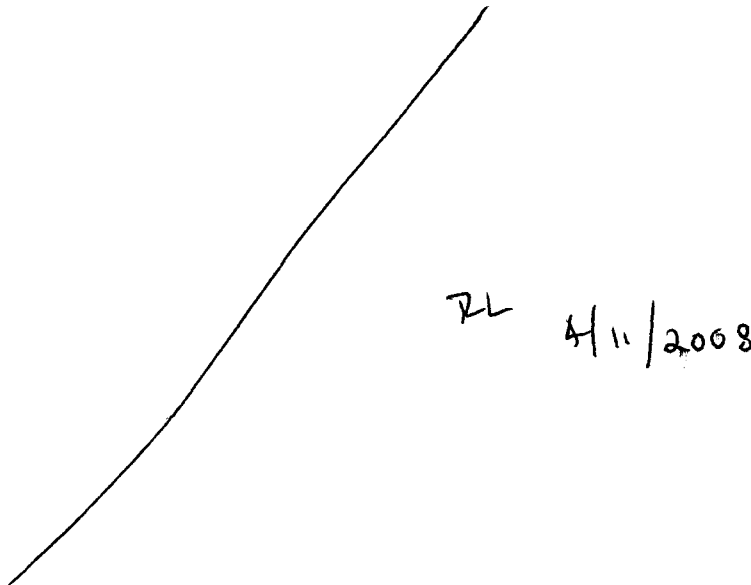
1. The transport of moisture from a high temperature wet surface to a lower temperature wet surface. This will be carried out as an analytical of an idealized 1-D geometry.
2. The transport of vapor from a pan of hot water on the floor of an enclosure to a cooled wall at the opposite end of the enclosure.

TEST CASE 1

This test case is based on the analytical treatment of a diffusion of water vapor and thermal energy in air from a hot wall to a cold wall in which both walls are saturated with liquid water. This scenario is described in Sections 16 and 17 of

Bird, R. B., Stewart, W. E., Lightfoot, E. N., **Transport Phenomena**, John Wiley and Sons, New York, 1960. Specifically, Sections 17 and 18 of this text provide the general equations and examples.

The analytical basis for this case is described in the Matchcad sheet 1-D_Heat_Mass.mcd
A listing of this file is given in the following 7 pages.



RL 4/11/2008

One dimensional Conduction and Mass Diffusion

Introduction

This document describes an analytical solution to the combined heat transfer and mass diffusion in a volume of two chemical species. The opposing surfaces are maintained at different temperatures and the surfaces are liquids of one species. The other species is not condensable. The heat transfer is by conduction only through the mixture.

The general equations of the two diffusion processes are presented and a specific example is investigated. The specific example is that of water vapor diffusing through air between one liquid surface held at 320 K and the other at 280 K.

This specific example serves as a validation test case for the software written to incorporate a vapor transport model into the computer program FLOW-3D.

References

The equations describing this process are given in

Bird, R. B., Stewart, W. E., Lightfoot, E. N. *Transport Phenomena*, John Wiley and Sons, New York, 1960. Specifically, Sections 17 and 18 of this text provide the general equations and examples.

General Case

Consider the scenario described in Figure 1.

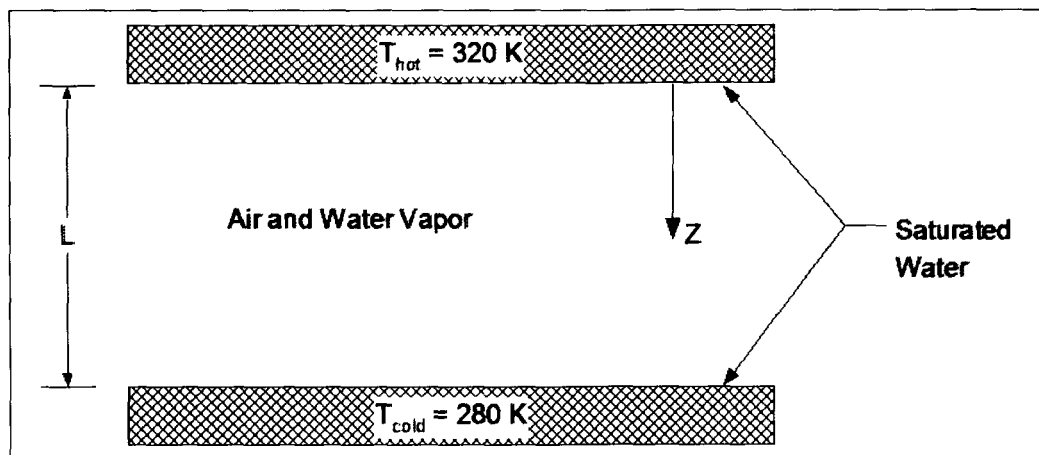


Figure 1. 1-D Conduction and Diffusion in a Mixture

A mixture of air and water vapor is maintained between two surfaces which are at two different temperatures. Each surface is able to maintain a liquid water interface that is in equilibrium with the water vapor adjacent to the wall. In this scenario we will assume that there is no advection of the bulk mixture and we will neglect the Soret and Dufour effects.

The water vapor evaporates from the hot surface, diffuses through the mixture and condenses on the cold surface. The air is incondensable and is stationary. We will also assume that the bulk properties of the mixture are uniform and constant.

Bird, Stewart and Lightfoot show that the energy flux at any point in the z-direction is given by

$$e(z) = -k_{\text{mix}} \left(\frac{d}{dz} T \right) + (h_a \cdot N_a + h_v \cdot N_v) \quad \text{Eq. 1}$$

where

- e energy flux
- k_{mix} mixture thermal conductivity
- T local mixture temperature
- h_a mole-specific enthalpy of air
- N_a mole flux of air
- h_v mole specific enthalpy of water vapor
- N_v mole specific enthalpy of water vapor

For the case considered here, $N_a = 0$. Assuming that both air and water vapor can be treated as ideal gases, Eq. 1 can be rewritten as

$$e(z) = -k_{\text{mix}} \left(\frac{d}{dz} T \right) + N_v \cdot C_{pa} (T - T_{\text{cold}}) \quad \text{Eq. 2}$$

We will use T_{cold} as the reference temperature for assigning enthalpy values. At steady conditions the energy flux is constant

$$\frac{d}{dz} e(z) = 0 \quad \text{Eq. 3}$$

Bird, Stewart and Lightfoot also show that the mole flux of vapor in this 1-D model is described by

$$N_v = -\rho_{\text{mix}} D_{va} \left(\frac{d}{dz} x_v \right) + x_v \cdot N_{\text{mix}} \quad \text{Eq. 4}$$

where

- N_v mole flux of water vapor
- ρ_{mix} mole density of the mixture
- D_{va} diffusion coefficient for water vapor and air
- x_v mole concentration of water vapor (mole per unit volume)
- N_{mix} mole flux of mixture

The mole flux of the mixture is

$$N_{\text{mix}} = N_v + N_a$$

but the air is stationary; so, $N_{\text{mix}} = N_v$. Eq. C becomes

$$N_v = -\frac{\rho_{\text{mix}} D_{va}}{1 - x_v} \frac{d}{dz} x_v \quad \text{Eq. 5}$$

Again, under steady conditions, the mole flux of vapor is constant,

$$\frac{d}{dz} N_v = 0 \quad \text{Eq. 6}$$

First, solve for the vapor concentration profile. Start by substituting Eq. 5 into Eq. 6 and rearranging

$$\frac{d}{dz} \left(\frac{\rho_{\text{mix}} D_{\text{va}}}{1 - x_v} \frac{d}{dz} x_v \right) = 0$$

$$\frac{d}{dz} \left[\frac{1}{(1 - x_v)} \frac{d}{dz} x_v \right] = 0$$

with the boundary conditions

$$x_v = x_{v,L} \quad \text{at} \quad z=L$$

$$x_v = x_{v,0} \quad \text{at} \quad z=0$$

Integrate once to yield

$$\frac{1}{(1 - x_v)} \frac{d}{dz} x_v = C_1$$

Integrate again to yield

$$-\ln(1 - x_v) = C_1 \cdot z + C_2$$

Applying the boundary conditions provides the required solution

$$\frac{1 - x_v}{1 - x_{v,0}} = \left(\frac{1 - x_{v,L}}{1 - x_{v,0}} \right)^{\frac{z}{z_L}}$$

or

$$x_v = 1 - (1 - x_{v,0}) \left(\frac{1 - x_{v,L}}{1 - x_{v,0}} \right)^{\frac{z}{z_L}}$$

Eq. 7

The vapor mole flux can be obtained by substituting Eq. 7 back into Eq. 5,

$$N_v = \frac{\rho_{\text{mix}} D_{\text{va}}}{z_L} \cdot \ln \left(\frac{1 - x_{v,L}}{1 - x_{v,0}} \right)$$

Eq. 8

The water vapor mole flux is defined relative to the coordinate system. The value is negative in Eq. 8 if the hot surface is at $z=L$ (instead of as shown) because the mole flux would be in the negative z -direction in that case.

Also, note that the concentration profile is nonlinear. This is a result of the overall flow of vapor through the domain.

Now, the temperature distribution can be derived. Eq. 2 can be rewritten as

$$-k \cdot (T_L - T_0) \cdot \left(\frac{d}{dz} T' \right) + N_a \cdot C_{pv} \cdot (T_L - T_0) \cdot T' = e$$

where $T' = \frac{T - T_0}{T_L - T_0}$

The boundary conditions are

$$T' = 0 \quad \text{at} \quad z = 0$$

$$T' = 1 \quad \text{at} \quad z = L$$

This expression is rearranged as

$$\left(\frac{d}{dz} T' \right) - \frac{N_a \cdot C_{pv}}{k} \cdot T' = -\frac{e}{k \cdot (T_L - T_0)}$$

This first order differential equation can be solved by multiplying first by the appropriate integrating factor, $\exp\left(-\frac{N_v \cdot C_{pv}}{k} \cdot z\right)$

$$\frac{d}{dz} \left(T' \cdot \exp\left(-\frac{N_v \cdot C_{pv}}{k} \cdot z\right) \right) = -\frac{e}{k \cdot (T_L - T_0)} \cdot \exp\left(-\frac{N_v \cdot C_{pv}}{k} \cdot z\right)$$

This is finally solved,

$$T' = \frac{e}{(T_L - T_0) \cdot N_v \cdot C_{pv}} + C_2 \cdot \exp\left(\frac{N_v \cdot C_{pv}}{k} \cdot z\right) \tag{Eq. 9}$$

Apply the condition at z=0

$$C_2 = -\frac{e}{(T_L - T_0) \cdot N_v \cdot C_{pv}}$$

Substitute this into Eq. 9

$$T' = \frac{e}{(T_L - T_0) \cdot N_v \cdot C_{pv}} \cdot \left(1 - \exp\left(\frac{N_v \cdot C_{pv}}{k} \cdot z\right) \right)$$

Apply the condition at z=L

$$\frac{e}{(T_L - T_0) \cdot N_v \cdot C_{pv}} = \frac{1}{\left(1 - \exp\left(\frac{N_v \cdot C_{pv}}{k} \cdot z_L\right) \right)}$$

Finally, the required solution is

$$T' = \frac{1 - \exp\left(\frac{N_v \cdot C_{pv}}{k} \cdot z\right)}{1 - \exp\left(\frac{N_v \cdot C_{pv}}{k} \cdot z_L\right)} \quad \text{or} \quad T(z) = T_0 + (T_L - T_0) \cdot \frac{1 - \exp\left(\frac{N_v \cdot C_{pv}}{k} \cdot z\right)}{1 - \exp\left(\frac{N_v \cdot C_{pv}}{k} \cdot z_L\right)} \tag{Eq. 10}$$

As with the concentration profile, the temperature distribution is nonlinear. The deviation from a linear profile is governed by the fluid properties and the mole flux.

Example Calculation

The example calculations are for the case described in Figure 1 where

$$T_L := 280 \cdot K \quad T_0 := 320 \cdot K$$

$$z_L := 0.2 \cdot m \quad \text{Distance between surfaces}$$

$$P_{mix} := 1 \cdot atm \quad \text{Total pressure of mixture, assumed uniform, constant}$$

To define the saturation vapor pressure of water vapor, us the correlation of Keenan, Keyes, Hill, and Moore.

$$E_0 := -741.9242 \quad F_4 := 0.1094098$$

$$F_1 := -29.721 \quad F_5 := 0.439993$$

$$F_2 := -11.55286 \quad F_6 := 0.2520658$$

$$F_3 := -0.8685635 \quad F_7 := 0.05218684$$

$$FPvsat(T) := 217.99 \cdot \exp \left[\frac{0.01}{T} \cdot [374.136 - (T - 273.15)] \cdot \sum_{k=0}^7 [F_k \cdot [0.65 - 0.01 \cdot (T - 273.15)]^k] \right] atm$$

$$P_{mix} = 101325 Pa$$

This expression gives the vapor pressure in atm when the temperature is provided in K.

The material properties of water vapor and air are taken from handbook values.

$$R_{gas} := 8.3143 \cdot \frac{joule}{mol \cdot K} \quad \text{Universal gas constant}$$

$$MW_{vap} := 18.01534 \cdot \frac{gm}{mol} \quad MW_{air} := 28.9645 \cdot \frac{gm}{mol} \quad \text{Molecular weights}$$

$$C_{pv} := 1872.3 \cdot \frac{joule}{kg \cdot K} \cdot MW_{vap} \quad \text{Mole-specific heat of water vapor}$$

$$D_{va} := 2.6 \cdot 10^{-5} \cdot \frac{m^2}{sec} \quad \text{Species diffusion coefficient for air - water vapor}$$

$$k_{mix} := 0.026 \cdot \frac{watt}{m \cdot K} \quad \text{Mixture thermal conductivity, assumed constant}$$

The vapor conditions adjacent to each surface are now computed

$$P_{v.sat.0} := FPvsat \left(\frac{T_0}{K} \right)$$

$$P_{v.sat.0} = 1.054 \times 10^4 Pa$$

$$P_{v.sat.L} := FPvsat \left(\frac{T_L}{K} \right)$$

$$P_{v.sat.L} = 991.24 Pa$$

$$C_{pv} = 33.73 \cdot \frac{kgm^2}{s^2 \cdot K mol}$$

$$x_{v.sat.0} := \frac{P_{v.sat.0}}{P_{mix}}$$

$$x_{v.sat.L} := \frac{P_{v.sat.L}}{P_{mix}}$$

RL
4/11/2008

Assume a linear temperature profile to estimate the average temperature for computing the bulk molar density

$$T_{avg} := 0.5 \cdot (T_0 + T_L) \quad \rho_{n,mix} := \frac{P_{mix}}{R_{gas} \cdot T_{avg}} \quad \text{Bulk molar density}$$

$$x_v(z) := 1 - (1 - x_{v,sat,0}) \cdot \left[\frac{(1 - x_{v,sat,L})}{1 - x_{v,sat,0}} \right]^{\frac{z}{z_L}} \quad \text{Vapor concentration profile}$$

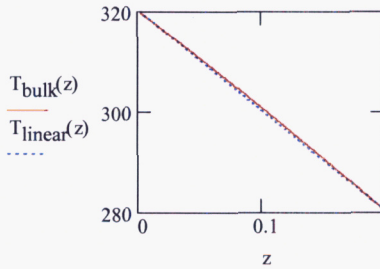
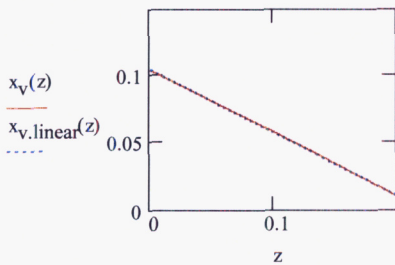
$$N_v := \frac{\rho_{n,mix} \cdot D_{va}}{z_L} \cdot \ln \left(\frac{1 - x_{v,sat,L}}{1 - x_{v,sat,0}} \right) \quad N_v = 5.283 \times 10^{-4} \frac{\text{mol}}{\text{m}^2 \cdot \text{s}} \quad \text{Mol flux of vapor}$$

$$N_v \cdot MW_{vap} = 9.518 \times 10^{-6} \frac{\text{kg}}{\text{m}^2 \cdot \text{s}} \quad \text{Mass flux of vapor}$$

$$T_{bulk}(z) := T_0 + (T_L - T_0) \cdot \frac{\left(1 - \exp \left(\frac{N_v \cdot C_{pv}}{k_{mix}} \cdot z \right) \right)}{\left(1 - \exp \left(\frac{N_v \cdot C_{pv}}{k_{mix}} \cdot z_L \right) \right)} \quad \text{Temperature profile}$$

$$x_{v,linear}(z) := x_{v,sat,0} + \frac{z}{z_L} \cdot (x_{v,sat,L} - x_{v,sat,0})$$

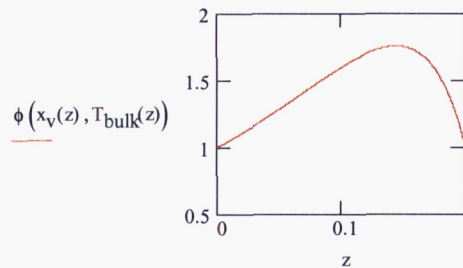
$$T_{linear}(z) := T_0 + \frac{z}{z_L} \cdot (T_L - T_0) \quad \text{Linear profiles for reference}$$



The concentration and temperature distributions are very nearly linear for this example case.

$$\phi(x_v, T_v) := \frac{x_v \cdot P_{mix}}{FP_{vsat} \left(\frac{T_v}{K} \right)} \quad \text{Relative humidity}$$

The relative humidity is greater than 100% except at the two boundaries. The model equations are based on the ideal gas assumption and do not allow for the possibility that the partial pressure of one component can exceed its saturation vapor pressure as a result of the temperature distribution.



$$i := 0..50$$

$$z_i := \frac{i}{50} \cdot z_L$$

$$z_L = 0.2\text{m}$$

$$x_v(z_L) = 9.783 \times 10^{-3}$$

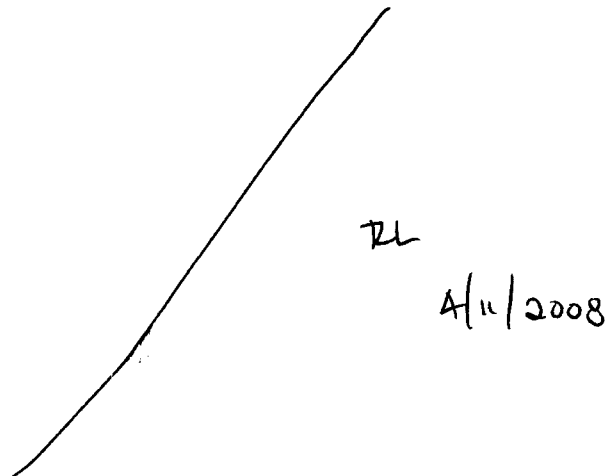
$$a_{i,0} := \frac{z_i}{\text{m}}$$

$$a_{i,1} := \frac{T_{\text{bulk}}(z_i)}{\text{K}}$$

$$a_{i,2} := x_v(z_i)$$

	0	1	2
0	0	320	0.104
1	$4 \cdot 10^{-3}$	319.253	0.102
2	$8 \cdot 10^{-3}$	318.503	0.1
3	0.012	317.752	0.099
4	0.016	316.998	0.097
5	0.02	316.242	0.095
6	0.024	315.484	0.093
7	0.028	314.725	0.091
8	0.032	313.963	0.09
9	0.036	313.199	0.088
10	0.04	312.433	0.086
11	0.044	311.664	0.084
12	0.048	310.894	0.082
13	0.052	310.122	0.08
14	0.056	309.347	0.079
15	0.06	308.57	0.077

WRITEPRN("1-D_Heat_Mass.txt") := a



A FLOW-3D prepin file was prepared to specify the model conditions described in the Mathcad sheet above. This prepin file is entitled

prepin.1-D FULL 40 diff Twall

Nat Conv Box wet, 20cm Sq., Right=320K, Left=280K DIFFUSION ONLY TWALL

5-12-05

Tests the transport of vapor and thermal energy by concentration gradients only.

\$xput

```
remark='units are SI',
itb=0, ifvis=0, ifenrg=2, ifrho=1, ihtc=2, ipdis=1,
iwsh=1,
iadiz=1,
iusrd=1,
delt=1.e-4, pltdt=20.,
twfin=1000.,
isolid=0,
rmrhoe=1.,
rmrho=1.,
```

\$end

\$limits

\$end

\$props

```
rhof=1.097,
mu1=2.e-05, units='si',
cv1=717., thc1=0.026,
```

\$end

\$scalar

```
nsc=6,
isclr(1)=3, cmisc(1)=0.26e-04, scltit(1)='Tot.Water', rmisc=1.,
isclr(2)=0, cmisc(2)=0., scltit(2)='Liq.Flux',
isclr(3)=0, cmisc(3)=0., scltit(3)='Rel.Hum',
isclr(4)=0, cmisc(4)=0., scltit(4)='Net.Liq',
isclr(5)=0, cmisc(5)=0., scltit(5)='Vap.Wat',
isclr(6)=0, cmisc(6)=0., scltit(6)='Liq.Wat',
```

\$end

\$bcdata

```
wl=2, wr=2,
wf=1, wbk=1,
wb=1, wt=1,
```

\$end

\$mesh

```
px(1)=-0.005, py(1)=0., pz(1)=0.,
```

```
    px(2)=0.205,    py(2)=1.,    pz(2)=1.,
    nxcelt=42,     nycelt=1,     nzcelt=1,
$end

$obs
    avrck=-3.1,
    nob =2,
    tobs(1)=0., tobs(2)=95., tobs(3)=100., tobs(4)=195., tobs(5)=200.,
tobs(6)=1000.,
    remark='Obstacle 1. Left hot wall',
    xl(1)=-0.02, xh(1)=0.0,
    twobs(1,1)=320.,
    remark='Obstacle 2. Cold right wall',
    xl(2)= 0.2,    xh(2)=0.22,
    twobs(1,2)=280.,
$end
$fl
    remark=' No vapor in fluid',
    sclri(1)=0.0,
    presi=101300.,
$end
    remark=' Sat. at 300 K',
    sclri(1)=0.021994,

$bf
$end

$temp
    ntmp=1,
    tempi=300.,
$end

$motn
$end

$grafic
$end

$parts
$end

$usrdat
    istwtf_stg = 'tw',
    imoist_stg(1)=-1,
    imoist_stg(2)=-2,
    isvap_stg = 1,
    isliq_stg = 2,
    isrh_stg = 3,
    istlq_stg = 4,
    isyvw_stg=5,
    isywl_stg=6,
    hvvap_stg=2300000.,
    cvvap_stg=1411.,
    rvap_stg=416.,
    rgas_stg=289.,
    vaprlx_stg=0.5,
$end
```

The analysis predictions and the FLOW-3D predictions for the temperature and vapor concentration profile were copied into an Excel spreadsheet entitled

1-D_Mass_Heat.xls

for convenient plotting. The predictions are compared in Figure 5-16-05-A below.

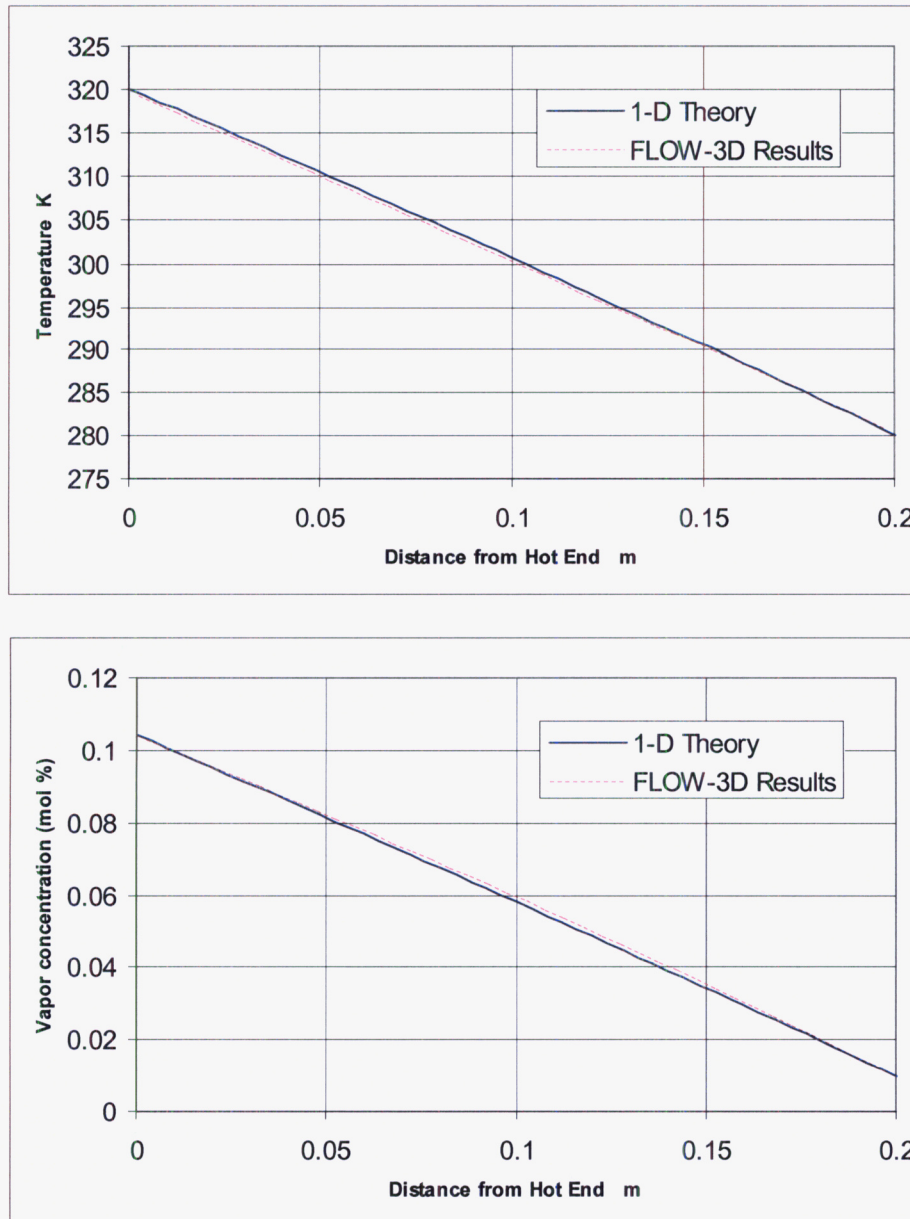


Figure 6-16-05-A. Temperature and Vapor Molar Concentration for 1-D Diffusion of Water through Air.

The FLOW-3D results closely agree with the theoretical model.

The theoretical analysis shows an important feature that is probably not realistic. Not on the next to last page of the Mathcad sheet (page 149 of this notebook) that the relative humidity is predicted to be well in excess of 100%. The slight supersaturation of air with water vapor (i.e., $RH > 100\%$) is well known, but RH values of 180% are NOT realistic. This means that the FLOW-3D model is also not realistic in that it too will predict vapor concentrations well in excess of the saturation values. These relative humidity predictions are compared in Figure 5-16-05-B.

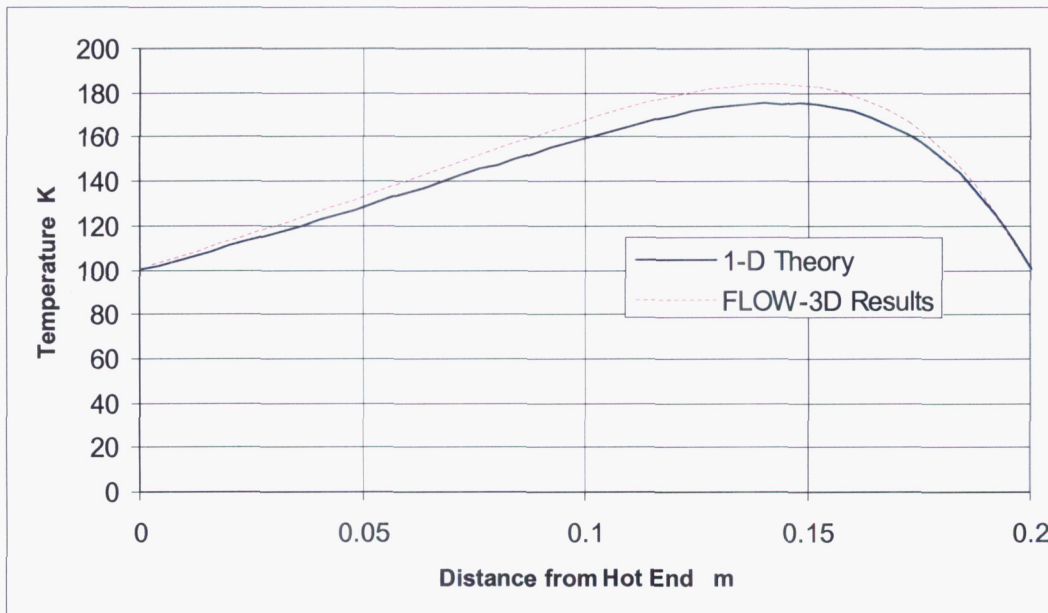


Figure 6-16-05-B. Relative Humidity 1-D Diffusion of Water through Air.
(Supersaturation of water vapor is unlimited)

Consequently, the vapor transport model must be modified to limit the vapor concentration to a maximum of 100%. The excess vapor will condense as fine droplets. In the physical case, this mist could agglomerate and fall like rain. This is a very complex modeling task; so, it will be assumed that the excess water will remain as a mist and be transported and diffused in the same way that the water vapor is diffused and advected.

END OF ENTRY FOR 5-16-05

STG

6/23/05 *STG*

In the previous entry, 5-16-05, it was shown that the vapor transport model needed to be modified to limit the vapor concentration to a maximum of 100 %. This entry documents the resulting software changes to the special FLOW-3D subroutines

qsadd_moist_stg.F

teval_stg.F

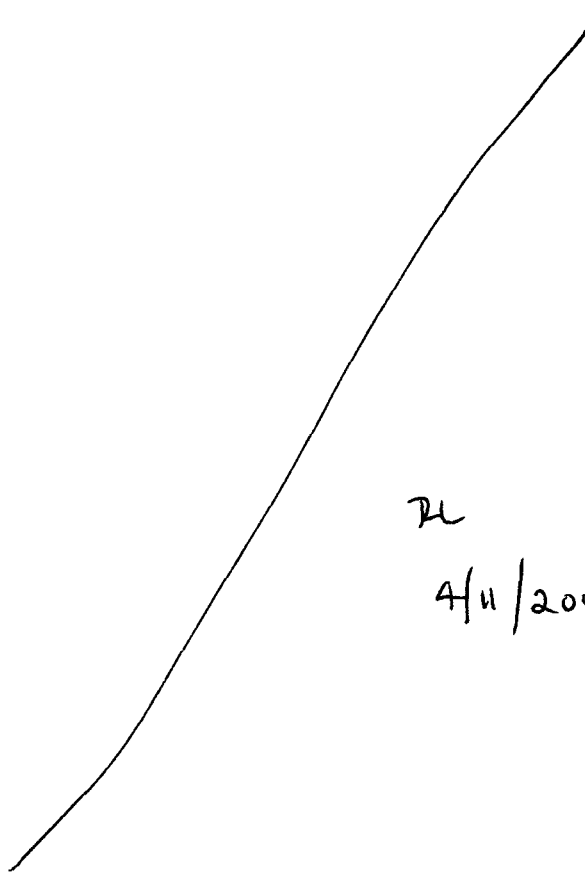
rusrd_stg.F

prusrd_stg.F

rhoec1_stg.F

rhocal_stg.F

to allow for liquid water mist as a separate scalar species that is tracked



RL

4/11/2008